Membrane interaction of the CLIC1 transmembrane domain

Bradley Peter 300215

October 2014

A Thesis submitted to the Faculty of Science, University of the Witwatersrand, Johannesburg in fulfilment of the requirements for the degree of Doctor of Philosophy

Supervisor: Professor Heini W. Dirr

Co-Supervisor: Doctor Sylvia Fanucchi

Declaration

I, Bradley Peter (300215), am a student registered for the degree of Doctor of Philosophy (PhD) in the academic year 2014.

I hereby declare the following:

- I am aware that plagiarism (the use of someone else's work without their permission and/or without acknowledging the original source) is wrong.
- I confirm that the work submitted for assessment for the above degree is my own unaided work except where explicitly indicated otherwise.
- I have followed the required conventions in referencing the thoughts and ideas of others.
- I understand that the University of the Witwatersrand may take disciplinary action against me if there is a belief that this is not my own unaided work or that I have failed to acknowledge the source of the ideas or words in my writing.

Signature:  Date:

Abstract

The chloride intracellular channel protein 1 (CLIC1) is a dual-state protein that can exist either as a soluble monomer or in an integral membrane form. Dysfunction in membrane insertion has been implicated in several pathologies including apoptosis, cancer and homeostatic imbalance. The transmembrane domain (TMD) is implicated in membrane penetration and pore formation and is therefore a key target for understanding amphitropism in CLIC1. The mechanism by which the TMD binds, inserts and oligomerises in membranes to form a functional chloride channel is unknown. Here the secondary, tertiary and quaternary structural changes of the CLIC1 TMD and several TMD mutants are reported in an attempt to elucidate the membrane insertion mechanism. A synthetic 30-mer peptide comprising the TMD was examined in 2,2,2-trifluoroethanol (TFE), SDS micelles and POPC liposomes using far-UV CD, fluorescence and UV absorbance spectroscopy. The results suggest a four-step mechanism whereby the TMD, which is unfolded in buffer, refolds into a helix which partitions onto the membrane, followed by insertion and dimerisation to form a membrane-competent protopore complex. These helices associate via a Lys37-mediated cation-π interaction to form weakly active dimers. The complex is then tethered to the membrane by a cationic motif acting as an electrostatic plug. Thus, electrostatic interactions provide both a strong thermodynamic driving force for helix-helix association as well as structural integrity within the membrane. This represents an important step towards understanding how amphitropism occurs in CLIC1 and offers a unique insight into how CLIC1 and other proteins defy the 'one-sequence one-fold' hypothesis.

Research Outputs

Original Publications

1. Peter, B., Ngubane, N. C., Fanucchi, S. and Dirr, H. W. (2013). Membrane mimetics induce helix formation and oligomerisation of the chloride intracellular channel protein 1 transmembrane domain. *Biochemistry*, **52(16):** 2739-49
2. Peter, B., Polyansky, A. A., Fanucchi, S. and Dirr, H. W. (2014). A Lys-Trp cation-π interaction mediates the dimerisation and function of the chloride intracellular channel protein 1 transmembrane domain. *Biochemistry*, **53(1):** 57-67
3. Peter, B., Fanucchi, S. and Dirr, H. W. (2014). A conserved cationic motif enhances membrane binding and insertion of the chloride intracellular channel protein 1 transmembrane domain. *Eur Biophys J* (DOI: 10.1007/s00249-014-0972-y)

Conference Presentations

1. Molecular Biosciences Research Thrust research day, Johannesburg (2013). *Oral Presentation*. "Membrane insertion mechanism of the chloride intracellular channel protein 1". Bradley Peter, Sylvia Fanucchi and Heini W. Dirr
2. University of the Witwatersrand postgraduate symposium (2013). *Poster Presentation*. "The transmembrane domain of CLIC1 facilitates dimerisation, insertion and chloride transport". Bradley Peter, Sylvia Fanucchi and Heini W. Dirr
3. 27th Symposium of the Protein Society, Boston (2013). *Poster Presentation*. "The transmembrane domain of CLIC1 facilitates dimerisation, insertion and chloride transport". Bradley Peter, Sylvia Fanucchi and Heini W. Dirr
4. Molecular Biosciences Research Thrust research day, Johannesburg (2012). *Poster Presentation*. "Membrane Mimetics Induce Helix Formation and Dimerisation of the CLIC1 Transmembrane Domain". Bradley Peter, Sylvia Fanucchi and Heini W. Dirr

5. University of the Witwatersrand postgraduate symposium (2012). *Poster Presentation*. "Membrane Mimetics Induce Helix Formation and Dimerisation of the CLIC1 Transmembrane Domain". Bradley Peter, Sylvia Fanucchi and Heini W. Dirr

Acknowledgements

I would like to thank my supervisors Professor H. Dirr and Doctor S. Fanucchi for their unwavering support and supervision throughout the course of my studies. Their passion and dedication have inspired and motivated me and I hope to carry this with me in my future endeavours.

To the members of the Protein Structure-Function Research Unit, I would be nowhere without you. You took me in and taught me everything I know- for that I am truly grateful. Special thanks to Megan Cross, Helen Letseka and Derryn Legg-E'Silva

I am also grateful to the National Research Foundation and University of the Witwatersrand for financial assistance without which this work would not have been possible.

Lastly, I would like to thank my close friends and family for putting up with me for the past few years. Your love and support are everything to me.

"If I have seen further than others, it is by standing upon the shoulders of giants"

- Isaac Newton

Contents

List of Figures

List of Tables

List of Abbreviations

CD	circular dichroism
Cl^-	chloride ion
CLIC	chloride intracellular channel protein
GST	glutathione *S*-transferase
GUV	giant unilamellar vesicle
LUV	large unilamellar vesicle
MLV	multilamellar vesicle
PFT	pore-forming toxin
POPC	1-palmitoyl-2-oleoyl-*sn*-glycero-3-phosphocholine
PTM	putative transmembrane region
SDS	sodium dodecyl sulphate
SUV	small unilamellar vesicle
TFE	2,2,2-trifluoroethanol
TMD	transmembrane domain

Chapter 1

Introduction

Membrane proteins account for nearly one-quarter of proteins in eukaryotic cells and constitute approximately 50 % of all current drug targets (Caffrey, 2003). These proteins are implicated in vital cellular processes ranging from cell signalling to structural support and molecular transport (Caffrey, 2003). Despite their clear biological significance, only a handful of membrane proteins have been structurally classified. As a result, the mechanisms by which many membrane proteins bind to and insert into membranes remain relatively unknown. In order to determine how membrane proteins interact with membranes, it is important to establish the features of biological membranes and how these may influence protein-membrane interactions.

1.1 Biological Membranes

Biological membranes establish cellular compartmentalisation, act as highly-selective barriers to the external environment and play key roles in maintaining the homeostatic balance of the cell. These functions are largely determined by the physicochemical properties of the membrane as well as the proteins bound to/embedded within it.

1.1.1 Structure and Physicochemistry

1.1.1.1 Composition

Biological membranes are composed of amphipathic lipid molecules arranged into a continuous bilayered structure. These lipids comprise a hydrophobic head attached, via a glycerol or ceramide moiety, to one or more hydrophobic hydrocarbon chains (Spector and Yorek, 1985) (Figure 1 A). The head sections may contain either phosphate or carbohydrate

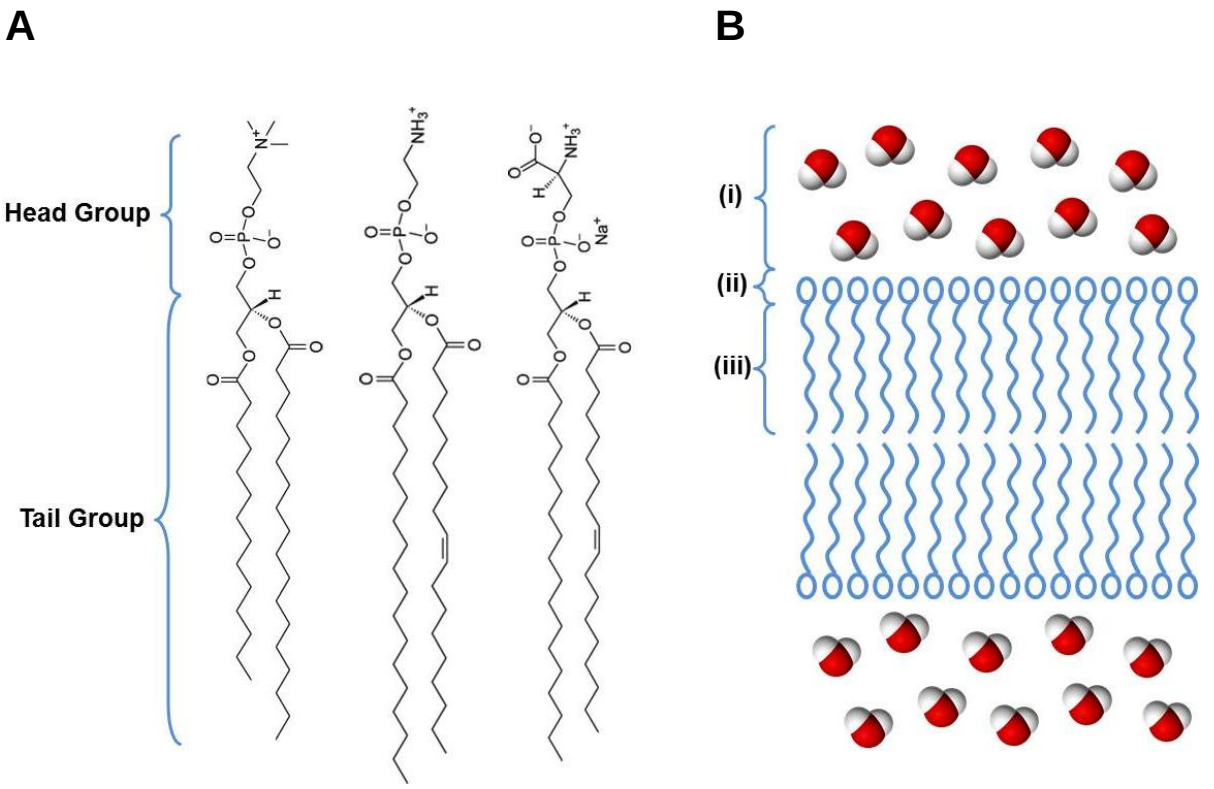

Figure 1 Typical structure of a bilayered membrane and its constituent phospholipids. **(A)** The three most abundant phospholipids include phosphatidylcholine (left), phoshpotidylethanolamine (centre) and phosphatidylserine (right). The amphipathic nature of these phospholipids is a result of the hydrophilic head group coupled to a hydrophobic hydrocarbon tail via a glycerol moiety. **(B)** The plasma membrane comprises three distinct regions: (i) the aqueous solvent belt, (ii) the charged phospholipid head groups and (iii) the hydrophobic core. Lipid asymmetry within the membrane generates ionic and pH gradients which can influence the binding and insertion of membrane proteins. Adapted from Dowhan (1997)

esters, yielding phospholipids or glycolipids respectively. Phospholipids make up ~ 70 % of the total lipid content (Bretscher, 1973) and are particularly amenable to chemical modifications, resulting in a large number of phospholipid derivatives (Figure 1 A). The distribution of these phospholipids varies according to the membrane type and tissue location, thus making the lipid bilayer a structurally and chemically heterogeneous environment.

The bilayer configuration of biological membranes is a direct result of the hydrophobic effect acting on these amphiphilic phospholipids (Spector and Yorek, 1985). In the cytosol, water-lipid interactions are thermodynamically unfavourable and result in vast entropic losses. The interaction between water and the charged lipid heads, however, is favourable. As a result, the phospholipids arrange themselves so that the hydrocarbon tails face one another and are shielded from the solvent whilst the hydrophobic head groups remain solvent exposed (Bretscher, 1973). This arrangement produces three-distinct regions: (i) the central hydrophobic core (~30 Å thick) which can accommodate a protein helix of ~21 residues in length (Nagle and Tristram-Nagle, 2000; Lee, 2003); (ii) the outer phospholipid heads (~ 10-15 Å thick) and; (iii) the flanking solvent/aqueous belt which forms the interfacial region (Figure 1 B). This solvent belt, coupled with the surface charge on the lipid heads, promotes the formation of solute and pH gradients at the membrane surface (White and Wimley, 1999).

1.1.1.2 Fluidity

The membrane is a fluid semi-crystalline assembly that can adapt and change depending on its external environment and functional requirements. The fluidity of biological membranes is attributed to the dynamic nature of its constituent lipids. Lipids are capable of three types of movement: (i) laterally in the plane of the lipid bilayer; (ii) rotationally around the carbon-carbon bonds of the hydrocarbon lipid chains; and (iii) a transversion 'flip-flop' movement of phospholipids from one leaflet to the other (Bergers *et al*., 1993; Rawicz, 2000). These

motions are dependent on the phase transition temperature (T_m) of the lipids as well as the strength of the attractive van der Waals interactions between neighbouring lipid molecules (Träuble and Eibl, 1974; Rawicz, 2000). The degree of unsaturation of the hydrocarbon chains as well as the presence of cholesterol also influences membrane fluidity (Brown, 2000). Importantly, the transmembrane domains (TMDs) of membrane proteins can interact with and alter the packing of lipid molecules (Sanchez *et al*., 2010). The opposite is also true, with membrane fluidity strongly regulating membrane protein binding and insertion.

1.1.1.3 Asymmetry and Electrostatics

A unique feature of biological membranes, in addition to their fluid nature, is that the inner and outer leaflets differ in composition and physicochemical properties. This asymmetry allows membrane properties to be independently adjusted in order to meet the requirements of various membrane proteins in different cellular compartments (Yeagle, 1989; Anderson and Koeppe, 2007; Nyholm *et al*., 2007). Asymmetry typically takes the form of differentially-distributed phospholipids and the resulting differences in membrane surface chemistry. Such differences in surface chemistry play crucial roles in promoting or preventing the binding and insertion of membrane proteins (Lawson *et al*., 1977). Different membranes may thus be more prone to protein insertion than others based on their lipid content.

Charge imbalances resulting from membrane asymmetry create an electrostatic potential across the membrane. This comprises: (i) a transmembrane potential; (ii) a surface potential; and (iii) an internal potential (Honig *et al*., 1986). Transmembrane potentials are a result of charge separation across the *cis* and *trans* faces of the membrane (Gurtovenko and Vattulainen, 2008) whereas surface potentials arise from charge differences between the membrane interface and the cytosol. Internal potentials, which stem from dipoles within the hydrophobic core, produce a powerful electrical field which can dictate both the folding and

insertion of membrane proteins (Honig *et al*., 1986). In addition, these large electrostatic energy barriers virtually exclude most small ions from passing through the hydrocarbon core (Mimms *et al*., 1981; Paula *et al*., 1998). Electrostatic interactions are thus important regulators of both solute diffusion and protein binding.

1.1.2 Model Membrane Systems

The complex liquid crystalline nature of the lipid bilayer has proved a formidable barrier to the study of protein-membrane interactions. Simplified model systems which retain the essential characteristics of the lipid bilayer are thus required in order to probe the association of proteins with membranes. Isotropic solvents, detergent micelles/bicelles and phospholipid liposomes are among the most commonly employed membrane mimetics.

1.1.2.1 Isotropic Solvents

Isotropic solvents are characterised by a homogeneous dielectric constant/scalar permittivity (Mennucci *et al*., 1997). Thus they provide a uniform set of environmental conditions with dielectric constants that match that of the hydrophobic core of biological membranes (~ 2-10) (Mennucci *et al*., 1997). These compounds can interact with membrane proteins via non-specific (dielectric enrichment) and specific (hydrogen bonding, proton/charge transfer) interactions (Zakerhamidi *et al*., 2012). These solvents include benzene, toluene, n-butyl stearate and trifluoroethanol (TFE). TFE is by far the most widely-used isotropic membrane mimetic. TFE (Figure 2 A) essentially increases the order of the solvent, making solvent-protein interactions energetically unfavourable and subsequently promoting interactions between the protein backbone (secondary structure) (Roccatano *et al*., 2002). Despite their ease of use, isotropic solvents do not mimic the heterogeneity of lipid bilayers and are thus a crude and preliminary means of analysing membrane proteins.

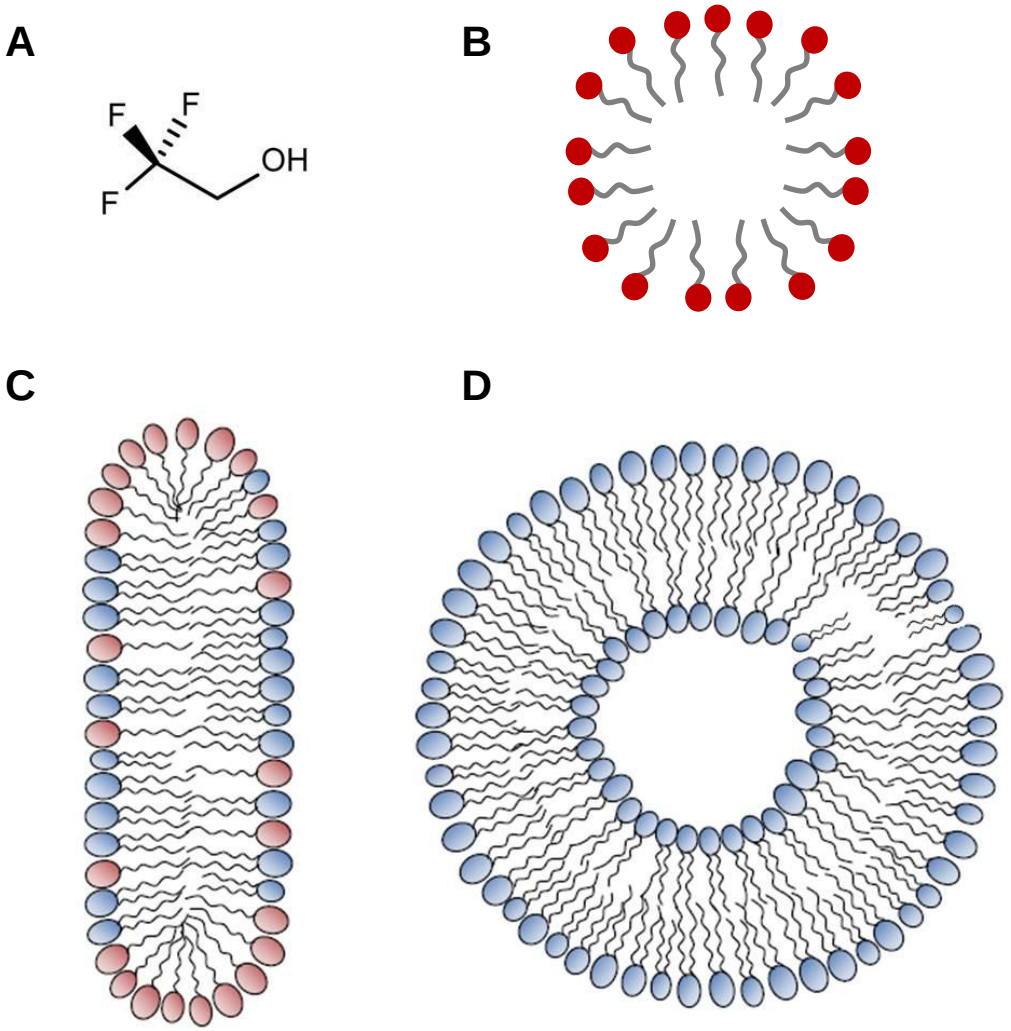

Figure 2 Model membrane systems used to analyse protein-membrane interactions. (A) The isotropic solvent 2,2,2-trifluoroethanol (TFE) provides a chemically homogeneous environment with a dielectric constant that matches the hydrophobic core of biological membranes. **(B)** The small spherical nature of micelles is derived from the self-association of detergent monomers (red) due to the hydrophobic effect. **(C)** Bicelles are disc-like collections of detergents (blue) and lipids (red) which lack an aqueous interior. **(D)** Liposomes are bilayered phospholipid vesicles which enclose an aqueous interior and closely match the heterogeneity of biological membranes

1.1.2.2 Detergent Micelles/Bicelles

Micelles are spherical structures formed by the self-association of detergent monomers above a concentration threshold (Figure 2 B) (Garavito and Ferguson-Miller, 2001). The detergent monomers, like phospholipids, are amphipathic and may either be ionic, non-ionic or zwitterionic (Wennerström and Lindman, 1979). Detergents are preferable to isotropic solvents since they simulate protein-lipid interactions whilst simultaneously solubilising membrane proteins from their native environment (Thomas *et al*., 1999). However, they are relatively unstable and permeable to the external environment (Rosen, 1969; Thomas *et al*., 1999; Garavito and Ferguson-Miller, 2001).

Bicelles are more structurally complex than micelles and are composed of a mixture of detergents and lipids which form a stable and bilayered disc-like structure (Figure 2 C) (Diller *et al*., 2009). Bicelles more accurately mimic the asymmetry of biological membranes but are poorly suited to the functional characterisation of many membrane proteins owing to the absence of an aqueous interior (Sanders and Landis, 1995; Diller *et al*., 2009). In addition, the spherical nature and relatively small size of both micelles and bicelles does not account for the lateral organisation of biological membranes (Diller *et al*., 2009).

1.1.2.3 Phospholipid Liposomes

Liposomes are bilayered lipid vesicles which enclose an aqueous interior and form as a result of hydrophobic interactions between lipid and water molecules (Figure 2 D) (Mozafari, 2005) Because of their larger size and lipid content, liposomes more accurately mimic the asymmetry, curvature and lateral organisation of biological membranes. Liposomes comprise four classes based on size: (i) small unilamellar vesicles/SUVs (30-70 nm diameter); (ii) large unilamellar vesicles/LUVs (100-1000 nm diameter); (iii) giant unilamellar vesicles/GUVs (10-100 μm diameter); and (iv) multilamellar vesicles/MLVs (Winterhalter and Lasic, 1993).

Of all the membrane mimetics, liposomes are perhaps the most widely-used for structural studies of membrane proteins due to their diversity in size, coupled with adjustable fluidity, charge and phospholipid composition. Such a system may be tailored to suit the requirements of specific membrane proteins, thereby maximising insertion and/or function.

1.2 Membrane Proteins

The membrane environment influences the structure, stability and folding of membrane proteins as well as their ability to insert into membranes. In order to maximise their functional versatility, membrane proteins have adapted their structure to suit the unique environment of the lipid bilayer.

1.2.1 Structure and Classes

Membrane proteins can be classified according to their relationship with the membrane and may be either (i) peripheral; (ii) integral or; (iii) amphitropic (White *et al*., 2001). Peripheral membrane proteins reversibly associate with the outer regions of the membrane or other integral membrane proteins via electrostatic, hydrophobic and other non-covalent interactions (Klein *et al*., 1985; Buckland *et al*., 2000; Mulgrew-Nesbitt *et al*., 2006). Integral membrane proteins, however, utilise strong non-covalent interactions to permanently embed themselves within membranes (Tusnady, 1998). These proteins may either span the membrane (polytopic) or remain partially embedded (monotopic) (Klein *et al*., 1985; Smith *et al*., 2001). In order to conform to the dual cytosol-membrane environment, integral polytopic proteins are amphiphilic in nature. Unlike integral and peripheral membrane proteins, amphitropic proteins can adopt multiple stable native states and undergo large-scale structural rearrangements upon association with the lipid bilayer. This results in the spontaneous conversion from a water-soluble to a membrane-bound form (Johnson and Cornell, 1999; Bryan and Orban, 2010). Such amphitropism requires major secondary and tertiary structural

alterations as well as interactions which are favourable in both aqueous and membrane environments. Although the energy barriers to structural plasticity may seem high, amphitropism is widely observed and occurs in many bacterial pore-forming toxins, apoptotic proteins and the eukaryotic chloride intracellular channel (CLIC) protein family (Littler *et al*., 2004; Parker and Feil, 2005; Thuduppathy *et al*., 2006, 2012).

Regardless of their relationship to the membrane, all membrane proteins require a transmembrane domain(s) (TMD) in order to interact with the lipid bilayer. Whilst solvent-exposed domains can adopt a wide variety of protein folds, transmembrane domains are limited in their design and are influenced by the physicochemical properties of the lipid bilayer (White and Wimley, 1999; Popot and Engelmann, 2000).

1.2.2 Transmembrane Domains

1.2.2.1 Structure

Nearly all transmembrane regions identified to date comprise either alpha-helical segments/bundles or beta-barrel arrangements (White and Wimley, 1999; Käll *et al*., 2004). The amino acid content also remains highly conserved, with nearly all transmembrane domains containing: (i) a central span of predominantly apolar residues; and (ii) charged residues at the membrane interface (Landolt-Marticorena *et al*., 1993; Arkin and Brunger, 1998; Hunte *et al*., 2005). The structure of transmembrane domains is often described in terms of hydrophobic mismatch. This refers to the difference in length/thickness of the lipid bilayer versus the length of the hydrophobic region of a transmembrane domain which spans it (Duque *et al*., 2002). Ideally, these lengths are equal (~ 30 Å) but transmembrane domains often vary in length and/or residue composition. To compensate for this, transmembrane domains are pre-oriented/tilted within the lipid bilayer (Ren *et al*., 1997).

Transmembrane domains often contain numerous structural peculiarities such as proline kinks (Cordes *et al*., 2002; Rigoutsos *et al*., 2003), π-bulges and 3_{10}-helices (Popot and Engelman, 2000). These features reduce the overall number of intrachain hydrogen bonds which enhances tertiary interactions (Locher *et al*., 2003; Orzaez *et al*., 2004) and allows for structural flexibility (Chakrabarti and Chakrabarti, 1998). In addition, super-secondary structural elements such as N- and C-terminal capping motifs stabilise the folded conformation in membranes (Aurora and Rose, 1998; Gurezka *et al*., 1999; Quan *et al*., 2012). These features are only stable when exposed to appropriate environmental conditions (Hildebrand *et al*., 2004). This enables amphitropic proteins to maintain distinct cytoplasmic and membrane-bound conformations and hints at the transmembrane domain as being a key catalyst in the structural conversion.

1.2.2.2 Folding and Energetics

A unique feature of transmembrane domains is their ability to retain structural and functional integrity after being excised from the parent protein (Deutsch, 2002). This is possible since these domains are thermodynamically stable and follow a folding mechanism which is independent of the parent protein (Popot and Engelman, 2000).

The folding of transmembrane domains is dictated by the membrane environment and the resulting thermodynamic cost of peptide bond partitioning (Wimley and White, 1996). Desolvation of the peptide bond is thermodynamically costly (~ 1.2 $kcal.mol^{-1}$) and would limit folding and insertion into the membrane (Liu and Bolen, 1995; Wimley and White, 1996). These energetic costs can, however, be mitigated by replacing peptide-solvent interactions with peptide-peptide interactions at the membrane interface. As a result, the membrane interface is a key catalyst of secondary structure formation (White *et al*., 2001).

This concept of interface-induced peptide bond desolvation is used as a template for understanding α-helical membrane protein folding and insertion (White and Wimley, 1999).

The four-step folding model devised by White and Wimley (1999) is a composite of two related models proposed by Jacobs and White (1989) and Popot and Engelman (1990). This sequential model involves: (i) the partitioning of the unfolded domain onto the membrane interface; (ii) interfacial folding; (iii) the insertion of the folded domain into the membrane; and (iv) the association of individual domains to form functional complexes (Figure 3). These four steps can occur exclusively along the membrane interface or include several steps within the cytosol. Experimental evidence does, however, suggest that the interfacial pathway predominates under most conditions (White and Wimley, 1998; White and Wimley, 1999). This is likely a result of the free energy well provided by the bilayer interface which supports the initial binding and folding of transmembrane domains (White and Wimley, 1999).

1.2.3 Membrane Binding Mechanisms

The four-step mechanism of transmembrane helix insertion only describes the general processes of folding and insertion. The specific molecular interactions which mediate these events are equally as important and are responsible for the wide range of membrane binding mechanisms seen in membrane proteins. Membrane proteins may or may not contain membrane targeting/topogenic signal sequences (von Heijne and Gavel, 1988). Those that do are often targeted to membranes via the secretory pathway (Kelly, 1985; Pelham and Munro, 1993). Of interest to this study are those proteins which bypass conventional membrane insertion pathways and spontaneously insert into membranes via alternate mechanisms. These proteins typically exploit reversible hydrophobic and electrostatic interactions to mediate membrane insertion.

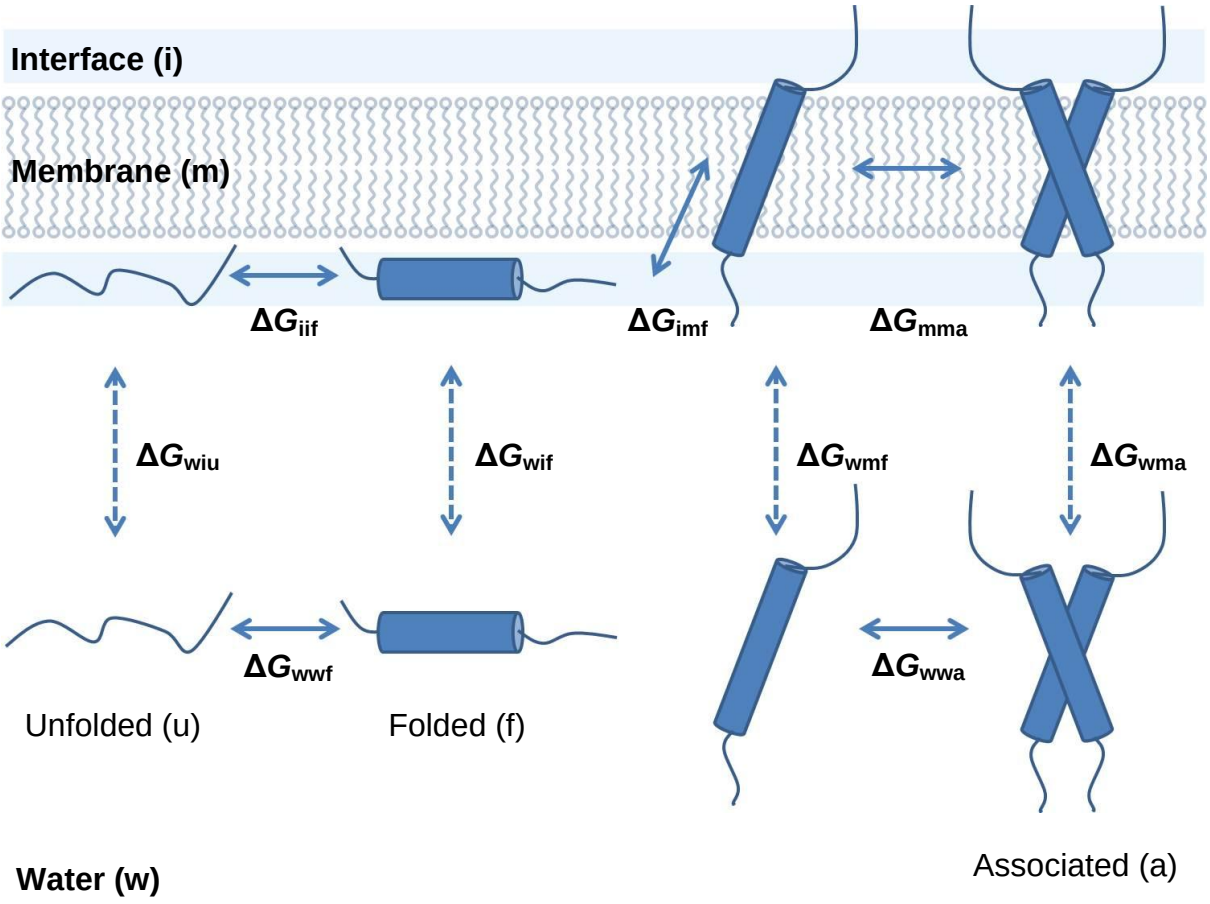

Figure 3 Energetics associated with membrane insertion of a transmembrane domain. The insertion of a transmembrane domain into membranes comprises four-steps: (i) partitioning onto the membrane surface; (ii) folding; (iii) membrane insertion and; (iv) self-association. This process may take place along the membrane interface, in water (cytosol) or a combination of the two. The standard transfer free energies are indicated by the ΔG symbols. The first two subscripts indicate the change in phase whilst the third subscript indicates the final structure assumed by the domain. The subscripts denote the membrane interface (i), membrane core (m), water/cytosol (w), unfolded domain (u), folded domain (f) and associated/oligomeric domains (a)

1.2.3.1 Hydrophobic and Protein-Lipid Interactions

Membrane proteins may non-covalently interact with lipids to facilitate membrane adhesion and/or insertion (Hunte, 2005). These lipids may either surround the protein (annular), insert into surface cavities (non-annular) or insert deep into the protein (Hunte, 2005; Lee, 2005). The aromatic residues tryptophan and tyrosine are thought to mediate these interactions by anchoring transmembrane helices at the membrane surface (Landolt-Marticorena *et al*., 1993; Koeppe, 2007). The formation of salt bridges between aspartate/glutamate residues and phosphate head groups has also been shown to play a key role in stabilising protein-lipid interactions (Lee, 2005).

1.2.3.2 Electrostatic Interactions

As proteins approach the membrane interface, two competing short-range interactions are in motion: the unfavourable desolvation of polar groups on the membrane/protein and the favourable partitioning of non-polar groups into the membrane (Mulgrew-Nesbitt *et al*., 2006). The negative charge and low pH at the interface can alter a protein's electrostatic properties such that proteins with large net negative charges will encounter repulsive forces at the anionic membrane interface (Honig *et al*., 1986; McLaughlin *et al*., 2005). This repulsion may inhibit membrane binding and insertion. Many membrane proteins exploit these phenomena by (i) neutralising glutamate and aspartate residues via salt-bridges, thereby decreasing charge repulsion (Mulgrew-Nesbitt *et al*., 2006); or (ii) protonating histidine, arginine and lysine residues, thereby increasing charge attraction. Positively-charged regions within transmembrane domains may also act as topology determinants involved in the binding, insertion and orientation of proteins in membranes (von Heijne, 1984; Wallin and von Heijne, 1995). Electrostatic interactions may thus prime proteins for membrane targeting and insertion. Since these interactions are reversible, they are of particular importance for proteins which adopt multiple stable native states.

1.2.3.3 Membrane Insertion Mechanisms of Amphitropic Proteins

Amphitropic proteins utilise a combination of structural changes coupled with electrostatic and hydrophobic interactions to bring about membrane binding and insertion. Pore-forming toxins (PFTs) and apoptotic proteins have been extensively studied and used as models for understanding reversible membrane binding.

PFTs typically comprise a central transmembrane helical hairpin surrounded by a cluster of hydrophilic helices (Figure 4 A-E) (van der Goot *et al.*, 1991; Parker *et al.*, 1992; Grochulski *et al.*, 1995). Membrane insertion follows the 'Umbrella' model whereby insertion is initiated by hydrophobic interactions between the membrane and the transmembrane helical hairpin. The surrounding helical cluster subsequently opens up and is anchored to surface of the membrane (Parker *et al.*, 1990; Choe *et al.*, 1992). This process is driven by a combination of electrostatic and hydrophobic events. The low pH at the membrane interface assists membrane insertion by (i) increasing the protein's overall hydrophobicity via charge neutralisation and (ii) lowering the energy barrier to membrane insertion via the formation of a destabilised molten globule intermediate (Thuduppathy and Hill, 2006). In addition, certain toxins utilise clusters of surface aromatic residues to initiate membrane insertion (Belmonte *et al.*, 1993, Tejuca *et al.*, 1996) whilst others use electrostatic interactions to bind to cell surface receptors (Parker and Pattus, 1993).

The apoptotic proteins Bax, Bcl-2 and Bcl-x_L are structurally similar to the PFTs (Figure 4 F, G) and follow a similar membrane insertion mechanism (Nguyen *et al.*, 1993; Adams and Cory, 1998). The energy barrier to insertion, however, is lowered by side chain protonation rather than acid-induced conformational destabilisation (Ramsay *et al.*, 1989; Schendel and Cramer, 1994; Sathish *et al*., 2002; Thuduppathy and Hill, 2006).

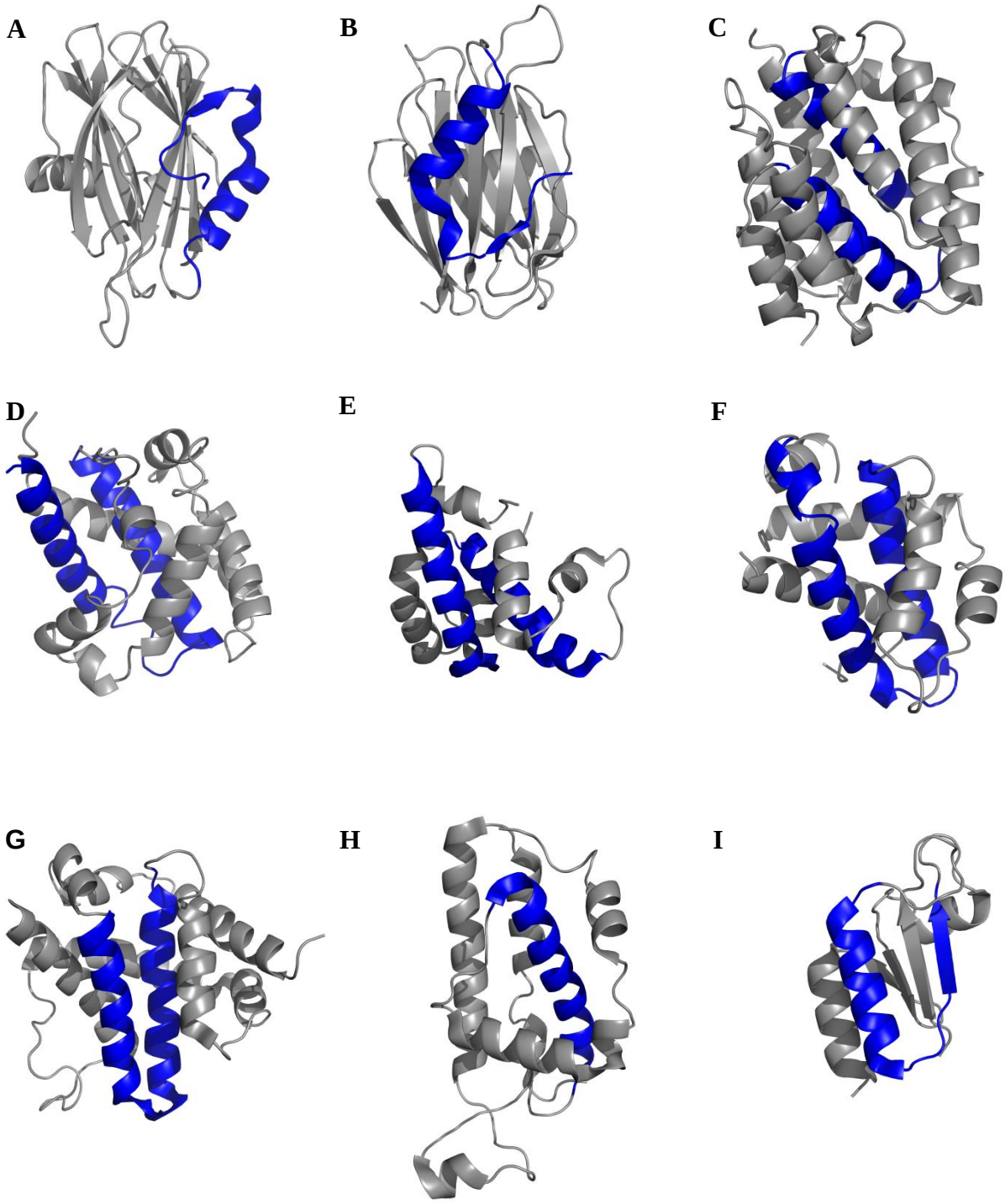

Figure 4 Transmembrane domains of dimorphic pore-forming proteins. The transmembrane domains of bacterial toxins **(A-E)** and apoptotic proteins **(F,G)** as well as the putative transmembrane domains of CLIC1 **(H,I)** are shown in blue. The topology of the domains is similar, with almost all showing a helix-turn-helix or helix-turn-sheet motif. The

CLIC1 C-domain is an exception, comprising a single α-helix. However, this domain has subsequently been shown to remain in the cytoplasm during membrane binding (Singh and Ashley, 2006). The topology of the transmembrane segments of the CLIC1 N-domain, actinoporin and equinatoxin II are similar and are predicted to be helical in the membrane. **(A)** Actinoporin, 1YAZ. **(B)** Equinatoxin II, 1IAZ. **(C)** Pore-forming domain of colicin A, 1COL. **(D)** Pore-forming domain of diptheria toxin, 1DDT. **(E)** Pore-forming domain II of exotoxin A, 1IKQ. **(F)** Bcl-XL, 1MAZ. **(G)** Bax, 1F16. **(H)** CLIC1 C-domain, 1K0M. **(I)** CLIC1 N-domain, 1K0M. Figures were generated using PyMol V 1.2.2 (DeLano Scientific, 2010)

The eukaryotic chloride intracellular channel 1 (CLIC1) protein is the most recently identified class of amphitropic protein and shares similar structural features to the PFTs and apoptotic proteins (Figure 4 H, I). Although little is known about the membrane insertion mechanism of CLIC1, its similarity to the PFTs and apoptotic proteins may hint at a comparable insertion model.

1.2.4 Membrane Transport Proteins

Whilst the primary role of PFTs and apoptotic proteins is to destroy the host cell, most eukaryotic membrane proteins work tirelessly to support and sustain life. Of the many roles played by membrane proteins, membrane transport proteins are perhaps the most functionally important given the impermeability of biological membranes.

The passive diffusion of polar solutes and water (osmosis) across the membrane is limited by the electrostatic barrier created by the membrane's apolar interior (Mulgrew-Nesbitt *et al.*, 2006). Transport proteins, comprising carrier proteins and ion channels, are therefore required to transport polar solutes into and out of the cell. Carrier proteins transport solutes by binding

the solute at one face of the membrane and transferring it to the other side via a series of conformational changes (Skou, 1957; Whittam and Chipperfield, 1975). This process may occur across a concentration gradient or via ATP-mediated active transport against a concentration gradient. On the other hand, ion channels are involved in passive ion transport across electrochemical gradients (Honig *et al*., 1986). Channel proteins can exist in either an open or closed state which may be voltage or chemically gated (Pethig and Kell, 1987; Catterall, 1988). These channels allow the transport of polar ions across the non-polar membrane by raising the dielectric constant within the pore (Honig *et al*., 1986). This is achieved by the presence of charged residues which line the pore interior. This not only compensates for the potential loss of solvation energy but also allows for ion selectivity based on charge-charge attraction and repulsion (Mulgrew-Nesbitt *et al*., 2006). The most commonly transported ions are sodium, potassium, calcium and chloride. Chloride ions are of particular interest since their associated channels are pathologically significant and structurally unique.

1.2.4.1 Chloride Channels

Chloride (Cl^-) is the most abundant anion in biological systems and is the predominant permeating species under most circumstances (Jentsch *et al*., 2002). Intracellular chloride channels are implicated in pH and cell volume regulation (Alvaro *et al*., 1993), apoptosis (Suh *et al*., 2004), cell migration and differentiation (Nilius, 2001). These channels comprise upwards of 20 members and have been divided into several groups based on sequence homology, structure and function (Jentsch *et al*., 2002). The structure, function and regulation of several channel families are summarised in Table 1. The CLICs are unique among all eukaryotic ion channels in that they are dimorphic and can exist in either a soluble or membrane-bound form (Harrop *et al*., 2001). The mechanism by which these CLIC proteins spontaneously insert into membranes is poorly understood.

Table 1 Intracellular chloride channel families. These proteins form a diverse collection of structurally and functionally unique complexes with the aim of transporting/regulating chloride ions within the cell

Chloride Channel	Channel Structure	Main Function(s)	Regulation
Ligand-gated acetylcholine receptor family[a]	Hetero-oligomeric pentamer comprising 4 TMDs per monomer	Synaptic neurotransmission	Binding of GABA and glycine, PKA phosphorylation
Cystic fibrosis transmembrane conductance regulator (CFTR)[b]	Monomer comprising 12 TMDs	Water homeostasis	Membrane potential (voltage), PKA phosphorylation
Voltage-gated chloride channels (CLC)[c]	Multipore homodimer comprising 12-13 TMDs	Transepithelial transport, organelle acidification, cell volume homeostasis	Membrane potential (voltage), PKA/PKC phosphorylation, pH
Calcium-activated chloride channels (CLCA)[d]	Hetero-oligomer comprising 4-5 TMDs with variable quaternary arrangements	Transepithelial transport, neuron/muscle excitation, Cl^- channel modulation	Binding of calcium, PKA phosphorylation
Chloride intracellular channels (CLIC)[e]	Membrane channel conformation unknown (likely a single TMD)	Regulates intra-organelle pH gradients, membrane potential and ion absorption	Membrane potential (voltage), PKA phosphorylation, pH, oxidation

[a]Betz, 1990; Reichling *et al*., 1994; Lindstrom *et al*., 1995; Owens *et al*., 1996; Ben-Ari *et al*., 1997; Vannier and Triller, 1997; Rivera *et al*., 1999

[b]Riordan *et al*., 1989; Anderson *et al*., 1991; Bear *et al*., 1992; Sheppard *et al*., 1993

[c]Stuhmer *et al*., 1989; Jentsch *et al*., 1990; Chen and Miller, 1996; Bateman, 1997; Fahlke *et al*., 1997; Ponting, 1997; Schriever *et al*., 1999

[d]Lowe and Gold, 1993; Morris and Frizzell, 1993; Cunningham *et al*., 1995; Arreola *et al*., 1998; Kidd and Thorn, 2000

[e]Landry *et al*., 1989; Howell *et al*., 1996; Redhead *et al*., 1997; Nishizawa *et al*., 2000; Warton *et al*., 2002; Singh and Ashley, 2006

1.3 Chloride Intracellular Channel (CLIC) Proteins

CLIC proteins form part of the glutathione *S*-transferase (GST) superfamily and adopt a GST-like canonical topology in their reduced monomeric states.

1.3.1 Glutathione Transferase Superfamily

The GSTs (EC 2.5.1.18) are a diverse class of enzymes implicated in the detoxification of drugs and other xenobiotic compounds (Dirr *et al*., 1994; Wilce and Parker, 1994). They catalyse the conjugation of glutathione (GSH) to drugs or reactive oxygen species, thereby disabling their action (Sheehan *et al*., 2001).

Cytosolic GSTs predominantly exist as soluble homodimers with each subunit comprising two domains. The N-domain contains a topologically-conserved thioredoxin fold (βαβαββα motif) whilst the C-domain is entirely α-helical (Dirr *et al*., 1994). The hydrophobic domain interface plays a vital role in maintaining the stability of both GSTs and CLICs in the cytoplasm (Stoychev *et al*., 2009; Parbhoo *et al*., 2011). The N-domain is conserved across the GSTs and CLICs as is the glutaredoxin-like active site formed by a Cys-X-X-Cys/Ser motif (Wilce and Parker, 1994). Although CLIC proteins retain this active site, little catalytic activity has been identified (Littler *et al*., 2004). Despite their structural homology to the GSTs, CLICs remain monomeric in solution under reducing conditions and are not associated with cellular detoxification. In addition, their ability to reversibly bind to the lipid bilayer and function as chloride channels makes them unique members of the GST superfamily.

1.3.2 Chloride Intracellular Channel Protein Family

The CLIC family belongs to a class of anion channel transport proteins and comprises seven members: CLIC1 (Valenzuela *et al*., 1997), CLIC2 (Heiss and Poutska, 1997), CLIC3 (Qian *et al*., 1999), CLIC4 (Duncan *et al*., 1997), CLIC5A/B (Berryman and Bretscher, 2000) and CLIC6 (Nishizawa *et al.*, 2000; Friedli *et al.*, 2003) in vertebrates. These members share

sequence identities of between 47% and 76% and are highly conserved across a number of vertebrate species (Cromer *et al*., 2002; Berry *et al*., 2003). CLICs show a ubiquity across numerous tissue and cell types and have been localised to the plasma and nuclear membranes, mitochondria, golgi and secretory vesicles (Valenzuela *et al*., 1997; Edwards, 1999; Fernandez-Salas *et al*., 1999; Jentsch *et al*., 2002).

Structurally, CLIC proteins comprise a ~ 240 amino acid core which contains the thioredoxin N-domain and all α-helical C-domain characteristic of the GSTs (Wilce and Parker, 1994; Armstrong, 1997; Board *et al.*, 2000; Harrop *et al.*, 2001). Additional structural features, such as the hydrophilic N-terminal extensions of CLIC5B and CLIC6, are not conserved throughout the family. Despite being structurally well-characterised, the biological function of CLICs remains obscure. Their ion channel activity is thought to mediate homeostatic processes such as regulating membrane potential and ion absorption (Landry *et al*., 1989), bone resorption (Schlesinger *et al*., 1997), cell motility (Ronnov-Jessen *et al*., 2002) and apoptosis (Fernandez-Salas *et al*., 1999). In addition, changes in CLIC expression levels have been linked to several disease processes including Alzheimer's disease (Novarino *et al*., 2004; Milton *et al*., 2008) and colorectal cancer (Petrova *et al*., 2008). The structure, function and localisation of the CLIC members is summarised in Table 2.

The soluble nature of the CLICs poses a unique problem in that they must insert into biological membranes in order to exert ion channel activity. This dual-state existence is unique among eukaryotic ion channels and is further complicated by the lack of a membrane-targeting signal sequence (Harrop *et al*., 2001; Cromer *et al*., 2002). CLIC proteins thus remain in the cytoplasm and spontaneously insert into membranes under certain environmental conditions (Ponce *et al*., 1997; Littler *et al*., 2004). This behaviour is analogous to many bacterial pore-forming toxins, annexins and apoptotic proteins (Li *et al*.,

Table 2 Chloride intracellular channel protein family. The chloride intracellular channel (CLIC) protein family comprises a diverse group of anion-selective channels. These proteins are unique among eukaryotic ion channels in that they spontaneously switch between a soluble and membrane-bound conformation

Family Member	Structure	Subcellular Localisation	Chloride Channel Activity
CLIC1[f]	27 kDa monomer comprising a thioredoxin-like N-domain and an all α-helical C-domain; forms dimeric species upon oxidation; comprises a single TMD	Nuclear and plasma membranes, sub-apical vesicles, cytoplasm and nucleoplasm	Poorly selective and lipid-dependent anion channel activity regulated by pH and redox; channel activity is blocked by the inhibitor indanyloxyacetic acid 94 (IAA-94)
CLIC2[g]	28 kDa monomer with a similar canonical fold to CLIC1, interacts with and inhibits the cardiac ryanodine receptor (RyR2) Ca^{2+} channel	Sarcoplasmic reticulum, cytoplasm and nucleoplasm	Displays single-channel conductance at low pH; channel activity is blocked by dithiothreitol (DTT)
CLIC3[h]	24 kDa monomer; the N-domain lacks a significantly hydrophobic region which suggests that channel formation requires oligomerisation	Nuclear and plasma membranes, cytoplasm and nucleoplasm	Forms weakly-active channels at high concentrations
CLIC4[i]	29 kDa in size with a similar canonical fold to CLIC1; may exist as a monomer or hydrogen-bonded homotrimer; comprises a single TMD	Nuclear and plasma membranes, cytoplasm, golgi, endoplasmic reticulum, mitochondria, actin cytoskeleton and secretory vesicles	Lipid-dependent chloride-selective channel activity; chloride transport is attributed to the N-domain and is blocked by IAA-94 and N-terminal antibodies
CLIC5A[j]	28 kDa in size with a similar canonical fold to CLIC1	Cytoplasm and actin cytoskeleton	Forms poorly-selective anion channels; Channel activity is regulated by F-actin and is blocked by IAA-94
CLIC5B/p64[j]	49 kDa in size with 50-60 % sequence identity to CLIC1	Plasma membrane, intracellular membranes and cytoplasm	Shows voltage-dependent Cl^- conductance; channel activity is blocked by IAA-94
CLIC6/parchorin[k]	65 kDa in size with an extended N-terminal hydrophilic domain; the C-terminus is thought to resemble the canonical fold of CLIC1	Plasma membrane and perinuclear cytoplasm	No known channel activity

[f]Valenzuela *et al*., 1997; Valenzuela *et al*., 2000; Ulmasov *et al*., 2007

[g]Heiss and Proutska, 1997; Board *et al*., 2000; Harrop *et al*., 2001; Dulhunty *et al*., 2005

[h]Qian *et al*., 1999; Money *et al*., 2007

[i]Duncan *et al*., 1997; Suginta *et al*., 2001; Singh and Ashley, 2007

[j]Berryman and Bretscher, 2000; Berryman *et al*., 2004

[k]Nishizawa *et al*., 2000; Friedli *et al*., 2003; Griffon *et al*., 2003

1991; Hsu *et al*., 1997; Langen *et al*., 1998) although the structural basis of the soluble-membrane transition is poorly understood. The chloride intracellular channel protein 1 (CLIC1) is the most well-understood CLIC member and is thus a prime target for studies attempting to elucidate the membrane insertion mechanism of the CLICs.

1.3.3 Chloride Intracellular Channel Protein 1 (CLIC1)

CLIC1 is a 241 amino acid protein which shares the canonical fold of the GST superfamily (Figure 5 A). The N-domain contains the transmembrane domain required to span the membrane (see *1.3.3.1*) whilst the C-domain is entirely helical. CLIC1 localises predominantly to nuclear and vesicle membranes (Tonini *et al*., 2000; Valenzuela *et al*., 2000) where it is involved in acidifying compartments along the secretory pathway as well as regulating cell volume and the cell cycle (Valenzuela *et al*., 2000). CLIC1 also indirectly interacts with F-actin, suggesting a role in cell motility and vesicle transport (Singh and Ashley, 2007).

The soluble-membrane conversion of CLIC1 is thought to involve environmentally-induced structural changes which expose the transmembrane domain (Figure 5 A). In particular, pH and oxidation have been implicated in promoting membrane binding and insertion. CLIC1 ion channel formation and activity is maximal at low pH (Tulk *et al*., 2002; Warton *et al*., 2002; Berry and Hobert, 2006). The low pH at membrane interfaces is thought to prime CLIC1 for membrane insertion by lowering the activation energy barrier of transmembrane domain exposure (Manceva *et al*., 2004; Fanucchi *et al*., 2008; Stoychev *et al*., 2009). The conformational dynamics of the regions surrounding the transmembrane domain are significantly increased at low pH (Stoychev *et al*., 2009) and are accompanied by the formation of a molten globule-like intermediate (Fanucchi *et al*., 2008). This collectively promotes membrane binding and may be responsible for the pH dependence seen in CLIC1.

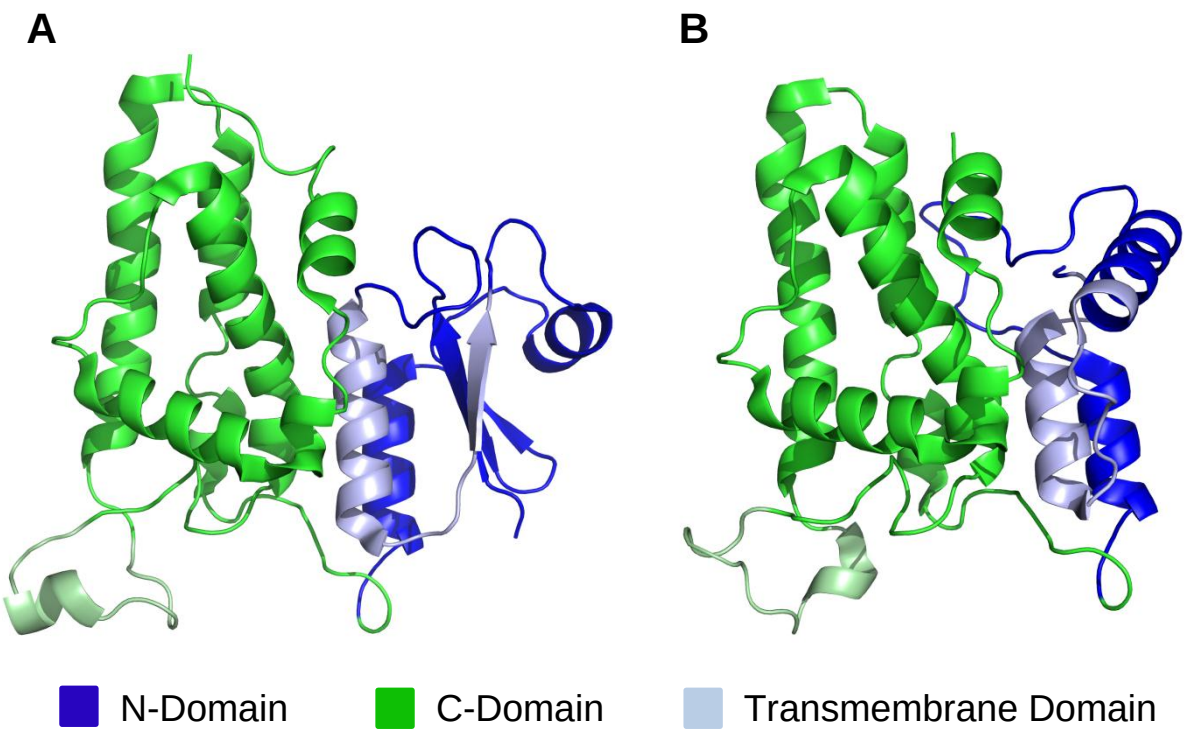

Figure 5 Structure of soluble CLIC1. (A) Reduced CLIC1 (1K0M; Harrop *et al*., 2001) consists of a thioredoxin N-domain (blue; residues 1-90) and all α-helical C-domain (green; 91-241). The transmembrane domain (light blue; 24-46) comprises α-helix 1 and β-sheet 2 of the N-domain. **(B)** Oxidised CLIC1 (1RK4; Littler *et al*., 2005). The mixed α/β thioredoxin motif is replaced by α-helices upon oxidation. The altered conformation is stabilised by an intramolecular disulphide bond between Cys24 and Cys59. Figures were rendered using PyMol V 1.3 (DeLano, 2004)

The presence of several redox-sensitive cysteine residues also implicates oxidation state as an important regulator of CLIC1 structure (Littler *et al*., 2004). Chemically-induced oxidation causes a dramatic structural rearrangement of CLIC1 (Figure 5 B) (Littler *et al*., 2004). Upon oxidation, the thioredoxin fold within the N-domain becomes entirely α-helical. The resulting helix-rich domain forms a flat, hydrophobic surface which enhances membrane insertion (Goodchild *et al*., 2009; Goodchild *et al*., 2010; Goodchild *et al*., 2011).

Both pH and oxidation target the transmembrane domain of CLIC1 and likely ensure that the domain is primed for membrane insertion. As with most membrane-spanning channel proteins, the transmembrane domain is the most functionally relevant region of the protein. As such, much energy is devoted to ensure that the domain is (i) correctly folded and (ii) membrane-insertion competent. Understanding how the transmembrane domain of CLIC1 achieves a membrane-competent form is therefore of utmost importance.

1.3.3.1 The Transmembrane Domain of CLIC1

Sequence comparisons between members of the vertebrate CLIC family have suggested that two putative transmembrane (PTM) regions of sufficient hydrophobicity exist (Cromer *et al*., 2002). The first comprises α-helix 1 and β-strand 2 of the N-domain whilst the second encompasses α-helix 6 of the C-domain (Berryman and Bretscher, 2000). The former was initially thought too stable to readily unfold to yield a membrane-interacting domain, given its evolutionary relationship with the thioredoxin superfamily (Cromer *et al*., 2002). However, mounting evidence suggests that the transmembrane domain lies within the N-domain. Studies using proteinase K digestion (Duncan *et al*., 1997), FLAG epitopes (Tonini *et al*., 2000) and terminal-directed antibodies (Proutski *et al*., 2002) of membrane inserted CLIC1 suggest that the C-domain remains cytoplasmic whilst the N-terminus inserts into the membrane. This evidence coupled with the work of Berry and Hobert (2006) and analyses

using the TMPred algorithm (Hofmann and Stoffel, 1993) and hydrophobicity plots (Figure 6 A) identifies residues 24 to 46 as the likely transmembrane domain of CLIC1. This 23 residue fragment is highly conserved amongst CLIC proteins (Figure 6 B), is of sufficient length to span the lipid bilayer and has a high helical propensity (Muňoz and Serrano, 1997; Lacroix *et al*., 1998). The energy required to transfer the domain from water to octanol (~ 18.8 kcal.mol^{-1}) is within the feasible range for transmembrane domains (Wimley and White, 1996). Fluorescence quenching studies confirm that Trp35 of the N-domain is located within the plasma membrane in the membrane-bound state (Goodchild *et al*., 2009; Goodchild *et al*., 2010).

The CLIC1 transmembrane domain comprises a predominantly apolar sequence flanked by a series of cationic residues. This apolar-cation motif is common for many transmembrane domains and is thought to (i) promote membrane binding by electrostatic attraction (Sakai and Tsukihara, 1998; Mulgrew-Nesbitt *et al*., 2006) and (ii) correctly orient the domain across the membrane (von Heijne and Gavel, 1988). The latter is consistent with the 'positive inside' model of membrane protein insertion (von Heijne and Gavel, 1988), whereby solvent-exposed lysine and arginine residues populate the *trans*-face of membranes. A lysine residue (Lys37) is present in the centre of the domain and would theoretically lie deep within the hydrophobic core of the lipid bilayer. The membrane partitioning of this charged residue would be energetically costly. To compensate for this, Lys37 likely forms a series of interactions with surrounding residues within the membrane. The transmembrane domain also contains a lone tryptophan fluorescent probe (Trp35) as well as a conserved cysteine (Cys24). A disulfide bond between Cys24 and Cys59 stabilises the alternative conformation of oxidised CLIC1 (Figure 5 B). This bond must be broken in order for the transmembrane domain to cross the membrane (Singh and Ashley, 2006), suggesting that membrane insertion is unlikely to be dependent on oxidation state.

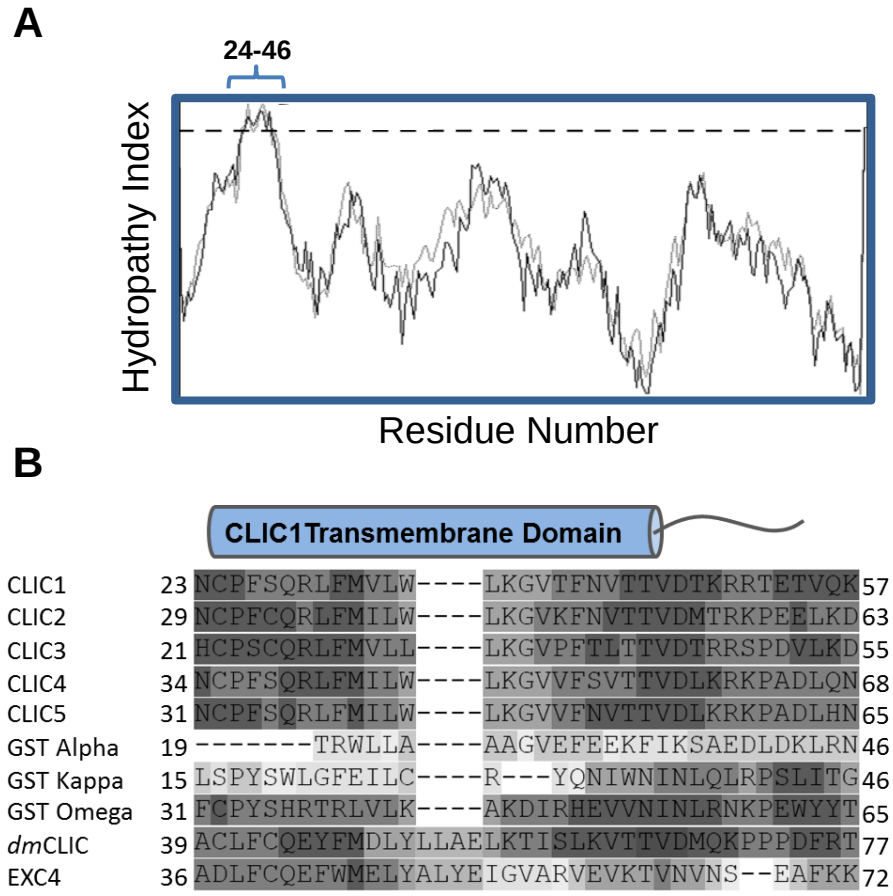

Figure 6 The transmembrane domain of CLIC1. (A) Kyte-Doolittle hydropathy plot. A region of sufficient hydrophobicity was identified and comprises residues 24-46 of the N-domain of CLIC1. The dashed line indicates a threshold hydropathy value. **(B)** A sequence alignment of this region shows that it is highly conserved amongst the vertebrate CLICs and shows considerable conservation amongst the GSTs and invertebrate CLIC homologs

The region comprising the transmembrane domain is conserved across all CLICs and has been implicated in membrane binding of CLIC1 (Singh and Ashley, 2007), CLIC4 (Singh and Ashley, 2007) and the invertebrate CLIC homolog EXC-4 (Berry and Hobert, 2003). A comparison of the equivalent transmembrane domains of the CLICs of known structure reveals a highly conserved structural element (Figure 7). All of the identified transmembrane domains share a αβ motif and are surrounded by structurally similar environments. This may suggest a common insertion mechanism but more importantly highlights the role of the transmembrane domain as the key element in membrane insertion.

1.3.4 Membrane Insertion Mechanism of the CLIC1 Transmembrane Domain

Initial similarities between CLIC proteins and bacterial pore-forming toxins led to the idea that they may share a similar membrane insertion mechanism (Tulk *et al*., 2002). Both α-PFTs and CLIC1 show pH-induced structural destabilisation which enables the former to partially unfold and expose a transmembrane helix. Insufficient data exists to show that CLICs also follow this mechanism, although aspects of the mechanism such as electrostatic and hydrophobic interactions are likely to be present.

The transmembrane domain of CLIC1 remains the focus of understanding how CLICs associate with and insert into membranes. Currently, it is believed that a large structural rearrangement is required in order to expose the transmembrane domain for insertion into the membrane. This event is presumably triggered by low pH, oxidation and/or the polarity of the membrane interface (Fanucchi *et al*., 2008; Stoychev *et al*., 2009). Such an event is likely to be mediated by electrostatic attraction between the transmembrane domain and the membrane interface as well as non-covalent interactions between the transmembrane domain and lipid moieties. Understanding how the transmembrane domain facilitates membrane insertion at the molecular level as well as how the domain responds to a membrane environment will prove

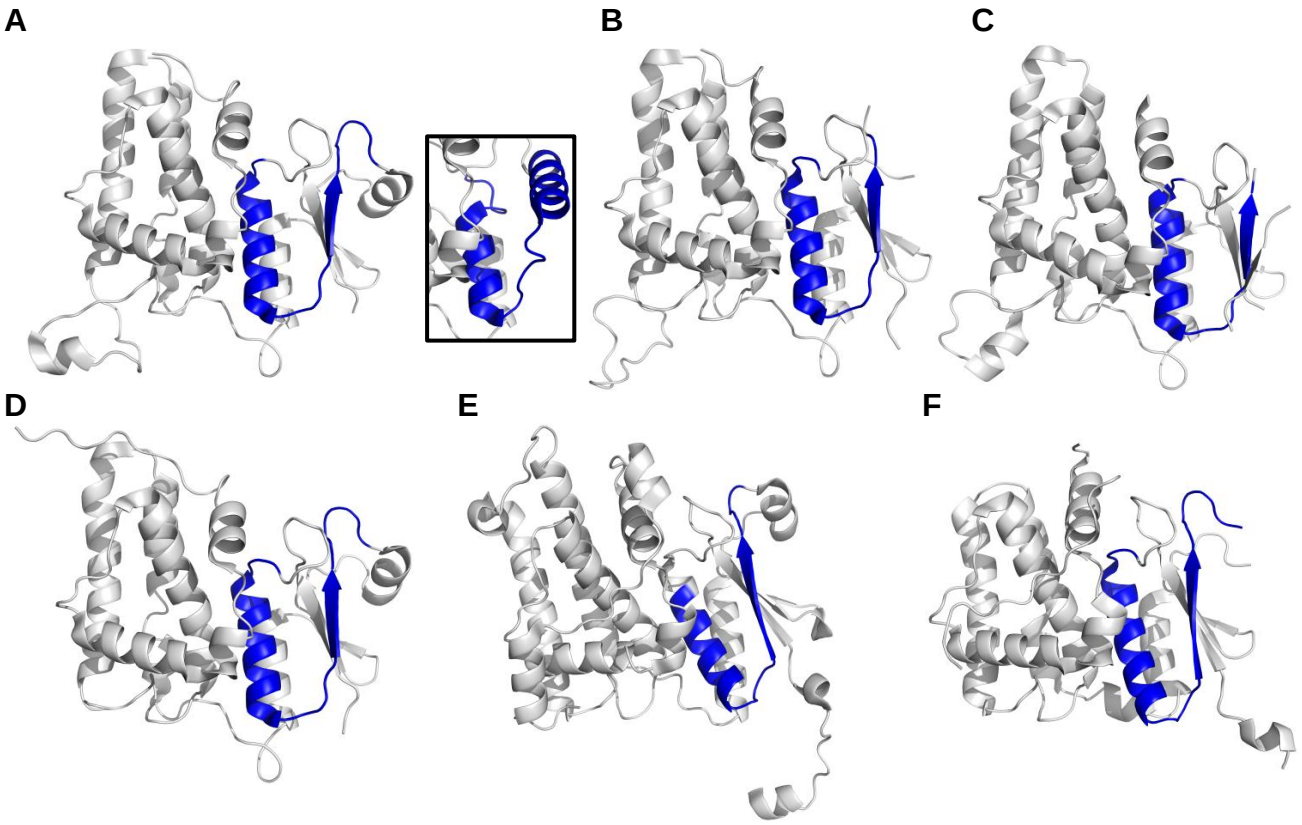

Figure 7 Transmembrane domains of human CLIC proteins and their invertebrate homologs. The putative transmembrane domains of CLIC and CLIC-like proteins of known structure are shown (blue). These regions were identified based on sequence alignments relative to CLIC1. The transmembrane domains of these proteins share both sequence and structure conservation, with a αβ motif being prevalent in all the proteins. The oxidised form of CLIC1 is the only exception where the transmembrane domain is entirely α-helical. **(A)** Reduced CLIC1, 1K0M (inset- oxidised CLIC1, 1RK4). **(B)** CLIC2, 2R4V. **(C)** CLIC3, 3FY7. **(D)** CLIC4, 2AHE. **(E)** *Drosophila melanogaster* CLIC, 2YV7. **(F)** *Caenorhabditis elegans* Exc-4, 2YV9

vital in understanding how CLICs are able to spontaneously convert between soluble and membrane-bound states.

1.4 Aim and Objectives

Despite the physiological importance of CLIC proteins, the mechanisms by which they spontaneously convert from a soluble to a membrane-bound form remain unknown. This is further hampered by the lack of structural data for the membrane-bound state. Elucidating the details of this conversion will largely lie in understanding the behaviour of the transmembrane domain as it partitions between an aqueous and membrane environment. The aim of this study was to contribute to a molecular understanding of amphitropism in CLIC1 by (i) assessing the membrane-induced structural plasticity of the transmembrane domain and (ii) probing specific molecular interactions within the transmembrane domain that are responsible for membrane binding and insertion.

The individual objectives of this research were as follows:

1. Design and synthesise a peptide comprising the transmembrane domain of CLIC1
2. Develop a model membrane system that can be used for the structural and functional characterisation of the CLIC1 transmembrane domain
3. Establish changes in the structure and stability of the CLIC1 transmembrane domain during membrane interaction using spectroscopic techniques
4. Evaluate membrane binding and channel activity of the CLIC1 transmembrane domain using equilibrium and kinetic methods
5. Identify structural determinants of membrane binding/insertion using site-specific mutagenesis

Chapter 2

Membrane mimetics induce helix formation and oligomerisation of the chloride intracellular channel protein 1 transmembrane domain

Peter, B., Ngubane, N. C., Fanucchi, S. and Dirr, H. W.
Biochemistry, **52(16):** 2739-49

In this publication, membrane-induced secondary, tertiary and quaternary structural changes of the CLIC1 transmembrane domain were identified. The transmembrane domain is thus able to independently direct folding, membrane insertion and self-association in the absence of the N- and C-domains.

Author contributions: Bradley Peter performed all experimental work, analysed the data and wrote the manuscript. Nomxolisi Ngubane performed initial solubility trials for the TMD peptide. Sylvia Fanucchi and Heini W. Dirr supervised the project and assisted in data analysis and interpretation.

BIOCHEMISTRY
including biophysical chemistry & molecular biology

Article

pubs.acs.org/biochemistry

Membrane Mimetics Induce Helix Formation and Oligomerization of the Chloride Intracellular Channel Protein 1 Transmembrane Domain

Bradley Peter, Nomxolisi Chloë Mina-Liz Ngubane, Sylvia Fanucchi, and Heini W. Dirr*

Protein Structure-Function Research Unit, School of Molecular and Cell Biology, University of the Witwatersrand, Johannesburg 2050, South Africa

Supporting Information

ABSTRACT: Chloride intracellular channel protein 1 (CLIC1) is a dual-state protein that can exist either as a soluble monomer or in an integral membrane form. The transmembrane domain (TMD), implicated in membrane penetration and pore formation, comprises helix α1 and strand β2 of the N-domain of soluble CLIC1. The mechanism by which the TMD binds, inserts, and oligomerizes in membranes to form a functional chloride channel is unknown. Here we report the secondary, tertiary, and quaternary structural changes of the CLIC1 TMD as it partitions between an aqueous and membrane-mimicking environment. A synthetic 30-mer peptide comprising the TMD was examined in 2,2,2-trifluoroethanol, sodium dodecyl sulfate (SDS) micelles, and 1-palmitoyl-2-oleoyl-*sn*-glycero-3-phosphocholine (POPC) liposomes using far-ultraviolet circular dichroism and fluorescence spectroscopy. Data obtained in the presence of SDS micelles and POPC liposomes show that Trp35 and Cys24 have reduced solvent accessibility, indicating that the peptide adopts an inserted orientation. The peptide assumes a helical structure in the presence of these mimetics, consistent with its predicted membrane conformation. This acquisition of secondary structure is concentration-dependent, suggesting an oligomerization event. Stable dimeric and trimeric species were subsequently identified using SDS−polyacrylamide gel electrophoresis. We propose that, in the vicinity of membranes, the mixed α/β TMD in CLIC1 rearranges to form a helix that then likely dimerizes via noncovalent helix−helix interactions to form a membrane-competent protopore complex. Such oligomerization would be essential for forming a functional ion channel, given that each CLIC1 monomer possesses only a single TMD. This work highlights the central role of the TMD in CLIC1 function: It is capable of promoting membrane insertion and dimerization in the absence of the C-domain and large portions of the N-domain.

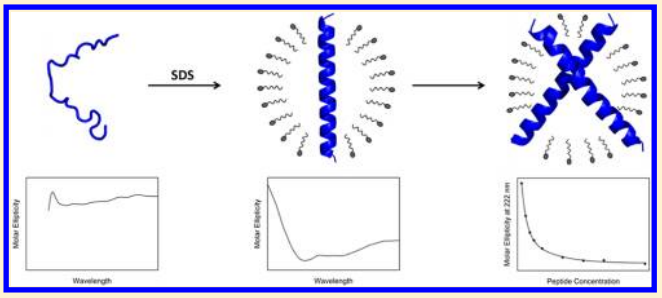

Membrane proteins play key physiological roles, accounting for nearly one-quarter of eukaryotic proteins and constituting approximately 50% of all current drug targets.[1] Despite their importance, the mechanisms by which membrane proteins bind and insert into membranes remain elusive. The two-state folding model proposed by Popot and Engelman[2] and the modified two-state model of White and Wimley[3] have been used to explain these interactions. Proteins capable of adopting multiple stable native states present an intriguing variation to these schemes. These proteins undergo large-scale structural rearrangements upon association with the lipid bilayer, resulting in the spontaneous conversion from a water-soluble to a membrane-bound form.[4] Structural metamorphism is a widely observed phenomenon and occurs in many bacterial pore-forming toxins,[5,6] apoptotic proteins,[7] and the eukaryotic chloride intracellular channel (CLIC) protein family.[8]

In their reduced monomeric state, the CLIC proteins adopt a topology similar to that of the GST superfamily, with a thioredoxin N-domain and an all-α-helical C-domain (Figure 1).[9] CLICs are unique among all eukaryotic ion channels in that they are dimorphic and can exist in either a soluble or membrane-bound form.[9] Unlike typical ion channels, most CLIC proteins lack a signal sequence and remain in the cytoplasm, spontaneously inserting into membranes under certain environmental conditions.[8,10] The structural basis of the soluble−membrane transition of CLIC1 is poorly understood but is thought to involve the exposure of putative transmembrane (PTM) domains.

Sequence comparisons between members of the vertebrate CLIC family identify two PTM regions of sufficient hydrophobicity.[11] The first comprises α-helix 1 and β-strand 2 of the N-domain (Figure 1A), while the second encompasses α-helix 6 of the C-domain.[12] The former was initially thought to be too stable to readily unfold to yield a membrane-interacting domain, given its evolutionary relationship with the thioredoxin superfamily.[11] However, studies using proteinase K digestion,[13] FLAG epitopes,[14] and terminally directed antibodies[15] of membrane-inserted CLIC1 showed that the C-domain remains cytoplasmic while the N-terminus inserts into the membrane with Cys24 localized at the trans face of the membrane.

Received: March 5, 2013
Revised: April 2, 2013
Published: April 2, 2013

   dx.doi.org/10.1021/bi4002776 | *Biochemistry* 2013, 52, 2739−2749

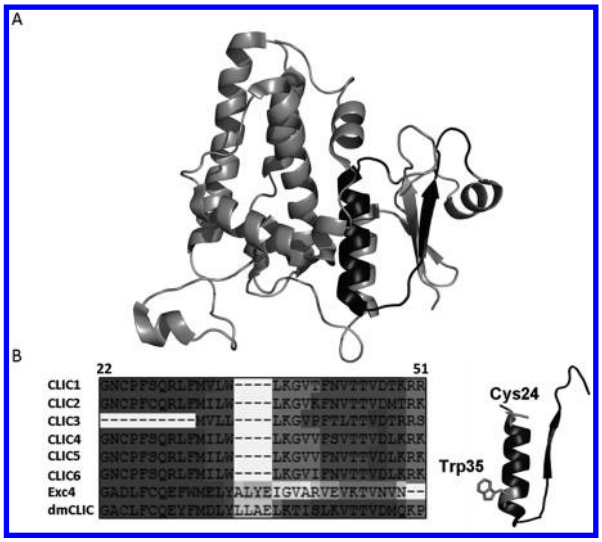

Figure 1. Structure and sequence conservation of the CLIC1 TMD. (A) The CLIC1 TMD (black) comprises residues 24−46, which include most of helix α1 and strand β2 of the N-domain. (B) This region, pictured, shows strong sequence conservation across the vertebrate CLICs as well as the invertebrate homologues Exc4 (*Caenorhabditis elegans*) and dmCLIC (*Drosophila melanogaster*).

On the basis of this evidence, coupled with results from hydrophobicity plots and the TMPred algorithm, Berry and Hobert[16] proposed that the CLIC1 transmembrane domain (TMD) was a 23-residue fragment comprising residues 24−46, a region that is highly conserved among CLIC proteins (Figure 1B). Recent studies by Goodchild et al.[17] used fluorescence quenching to confirm that Trp35 of the N-domain is indeed located within the plasma membrane in the membrane-bound state. The proposed CLIC1 TMD is of sufficient length to span the membrane and contains many conserved features characteristic of transmembrane domains,[18−20] including a central span of predominantly apolar residues and charged residues at the membrane interface. Although the structure of the membrane-bound form of CLIC1 is yet to be determined, the transmembrane segment is predicted to be helical,[8,21,22] with the AGADIR algorithm showing that this region has a high helical propensity.[22]

For the TMD to be exposed to the membrane, a large structural rearrangement of the CLIC1 N-domain is required. It has been proposed that the β1α1β2 motif detaches from the rest of the protein and refolds into the transmembrane conformation. This is presumably triggered by (i) lowered stability[22] and enhanced flexibility[23] at low pH, (ii) oxidation,[8,17] or (iii) the polarity of the membrane interface. This, however, remains speculative in the absence of structural data.

To improve our understanding of how CLIC1 refolds and inserts into membranes, we need to understand how the structure of the functionally relevant TMD behaves in a membrane environment. In this study, we examined the secondary, tertiary, and quaternary structural changes of the CLIC1 TMD as it partitions between an aqueous and membrane-mimicking environment. Our results show that the TMD undergoes structural modifications in a micellar environment, including the acquisition of helical secondary structure and dimerization. Fluorescence quenching of Trp35 shows that the acquisition of secondary structure correlates with the insertion of the peptide into SDS micelles and POPC liposomes, although whether these processes occur sequentially or in parallel is yet to be determined. This work shows that the TMD alone is sufficient to promote membrane insertion in the absence of a signal peptide, the C-domain, and the remainder of the N-domain. Similarly, the TMD is capable of forming stable, noncovalent dimers in the absence of the N- and C-domains.

MATERIALS AND METHODS

Peptide Design and Synthesis. The 30-residue CLIC1 TMD peptide (GNCPFSQRLFMVLWLKGVTFNVTTVDT-KRR) containing a carboxylated amino terminus and an amidated carboxyl terminus was synthesized using a solid phase continuous flow system by GL Biochem (Shanghai, China). Its purity was determined to be >95% using high-performance liquid chromatography.

Sample Preparation. For conformational studies, the hydrophobic peptide was solubilized in 100% (v/v) methanol to yield a 1 mM stock solution. For SDS work, the peptide was incorporated into SDS micelles as previously described.[24] Briefly, the peptide was added to 20 mM sodium phosphate buffer containing 15 mM SDS to yield a final peptide concentration of 5−50 μM. Samples were then vortexed, freeze-dried, and rehydrated in 20 mM sodium phosphate buffer containing 1 mM DTT (pH 5.5). The final SDS concentration was 15 mM. For TFE work, samples of the peptide in TFE were prepared by mixing the stock solution with TFE (Sigma-Aldrich) to a final TFE concentration of 40% (v/v). These samples were thoroughly mixed for 5 min and allowed to incubate at 20 °C for 1 h.

For liposome studies, the peptide was dissolved in chloroform containing 20 mg/mL POPC (Avanti Polar Lipids, Alabaster, AL). The sample was then incubated for 1 h and dried under a stream of N_2(g). The lipid film was resuspended in ddH_2O, frozen, and lyophilized overnight. The final peptide-containing liposomes were reconstituted in 20 mM sodium phosphate and 1 mM DTT (pH 5.5) to a final peptide:lipid concentration ratio of 20 μM:2.5 mM, followed by five cycles of freezing and thawing. The suspension was extruded through 100 nm polycarbonate membranes and clarified by centrifugation to remove any residual large liposomes. Samples were kept on ice for no more than 24 h prior to use.

CD Spectroscopy. Far-UV (far-ultraviolet) CD spectra were recorded in a 2 mm cuvette using a Jasco J-810 spectropolarimeter (Jasco, Tokyo, Japan) at 20 °C and are an average of four scans, using a scan speed of 50 nm/min. A 1 nm bandwidth and a 0.1 nm data pitch were used, with a response time of 1 s. The peptide concentration was 10 μM for standard spectra and between 2 and 30 μM for concentration dependence studies in TFE and SDS. Spectra were buffer corrected, smoothed using the negative exponential method, and normalized to mean residue ellipticity ($[\theta]$) using the equation

$$[\theta] = (100\theta)/(cnl)$$

where $[\theta]$ is the molar ellipticity (degrees square centimeter per decimole), θ is ellipticity (millidegrees), c is the protein concentration (millimolar), n is the number of residues in the peptide, and l is the path length (centimeters). For all far-UV CD analyses, n = 30 and l = 0.2 cm.

A quantitative estimation of the secondary structural content of the TMD peptide was made using CDPro,[25] which compares the peptide's CD spectra with those of known protein structures. A 43-protein reference set (SP43) with a wavelength

dx.doi.org/10.1021/bi4002776 | *Biochemistry* 2013, 52, 2739−2749

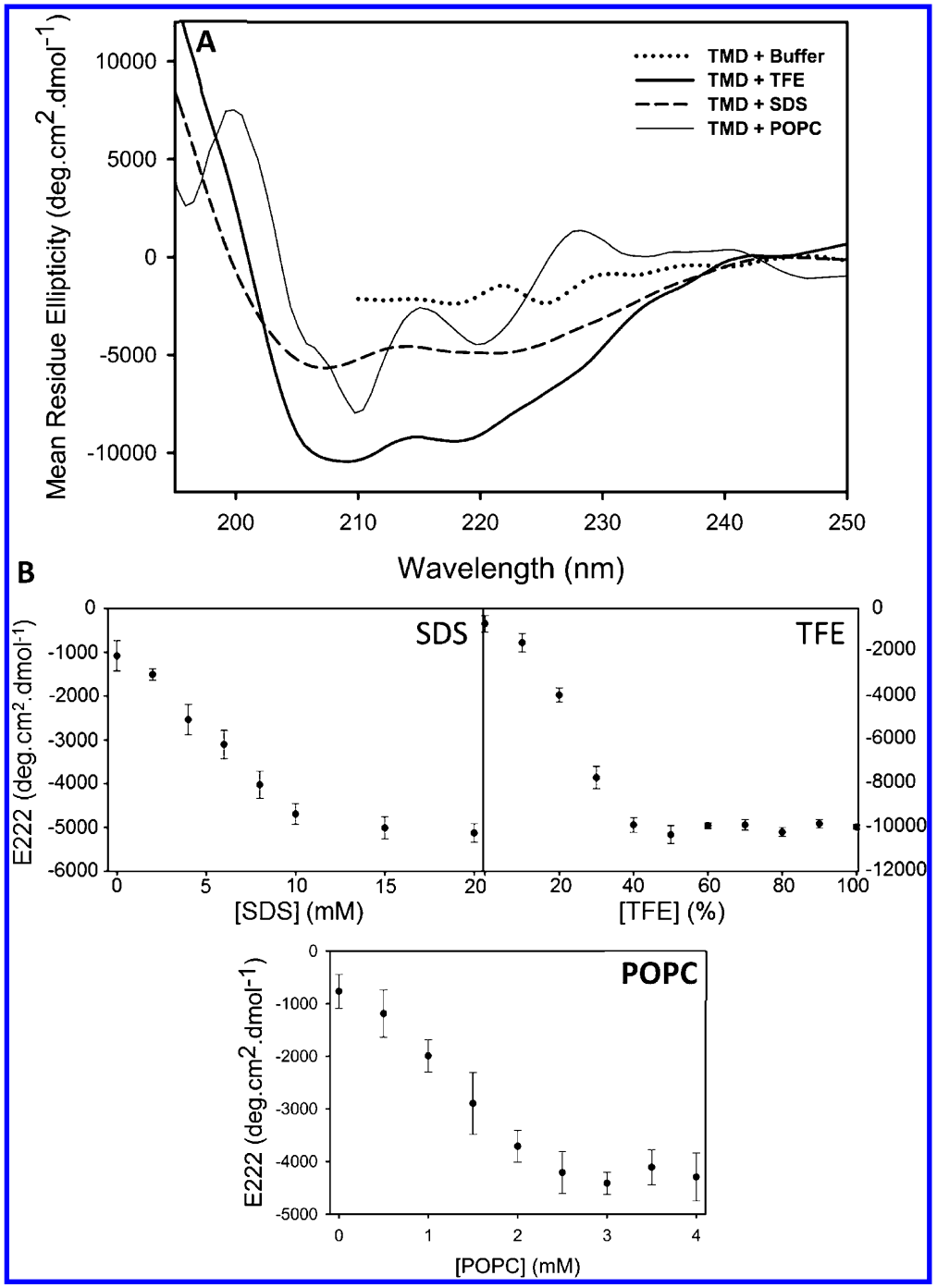

Figure 2. Membrane mimetics induce the α-helical secondary structure of the CLIC1 TMD peptide. (A) Far-UV CD spectra were recorded in buffer (dotted), 40% (v/v) TFE (thick solid), 15 mM SDS micelles (dashed), and 2.5 mM POPC (thin solid). In solution, the peptide is unstructured. Upon addition of TFE, SDS, and POPC, the peptide assumes an α-helical secondary structure. (B) The helical content of 15 μM peptide is maximal at 40% (v/v) TFE, 16 mM SDS, and 2.5 mM POPC, after which no further increase in helicity is observed. The buffer consisted of 20 mM sodium phosphate, 1 mM DTT, and 0.2% (w/v) NaN_3 (pH 5.5).

range of 190−240 nm was used.[26] The standard error of the secondary structural elements was determined from three separate CDPro analyses.

Fluorescence Spectroscopy. Fluorescence emission spectra were recorded between 300 and 450 nm using a Perkin-Elmer LS50B luminescence spectrometer (Perkin-Elmer, Waltham, MA) at 20 °C and are an average of three accumulations, using a scan speed of 250 nm/min and 7.5 nm slit widths. An excitation wavelength of 295 nm was used. Samples were analyzed in 20 mM sodium phosphate and 1 mM DTT (pH 5.5). Spectra were buffer corrected and smoothed using the negative exponential method. The peptide concentration was 10 μM for standard spectra and between 2 and 30 μM for concentration dependence studies in TFE and SDS. To analyze the effect of oxidation, 10 μM peptide was incubated with 2 mM H_2O_2 for 0−24 h and analyzed as described above.

For quenching studies, the TMD peptide was diluted to 15 μM in 0 to 0.4 M acrylamide or sodium iodide (prepared at pH 5.5 with 20 mM sodium phosphate buffer and 1 mM DTT) in the absence and presence of 15 mM SDS or 2.5 mM POPC.

dx.doi.org/10.1021/bi4002776 | *Biochemistry* 2013, 52, 2739−2749

Iodide quenching samples were supplemented with 0.4 to 0 M NaCl to maintain a constant ionic strength. The fluorescence intensity at 345 nm was monitored and analyzed according to the Stern−Volmer relationship:

$$F_0/F = 1 + K_{SV}[Q]$$

where F_0 and F are the emission intensities in the absence and presence of quencher, respectively, [Q] is the concentration of quencher, and K_{SV} is the Stern−Volmer constant. This constant reflects residue accessibility, with low values indicating residues with low levels of exposure and vice versa.[27]

DTNB Assay. DTNB [5,5′-dithio(2-nitrobenzoic acid)] is a water-soluble compound used to quantify free thiol (-SH) groups in solution based on their solvent accessibility. The CLIC1 TMD contains a single cysteine residue at position 24. A 20 mM DTNB stock was made in methanol and diluted to a working concentration of 0.2 mM in DTNB buffer [20 mM sodium phosphate and 1 mM EDTA (pH 7.0)] containing 10 μM peptide in the absence and presence of 15 mM SDS. In the case of liposome samples, two versions of the DTNB assay were performed: (i) as described above with extrinsic DTNB added to samples and (ii) using DTNB encapsulated within the liposomes. The latter was achieved by including DTNB (final concentration of 0.2 mM) in the reconstitution buffer during liposome preparation (see Sample Preparation). Free DTNB was removed by size-exclusion chromatography on a Sephadex G-25 column equilibrated with DTNB buffer. The aim of these two methods was to probe whether Cys24 is located at the cis or trans face of the membrane mimetic. The concentration of 2-nitro-5-thiobenzoic acid (NTB) was determined spectrophotometrically at 412 nm using an extinction coefficient of 13600 M^{-1} cm^{-1}.[28] The proportion of free thiols was obtained from the ratio of NTB concentration to peptide concentration.

Size-Exclusion Chromatography. Association of the peptide with SDS micelles was probed using size-exclusion chromatography, on the basis that SDS-bound peptide will elute in the void volume while unbound peptide will be retarded. Triplicate samples of 15 μM peptide with 15 mM SDS were loaded onto a Sephadex G-25 column (Amersham Biosciences) pre-equilibrated with buffer [20 mM sodium phosphate and 1 mM DTT (pH 5.5)]. Samples containing only 15 mM SDS or 15 μM NATA were used as controls for the void volume and total column volume, respectively. Oxidized samples were obtained by incubating 15 μM peptide with 2 mM H_2O_2 and 15 mM SDS for 4 h prior to loading. The elution profiles were corrected for scatter by SDS by running identical samples without peptide and subtracting the two elution profiles. The amount of peptide in each peak was subsequently estimated using the Beer−Lambert law:

$$A = \varepsilon_\lambda cl$$

where A is the absorbance at 280 nm, ε_λ is the molar extinction coefficient at wavelength λ, c is the concentration of the absorbing solution, and l is the path length of light through the cuvette. For this analysis, ε_λ is 5550 M^{-1} at 280 nm and l is 5 mm. The relative percentages of each peak were calculated by dividing the observed peptide concentration by the total peptide concentration. An identical experiment was performed using 2.5 mM POPC liposomes instead of SDS. Peptide bound to the liposomes was detected using a standard Bradford assay. The assay was corrected for scatter contribution by the liposomes using an identical sample in the absence of the TMD peptide.

Tricine Sodium Dodecyl Sulfate−Polyacrylamide Gel Electrophoresis (SDS−PAGE). The potential oligomeric state of the TMD peptide in SDS micelles was investigated by gel electrophoresis. A modified Tricine buffer system[29] with a 0.5% SDS gel was used. The peptide (5, 25, or 50 μM) was incubated in 20 mM sodium phosphate buffer at pH 7 or 5.5 in the presence of 15 mM SDS as described. A dimer control was included by incubating samples with 2 mM H_2O_2 in the absence of β-mercaptoethanol, thereby inducing the formation of a Cys24−Cys24 disulfide bond between the two peptides. The samples were boiled for 5 min before being loaded onto a 16% polyacrylamide gel. The gels were run and stained according to the method of Schägger and von Jagow.[29] Silver staining was performed using the SilverQuest kit (Life Technologies, Carlsbad, CA), according to the manufacturer's instructions. The peptide was sized using a Spectra multicolor low-range molecular marker (Fermentas, Glen Burnie, MD).

RESULTS

Secondary Structure Content. The far-UV CD spectra of the TMD peptide in aqueous buffer, TFE, SDS micelles, and POPC liposomes are shown in Figure 2. In solution, the peptide is relatively unstructured. Upon addition of TFE, SDS micelles, or POPC liposomes, the CD spectra exhibit two minima near 208 and 222 nm, which is characteristic of a predominantly α-helical conformation. POPC spectra displayed an additional maximum at ∼228 nm that can be attributed to aromatic side chains adopting an ordered conformation.[26] The molar ellipticity of the TMD peptide in TFE is substantially higher than that in either SDS micelles or POPC liposomes. This suggests that a greater proportion of peptide assumes an α-helical conformation under these conditions compared to a micellar/vesicle environment. Quantitative analysis using CDPro shows that the α-helical content increases substantially, from 18% (±5%) in buffer to 64% (±8%) in TFE, 59% (±10%) in SDS, and 56% (±9%) in POPC. In contrast, the amount of β-structures in buffer (23 ± 4%) was reduced 4-fold following the addition of TFE (9 ± 2%), SDS (7 ± 3%) and POPC (11 ± 6%). The amount of unordered structure decreased similarly, with less than 22% (±9%), 29% (±7%), and 31% (±11%) present in TFE-, SDS-, and POPC-containing samples, respectively. The α-helical content increased with increasing TFE and SDS concentrations, reaching a maximum at 40% (v/v) TFE or 16 mM SDS (Figure 2B). The NRMSD values for the analysis were 0.095 (TFE), 0.11 (SDS), and 0.17 (POPC). The thermal stability of the peptide was also analyzed by measuring the CD spectra in 40% TFE or 15 mM SDS at increasing temperature (Figure S1 of the Supporting Information). The unfolding was shown to be fully reversible but yielded a linear loss of ellipticity rather than a defined unfolding transition. The sequential, rather than simultaneous, disruption of amide hydrogen bonds resulting in this behavior is characteristic of transmembrane helices[30] and indicates unfolding reactions that are local and transient.

Tertiary Structure. The TMD peptide contains a lone tryptophan residue at position 35 that can be used as a reporter of local tertiary structural changes. In solution, the peptide exhibits a fluorescence emission spectrum typical of a solvent-exposed tryptophan with a moderately low emission intensity and an emission maximum wavelength (λ_{max}) of 355 nm (Figure 3). In the presence of TFE, the emission intensity was reduced by ∼25% without altering the λ_{max}, suggesting that the TFE-induced acquisition of secondary structure is not

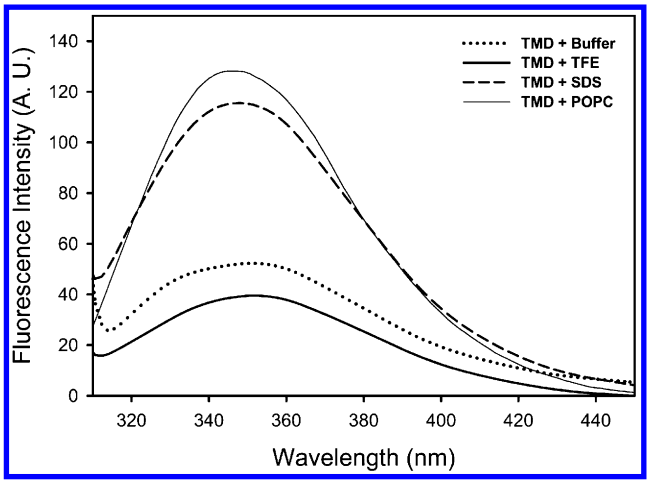

Figure 3. Tertiary structure of the CLIC1 TMD peptide. Tryptophan fluorescence emission spectra were recorded in buffer (dotted), 40% (v/v) TFE (thick solid), 15 mM SDS micelles (dashed), and 2.5 mM POPC (thin solid). In solution and in TFE, the peptide emits maximally at 355 nm whereas SDS and POPC induce both a blue-shifted λ_{max} (343 nm) and a 3-fold increase in emission intensity. This indicates that Trp35 becomes located in a hydrophobic environment, presumably inserted into the SDS micelles or POPC liposomes. The buffer consisted of 20 mM sodium phosphate, 1 mM DTT, and 0.2% (w/v) NaN_3 (pH 5.5).

accompanied by tertiary packing interactions. SDS and POPC, however, induced both a blue-shifted λ_{max} (343 nm) and a 3-fold increase in emission intensity. This indicates that, in the presence of SDS or POPC, Trp35 of the TMD peptide is located in a hydrophobic environment, presumably inserted into the SDS micelles or POPC liposomes. The local environment of Trp35 may also, however, be influenced by quaternary interactions in addition to interaction with the SDS micelles or POPC liposomes, particularly if Trp35 is located at or near an oligomer interface.

Under oxidizing conditions, the emission spectra of Trp35 respond in a manner that correlates well with the proposed solvent accessibility of the peptide in the various membrane mimetics (Figure 4). Oxidation of the indole ring to oxyindole quenches Trp35 fluorescence on the basis of solvent accessibility over time, with little to no quenching observed in SDS, minimal quenching in POPC (~5−10%) and TFE (~15%), and substantial quenching in solution (~50%) over 24 h. This likely reflects the nature of the mimetic, with the peptide being inserted into the POPC liposomes or SDS micelles and partially shielded by the TFE. This correlates well with the blue-shifted λ_{max} in POPC liposomes and SDS micelles and acts as confirmation of insertion. The observed reduction in Trp35 fluorescence in POPC at increasing H_2O_2 concentrations is likely a result of a small population of free peptide, with no change in fluorescence reduction observed over time.

Solvent Accessibility of Trp35 and Cys24 in POPC Liposomes and SDS Micelles. The association of the TMD peptide with the SDS micelles was probed using size-exclusion chromatography. The underlying basis was that micelle-associated peptide would elute in the void volume while free peptide would be retarded by the resin (Figure 5A). Approximately 66% of the total peptide eluted with the SDS micelles (Figure 5B), suggesting that a large population of the peptide interacts with the mimetic. The reduced monomer and oxidized dimer forms of the TMD were also identified in the absence of SDS (Figure 5C). The peptide was also shown to interact with POPC liposomes (Figure 5D), with most of the peptide coeluting with the liposomes. The total amount of peptide detected using the Bradford assay in the presence of POPC is comparable to that in the absence of the mimetic (Figure S3 of the Supporting Information). To determine whether the interaction between the TMD peptide and SDS micelles or POPC liposomes involves peripheral association or insertion, dynamic fluorescence quenching with acrylamide or iodide and a DTNB assay were conducted. Both acrylamide and iodide were chosen as complementary probes because of the ability of acrylamide to partially penetrate the interior of SDS micelles,[27] while iodide is excluded on the basis of its charge. Panels A and B of Figure 6 as well as Figure S4 of the Supporting Information show the Stern−Volmer constants (K_{SV}) obtained using acrylamide and iodide, respectively. This constant reflects residue accessibility, with low values indicating residues with low levels of exposure and vice versa.[27] In the absence of SDS micelles, both acrylamide (K_{SV} = 15.35 M^{-1}) and iodide (K_{SV} = 3.52 M^{-1}) quenching yield Stern−Volmer constants that are comparable to the values for free NATA in solution (16.15 and 3.88 M^{-1}, respectively). Upon addition of SDS micelles, a 3-fold reduction in solvent accessibility occurs, clearly indicating that Trp35 is protected from quenching by the micelles. Acrylamide quenching in the presence of POPC liposomes shows a similar reduction in K_{SV} values (15.35 and 7.01 M^{-1} in the absence and presence of POPC, respectively) (Figure 6A). A similar trend was observed using the DTNB assay, with an ~40% reduction in the fraction of free thiols following the addition of SDS micelles (Figure 6C). This suggests that Trp35 and Cys24 are fully and partially solvent excluded in the presence of SDS micelles, respectively (Figure S5 of the Supporting Information). A dual DTNB assay was employed in the case of POPC liposomes, whereby samples contained either extrinsic DTNB or DTNB encapsulated within the liposomes. The purpose of these two methods was to probe whether Cys24 was located at the cis (outer) or trans (inner) face of the liposomes. The data shown in Figure 6D suggest that a large proportion (~65%) of Cys24 reacts with the encapsulated DTNB reagent, whereas only 30−35% of the residues react with extrinsic DTNB. These combined values correlate with the total reactivity of the peptide in buffer (~100%).

Concentration Dependence of Secondary Structure. The concentration-dependent acquisition of secondary structure was also probed in an attempt to identify any oligomerization events. The normalized E_{222} values from peptide samples incubated in TFE showed little change over a wide range of peptide concentrations (Figure 7A). In the presence of SDS micelles, however, a 2-fold increase in molar ellipticity was observed (Figure 7A). This may be due to either the increased helical content or a positive shift in the population of peptides assuming helical structure. These data suggest that the TMD peptide associates in a concentration-dependent manner and forms the basis for subsequent investigations of its oligomeric state.

Oligomerization of the CLIC1 TMD in SDS Micelles. On the basis of the observed concentration-dependent secondary structure of the peptide, Tricine SDS−PAGE was conducted to identify potential oligomeric species in the presence of detergent micelles. The use of SDS−PAGE to monitor transmembrane domain association has been well-

dx.doi.org/10.1021/bi4002776 | Biochemistry 2013, 52, 2739−2749

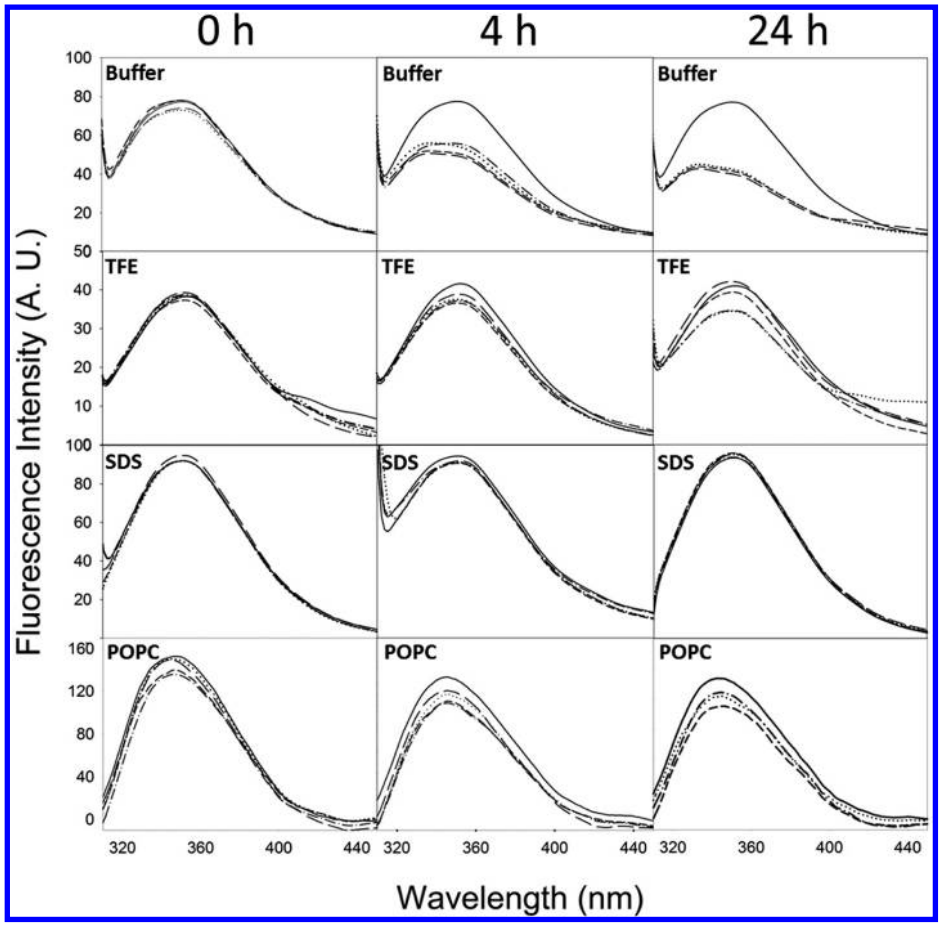

Figure 4. Oxidation quenches the fluorescence of Trp35 on the basis of solvent exposure. Samples were analyzed by fluorescence following the addition of 0 (solid), 0.5 (dash dotted), 1 (medium dash), 1.5 (short dash), or 2 mM H_2O_2 (dotted) in buffer only (top panels), 40% (v/v) TFE (top middle panels), 15 mM SDS micelles (bottom middle panels), or 2.5 mM POPC (bottom panels). Oxidation appears to quench Trp35 fluorescence on the basis of solvent accessibility over time, with no quenching observed in POPC or SDS, minimal quenching in TFE (~15%), and substantial quenching in solution (~50%) over 24 h. The buffer consisted of 20 mM sodium phosphate, 1 mM DTT, and 0.2% (w/v) NaN_3 (pH 5.5).

documented.[31,32] The data shown in Figure 7C show two bands of ~6.9 and ~10.2 kDa across all peptide concentrations tested. These are consistent with a homodimer and homotrimer of the ~3.4 kDa TMD peptide, respectively. Comparison with the disulfide-linked oxidized control sample confirms that the band at 6.9 kDa represents a stable dimeric species. At least 90% of the control peptide was shown to form a disulfide-linked dimer (Figure S2 of the Supporting Information). The absence of a band at 3.4 kDa suggests that the majority of the peptide exists as a dimer/trimer under the conditions tested. Smearing of the peptide band was evident at high peptide concentrations in the absence of aggregation, which suggests an equilibrium between the dimer and higher-order oligomers.[33,34] This is consistent both with the concentration-dependent CD signal and with the blue-shifted fluorescence at high peptide concentrations (Figure 7B). Interestingly, the migration patterns were independent of pH, denaturation, and reducing conditions. This agrees well with the reversible thermal denaturation (Figure S1 of the Supporting Information) and suggests that the helix–helix interactions between TMD peptides are noncovalent.

DISCUSSION

Membrane-bound CLIC1 plays key roles in cell signaling, homeostatic, and apoptotic processes.[35−37] Despite its physiological relevance, the structure of the membrane-bound form of CLIC1 is yet to be determined. In particular, the structural transition of the transmembrane domain (TMD) during membrane insertion is not well studied. Here we report the secondary, tertiary, and quaternary structural changes in the CLIC1 TMD as it partitions between an aqueous and membrane-mimicking environment. The use of synthetic TMD peptides as models for investigating the structure, assembly, and folding of membrane proteins has been well documented.[38,39]

In the presence of membrane mimetics, the TMD undergoes a dramatic structural rearrangement to form an α-helix. This conformation is consistent with the predicted membrane conformation of the TMD. The dependence of the secondary structure on both TFE and SDS concentration suggests that one conformation (the unstructured peptide) is progressively depopulated in favor of another (the helical peptide).[40] This transition from unstructured to helical is consistent with the membrane partitioning of a peptide in its transmembrane conformation.[41]

dx.doi.org/10.1021/bi4002776 | *Biochemistry* 2013, 52, 2739−2749

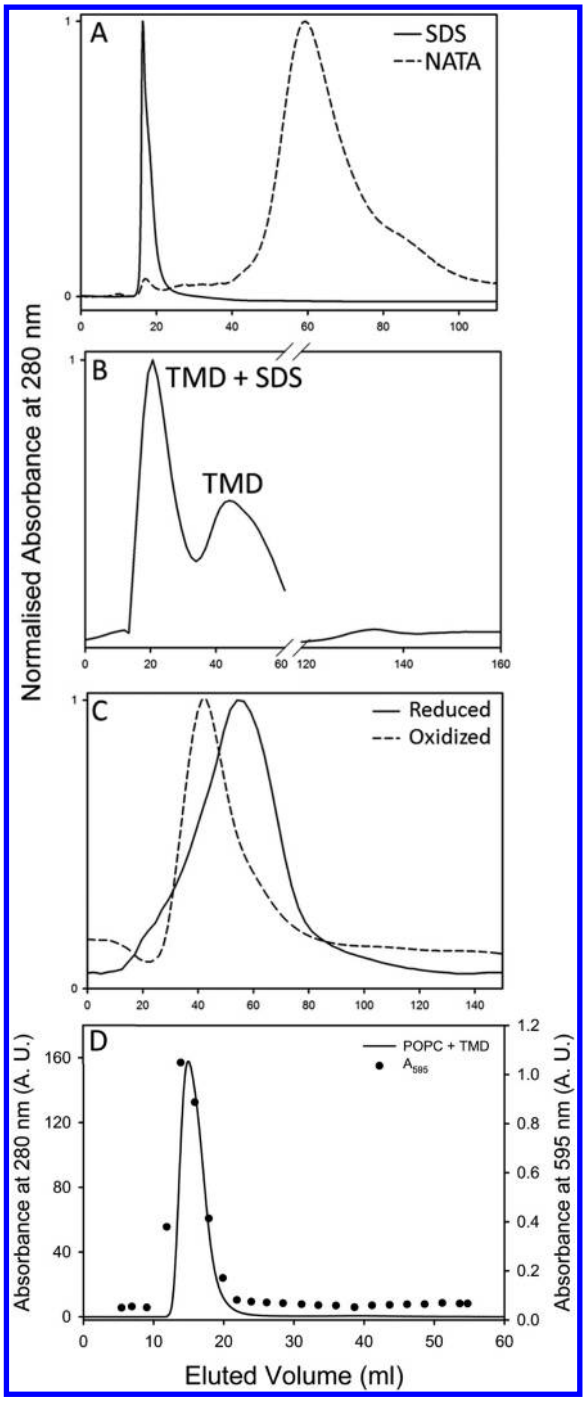

Figure 5. CLIC1 TMD peptide associates with SDS micelles and POPC liposomes. (A) Samples containing only SDS and only NATA were used to determine the void volume and total column volume, respectively. (B) A mixture containing 20 μM TMD peptide in 15 mM SDS was analyzed on a Sephadex G25 size-exclusion column to determine whether the peptide interacts with SDS micelles. The data show that 66% of the TMD peptide coelutes with the SDS micelles in the void volume. The profile shown has been corrected for scatter contribution by SDS. (C) Control sample containing only the reduced (solid) or oxidized (dashed) TMD peptide in buffer. (D) An identical assay was conducted using POPC liposomes, with the peptide-containing fractions detected using a Bradford assay. The Bradford assay was corrected for the contribution by liposome scatter using an identical sample without the TMD peptide. The buffer consisted of 20 mM sodium phosphate, 1 mM DTT, and 0.2% (w/v) NaN_3 (pH 5.5).

The membrane-mimetic effect of TFE is caused by an increase in the order of the solvent, making solvent−peptide interactions energetically unfavorable and subsequently promoting interactions between the peptide backbone (i.e., secondary structure).[42] However, isotropic solvents such as TFE lack the chemical and structural heterogeneity of lipid bilayers. In addition, TFE disrupts tertiary and quaternary contacts,[43] explaining the concentration independence of the peptide in TFE. The use of SDS micelles partially circumvents these issues by providing a heterogeneous environment with a polarity that more closely matches that of lipid bilayers.[44] Detergent micelles do, however, exist in equilibrium with detergent monomers and may thus form a hydrophobic surface that does not require insertion of the peptide. This necessitated the inclusion of the lipid bilayer (POPC) system, given that micelles are as likely to form around a peptide as a peptide is to insert into a preexisting micelle.

Fluorescence quenching studies indicate that the acquisition of secondary structure in the presence of SDS and POPC correlates with the insertion of the peptide into SDS micelles and POPC liposomes. Whether these events occur sequentially or in parallel remains unknown, although the two-state folding model of Popot and Engelman[2] tends to favor a sequential mechanism. In this study, the data show that the TMD alone is sufficient to promote membrane insertion in the absence of a signal peptide. This is in line with the work of Singh and Ashley,[45] which showed that the truncated N-domain of CLIC4 was capable of directing membrane insertion in the absence of the C-domain and large portions of the N-domain.

The spatial relationship between the micelles and the peptide is proposed in Figure S5 of the Supporting Information, corresponding to an orientation in which Trp35 is buried near the middle of the micelle. This compares favorably with its expected location within lipid bilayers, determined using brominated phospholipids.[17] Given the average internal diameter of SDS micelles (3−5 nm)[46] and the propensity for helices to extend in membrane environments,[47] the peptide may well be protruding from the micelles rather than being fully inserted (Figure S5A−C of the Supporting Information). The partial reactivity of Cys24 with DTNB confirms that a fraction of the micelle-associated peptide exhibits a protruding N-terminus. This is in line with the findings of Singh and Ashley[45] as well as work comprising FLAG epitopes[14] and terminally directed antibodies.[15] Interestingly, our data suggest that a large proportion (~70%) of the peptide is found in an orientation where Cys24 is exposed to the trans face of the membrane. This correlates with its expected location in the membrane[45] and is consistent with a transmembrane region that moves from the cytoplasm and inserts across an intracellular membrane.

Upon oxidation, wild-type CLIC1 undergoes a structural rearrangement stabilized by the formation of an intramolecular disulfide bond between Cys24 and Cys59.[8] This conformation is thought to promote membrane binding and insertion by increasing the hydrophobic surface area. The insertion of the CLIC1 TMD into SDS micelles and POPC liposomes was observed under reducing conditions and in the absence of Cys59. In addition, work performed using a C24S mutant has shown that the acquisition of helical structure does not require the presence of Cys24.[57] Therefore, the formation of an intramolecular disulfide between Cys24 and Cys59 and the resultant dimerization of full-length CLIC1[8] is unlikely to play a key role in the binding/insertion process. This is supported by

dx.doi.org/10.1021/bi4002776 | *Biochemistry* 2013, 52, 2739−2749

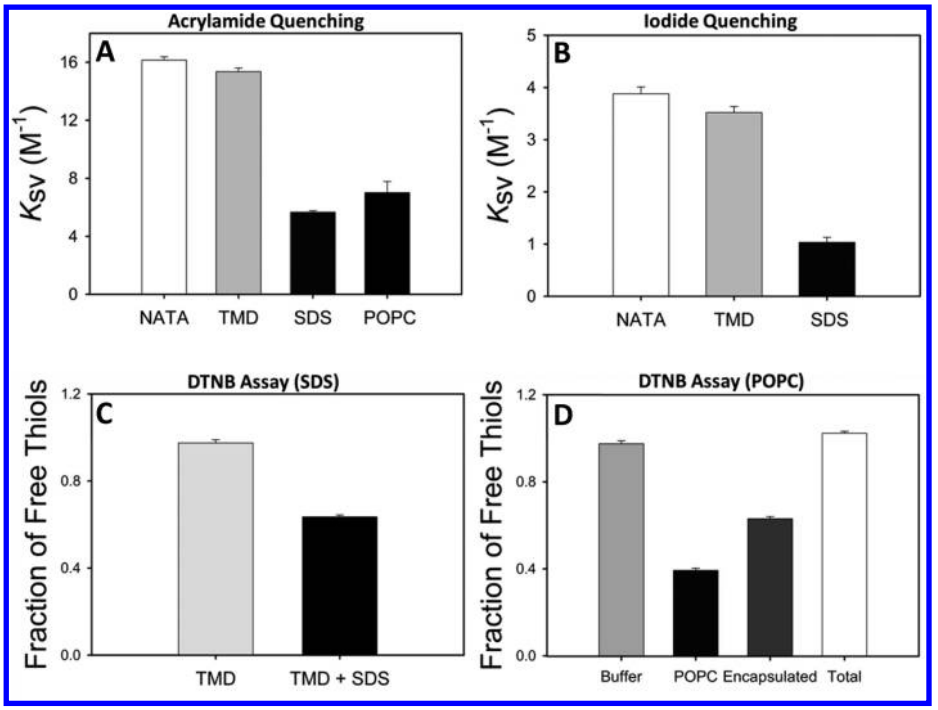

Figure 6. Solvent accessibility of the CLIC1 TMD peptide in SDS micelles and POPC liposomes. Dynamic acrylamide (A) and iodide (B) quenching and a DTNB assay (C and D) were performed in the absence and presence of 15 mM SDS or 2.5 mM POPC. In panel D, "buffer" refers to free TMD peptide in solution, "POPC" refers to external DTNB, and "encapsulated" refers to encapsulated DTNB. The buffer consisted of 20 mM sodium phosphate, 1 mM DTT, and 0.2% (w/v) NaN_3 (pH 5.5) (Quenching) or 20 mM sodium phosphate, 1 mM EDTA, and 0.2% (w/v) NaN_3 (pH 6.0) (DTNB Assay).

the fact that not all CLICs and CLIC homologues have a redox-active cysteine at their active sites.[48] Oxidation did, however, have a negative effect on the fluorescence emission of Trp35, consistent with reports of indole degradation by hydrogen peroxide.[49] This not only acts as a means of assessing solvent exposure, because buried tryptophans are inaccessible to H_2O_2, but also shows that care must be taken when using oxidation to study membrane insertion of CLIC1.[17,50]

In addition to oxidation, low pH has been implicated as a major driving force in membrane binding and/or insertion by both lowering the stability[22] and enhancing the flexibility[23] of the N-domain. This is thought to reduce the energy barrier required to expose and refold the TMD for membrane insertion. This pH dependence is due to the protonation and subsequent disruption of a stabilizing electrostatic network across the protein[51,52] as it moves from the cytosol (pH ∼7.4) to the membrane surface (pH ∼4−6). This network comprises residues not contained within the TMD, accounting for the pH insensitivity of the peptide's structure and self-association. This highlights the fact that membrane insertion and dimerization of the TMD itself is likely a pH-independent process, although pH may affect both the exposure of the TMD to the membrane and its ion conducting activity.[21,23] The pH-induced intermediate[22] and the oxidized dimer[8] of full-length CLIC1 are thought to expose hydrophobic regions of the protein, including the TMD. This not only facilitates membrane−protein interactions but also promotes protein−protein interactions (i.e., oligomerization).

Given that CLIC1 contains a single TMD, subsequent oligomerization is required to form a functional pore. This process, which completes the two-step folding model, has been poorly characterized in CLIC1 and forms the basis of much debate. The dimeric and trimeric TMD species identified here form under reducing conditions, again suggesting that oxidation is unlikely to play a role in this process. The poor staining of the trimeric species using Coomassie staining suggests that the dimer is likely the predominant species. The absence of the monomeric species coupled with data from size-exclusion chromatography (Figure 5) is troubling but may be a result of diffusion of the small peptide out of the gel coupled with poor staining by either Coomassie or silver staining methods. Alternatively, the peptide may display anomalous migration in the SDS−PAGE gel. This phenomenon has been observed for transmembrane peptides,[58,59] where monomeric species were shown to migrate as a dimer. In this study, then, the "dimer" bands may in fact represent the monomer while the "trimer" bands are likely representative of the true dimer. The smearing evident at high peptide concentrations does suggest that an equilibrium exists between the dimer and higher-order oligomers. This highlights possible differences in the thermodynamic stabilities of these species.

A dimer or trimer alone is unlikely to form an ion-conducting pore. Studies by Warton et al.[21] suggest that the dimer may represent a weakly active protopore that subsequently oligomerizes to form the fully active channel. Such behavior has been observed for other proteins that spontaneously insert into membranes, including diphtheria toxin,[53] Bax,[54] and Bcl-x_L.[7] To date, two models of the functional CLIC1 channel have been proposed. Singh[55] postulates that four protomers, each comprising four TMD helices, interact to form the ion channel. The second model comprises a large channel of at least four subunits, with each subunit comprising six to eight transmembrane helices.[50] Although Förster resonance energy transfer evidence supports this model, the large pore diameter of ∼120 Å does not appear to be physiologically feasible, given that other ion-conducting pores have diameters in the range of

dx.doi.org/10.1021/bi4002776 | *Biochemistry* 2013, 52, 2739−2749

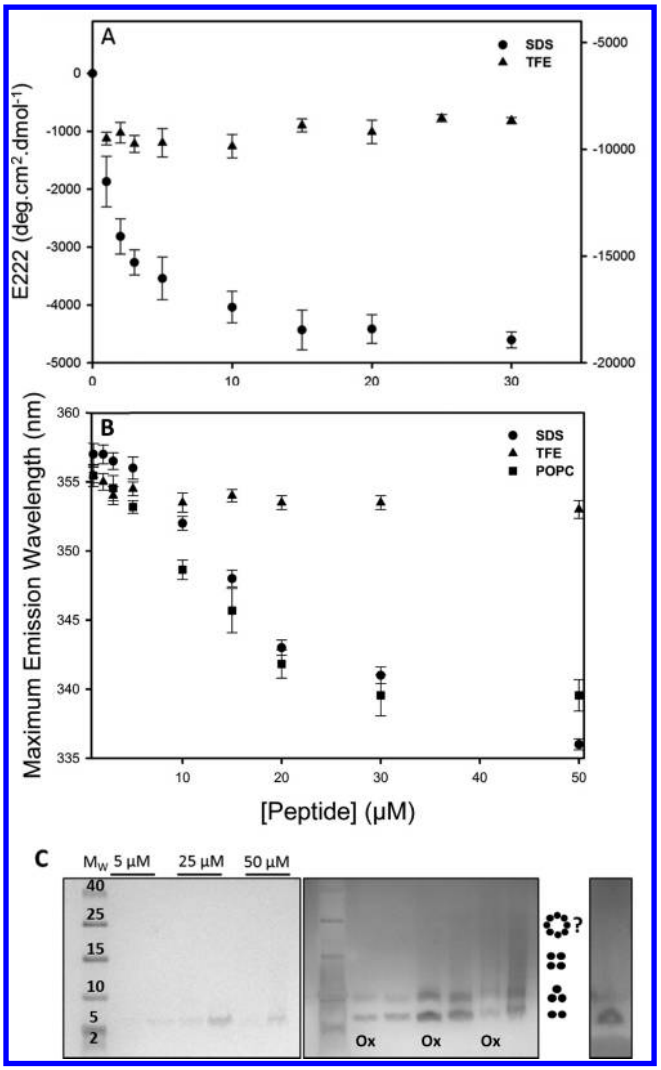

Figure 7. Concentration-dependent dimerization of the CLIC1 TMD peptide. (A) Upon conversion to mean residue ellipticity ($[\theta]$), the E_{222} values from peptide samples incubated in SDS micelles show a 2-fold increase at increasing peptide concentrations whereas those incubated in TFE show no such trend. The right-hand side *y*-axis represents E_{222} values in TFE, while that on the left represents those in SDS. (B) The maximal fluorescence emission wavelength also shows a blue shift at increasing peptide concentrations in SDS micelles and POPC liposomes. This suggests that the TMD peptide associates in a concentration-dependent manner in SDS micelles. (C) Stable dimeric (~6.9 kDa) and trimeric (~10.2 kDa) species were subsequently identified using SDS–PAGE under denaturing and reducing conditions. The smearing evident at high peptide concentrations may indicate higher-order tetrameric and octomeric species. The gel on the left was stained with Coomassie Brilliant Blue G-250, while that on the right was the same gel stained with silver. The lanes labeled "Ox" refer to the oxidized dimer control at each peptide concentration. An additional dimer control that was oxidized prior to being mixed with SDS is included at the far right.

3–5 Å (chloride channel),[56] being as large as 30 Å for Bax apoptotic proteins.[6,54] Further investigations into the oligomeric states of CLIC1 and its TMD are therefore warranted to gain a better understanding of how this soluble protein comes together to form a functional channel.

In conclusion, the results presented here represent the first analysis of the structure of the CLIC1 TMD in membrane-mimetic environments. The TMD peptide undergoes structural modifications in the micellar environment, including the acquisition of helical secondary structure and dimerization. We propose that, in the vicinity of membranes, the TMD refolds to form a helix, consistent with the predicted membrane conformation. The single helix then oligomerizes via non-covalent helix–helix interactions to form a membrane-competent protopore complex. Oligomerization does not, therefore, require the C-domain and large portions of the N-domain. However, much work is still needed to clarify both the nature of oligomerization and the forces that drive the peptide to spontaneously associate with micelles and/or membranes. Future work will involve analyzing the kinetics and thermodynamics of the interaction, although the gold standard will always be high-resolution structural data.

■ ASSOCIATED CONTENT

Supporting Information

Thermal unfolding of the CLIC1 TMD peptide in SDS and TFE (Figure S1), oxidation of Cys24 using a DTNB assay at 0 and 4 h (Figure S2), detection of free TMD peptide following size-exclusion chromatography (Figure S3), Stern–Volmer plots for acrylamide and iodide quenching (Figure S4), and a schematic representation of the possible orientations of the TMD peptide in SDS micelles and POPC liposomes (Figure S5). This material is available free of charge via the Internet at http://pubs.acs.org.

■ AUTHOR INFORMATION

Corresponding Author

*E-mail: heinrich.dirr@wits.ac.za. Telephone: +27 11 7176352. Fax: +27 11 7176351.

Funding

This work was supported by the University of the Witwatersrand, the South African National Research Foundation (Grants 60810, 65510, and 68898 to H.W.D.), and the South African Research Chairs Initiative of the Department of Science and Technology and National Research Foundation (Grant 64788 to H.W.D.).

Notes

The authors declare no competing financial interest.

■ ABBREVIATIONS

CD, circular dichroism; CLIC1, chloride intracellular channel protein 1; DTNB, 5,5′-dithio(2-nitrobenzoic acid); DTT, dithiothreitol; GST, glutathione transferase; NATA, *N*-acetyltryptophanamide; POPC, 1-palmitoyl-2-oleoyl-*sn*-glycero-3-phosphocholine; PTM, putative transmembrane domain; SDS, sodium dodecyl sulfate; TFE, 2,2,2-trifluoroethanol; TMD, transmembrane domain of CLIC1 (residues 24–46).

■ REFERENCES

(1) Overington, J. P., Al-Lazikani, B., and Hopkins, A. L. (2006) How many drug targets are there? *Nat. Rev. Drug Discovery 5*, 993–996.

(2) Popot, J. L., and Engelman, D. M. (1990) Membrane protein folding and oligomerization: The two-stage model. *Biochemistry 29*, 4031–4037.

(3) White, S. H., and Wimley, W. C. (1999) Membrane protein folding and stability: Physical principles. *Annu. Rev. Biophys. Biomol. Struct. 28*, 319–365.

(4) Johnson, J. E., and Cornell, R. B. (1999) Amphitropic proteins: Regulation by reversible membrane interactions. *Mol. Membr. Biol. 16*, 217–235.

(5) van der Goot, F. G., Gonzalez-Manas, J. M., Lakey, J. H., and Pattus, F. (1991) A 'molten-globule' membrane-insertion intermediate of the pore-forming domain of colicin A. *Nature 354*, 408−410.
(6) Parker, M. W., and Feil, S. C. (2005) Pore-forming protein toxins: From structure to function. *Prog. Biophys. Mol. Biol. 88*, 91−142.
(7) Thuduppathy, G. R., and Hill, R. B. (2006) Acid destabilization of the solution conformation of Bcl-xL does not drive its pH-dependent insertion into membranes. *Protein Sci. 15*, 248−257.
(8) Littler, D. R., Harrop, S. J., Fairlie, W. D., Brown, L. J., Pankhurst, G. J., Pankhurst, S., DeMaere, M. Z., Campbell, T. J., Bauskin, A. R., Tonini, R., Mazzanti, M., Breit, S. N., and Curmi, P. M. (2004) The intracellular chloride ion channel protein CLIC1 undergoes a redox-controlled structural transition. *J. Biol. Chem. 279*, 9298−9305.
(9) Harrop, S. J., DeMaere, M. Z., Fairlie, W. D., Reztsova, T., Valenzuela, S. M., Mazzanti, M., Tonini, R., Qiu, M. R., Jankova, L., Warton, K., Bauskin, A. R., Wu, W. M., Pankhurst, S., Campbell, T. J., Breit, S. N., and Curmi, P. M. (2001) Crystal structure of a soluble form of the intracellular chloride ion channel CLIC1 (NCC27) at 1.4-Å resolution. *J. Biol. Chem. 276*, 44993−45000.
(10) Ponce, A., Vega-Saenz de Miera, E., Kentros, C., Moreno, H., Thornhill, B., and Rudy, B. (1997) K^+ channel subunit isoforms with divergent carboxy-terminal sequences carry distinct membrane targeting signals. *J. Membr. Biol. 159*, 149−159.
(11) Cromer, B. A., Morton, C. J., Board, P. G., and Parker, M. W. (2002) From glutathione transferase to pore in a CLIC. *Eur. Biophys. J. 31*, 356−364.
(12) Berryman, M., and Bretscher, A. (2000) Identification of a novel member of the chloride intracellular channel gene family (CLIC5) that associates with the actin cytoskeleton of placental microvilli. *Mol. Biol. Cell 11*, 1509−1521.
(13) Duncan, R. R., Westwood, P. K., Boyd, A., and Ashley, R. H. (1997) Rat brain p64H1, expression of a new member of the p64 chloride channel protein family in endoplasmic reticulum. *J. Biol. Chem. 272*, 23880−23886.
(14) Tonini, R., Ferroni, A., Valenzuela, S. M., Warton, K., Campbell, T. J., Breit, S. N., and Mazzanti, M. (2000) Functional characterization of the NCC27 nuclear protein in stable transfected CHO-K1 cells. *FASEB J. 14*, 1171−1178.
(15) Proutski, I., Karoulias, N., and Ashley, R. H. (2002) Overexpressed chloride intracellular channel protein CLIC4 (p64H1) is an essential component of novel plasma membrane anion channels. *Biochem. Biophys. Res. Commun. 297*, 317−322.
(16) Berry, K. L., and Hobert, O. (2006) Mapping functional domains of chloride intracellular channel (CLIC) proteins in vivo. *J. Mol. Biol. 359*, 1316−1333.
(17) Goodchild, S. C., Howell, M. W., Cordina, N. M., Littler, D. R., Breit, S. N., Curmi, P. M., and Brown, L. J. (2009) Oxidation promotes insertion of the CLIC1 chloride intracellular channel into the membrane. *Eur. Biophys. J. 39*, 129−138.
(18) Landolt-Marticorena, C., Williams, K. A., Deber, C. M., and Reithmeier, R. A. (1993) Non-random distribution of amino acids in the transmembrane segments of human type I single span membrane proteins. *J. Mol. Biol. 229*, 602−608.
(19) Arkin, I. T., and Brunger, A. T. (1998) Statistical analysis of predicted transmembrane α-helices. *Biochim. Biophys. Acta 1429*, 113−128.
(20) Hunte, C., Screpanti, E., Venturi, M., Rimon, A., Padan, E., and Michel, H. (2005) Structure of a Na^+/H^+ antiporter and insights into mechanism of action and regulation by pH. *Nature 435*, 1197−1202.
(21) Warton, K., Tonini, R., Fairlie, W. D., Matthews, J. M., Valenzuela, S. M., Qiu, M. R., Wu, W. M., Pankhurst, S., Bauskin, A. R., Harrop, S. J., Campbell, T. J., Curmi, P. M., Breit, S. N., and Mazzanti, M. (2002) Recombinant CLIC1 (NCC27) assembles in lipid bilayers via a pH-dependent two-state process to form chloride ion channels with identical characteristics to those observed in Chinese hamster ovary cells expressing CLIC1. *J. Biol. Chem. 277*, 26003−26011.
(22) Fanucchi, S., Adamson, R. J., and Dirr, H. W. (2008) Formation of an unfolding intermediate state of soluble chloride intracellular channel protein CLIC1 at acidic pH. *Biochemistry 47*, 11674−11681.
(23) Stoychev, S. H., Nathaniel, C., Fanucchi, S., Brock, M., Li, S., Asmus, K., Woods, V. L., Jr., and Dirr, H. W. (2009) Structural dynamics of soluble chloride intracellular channel protein CLIC1 examined by amide hydrogen-deuterium exchange mass spectrometry. *Biochemistry 48*, 8413−8421.
(24) Killian, J. A., Trouard, T. P., Greathouse, D. V., Chupin, V., and Lindblom, G. (1994) A general method for the preparation of mixed micelles of hydrophobic peptides and sodium dodecyl sulphate. *FEBS Lett. 348*, 161−165.
(25) Sreerama, N., and Woody, R. W. (2000) Estimation of protein secondary structure from circular dichroism spectra: Comparison of CONTIN, SELCON, and CDSSTR methods with an expanded reference set. *Anal. Biochem. 287*, 252−260.
(26) Sreerama, N., Venyaminov, S. Y., and Woody, R. W. (2001) Analysis of protein circular dichroism spectra based on the tertiary structure classification. *Anal. Biochem. 299*, 271−274.
(27) Eftink, M. R., and Ghiron, C. A. (1981) Fluorescence quenching studies with proteins. *Anal. Biochem. 114*, 199−227.
(28) Habeeb, A. F. (1972) Reaction of protein sulfhydryl groups with Ellman's reagent. *Methods Enzymol. 25C*, 457−464.
(29) Schagger, H., and von Jagow, G. (1987) Tricine-sodium dodecyl sulfate-polyacrylamide gel electrophoresis for the separation of proteins in the range from 1 to 100 kDa. *Anal. Biochem. 166*, 368−379.
(30) Langosch, D., and Arkin, I. T. (2009) Interaction and conformational dynamics of membrane-spanning protein helices. *Protein Sci. 18*, 1343−1358.
(31) Wigley, W. C., Vijayakumar, S., Jones, J. D., Slaughter, C., and Thomas, P. J. (1998) Transmembrane domain of cystic fibrosis transmembrane conductance regulator: Design, characterization, and secondary structure of synthetic peptides m1-m6. *Biochemistry 37*, 844−853.
(32) Melnyk, R. A., Partridge, A. W., and Deber, C. M. (2001) Retention of native-like oligomerization states in transmembrane segment peptides: Application to the *Escherichia coli* aspartate receptor. *Biochemistry 40*, 11106−11113.
(33) Thanassi, D. G., Saulino, E. T., Lombardo, M. J., Roth, R., Heuser, J., and Hultgren, S. J. (1998) The PapC usher forms an oligomeric channel: Implications for pilus biogenesis across the outer membrane. *Proc. Natl. Acad. Sci. U.S.A. 95*, 3146−3151.
(34) Studer, S., and Narberhaus, F. (2000) Chaperone activity and homo- and hetero-oligomer formation of bacterial small heat shock proteins. *J. Biol. Chem. 275*, 37212−37218.
(35) Fernandez-Salas, E., Sagar, M., Cheng, C., Yuspa, S. H., and Weinberg, W. C. (1999) p53 and tumor necrosis factor α regulate the expression of a mitochondrial chloride channel protein. *J. Biol. Chem. 274*, 36488−36497.
(36) Landry, D. W., Akabas, M. H., Redhead, C., Edelman, A., Cragoe, E. J., Jr., and Al-Awqati, Q. (1989) Purification and reconstitution of chloride channels from kidney and trachea. *Science 244*, 1469−1472.
(37) Ronnov-Jessen, L., Villadsen, R., Edwards, J. C., and Petersen, O. W. (2002) Differential expression of a chloride intracellular channel gene, CLIC4, in transforming growth factor-β1-mediated conversion of fibroblasts to myofibroblasts. *Am. J. Pathol. 161*, 471−480.
(38) Aggeli, A., Bannister, M. L., Bell, M., Boden, N., Findlay, J. B., Hunter, M., Knowles, P. F., and Yang, J. C. (1998) Conformation and ion-channeling activity of a 27-residue peptide modeled on the single-transmembrane segment of the IsK (minK) protein. *Biochemistry 37*, 8121−8131.
(39) Yeagle, P. L., Danis, C., Choi, G., Alderfer, J. L., and Albert, A. D. (2000) Three dimensional structure of the seventh transmembrane helical domain of the G-protein receptor, rhodopsin. *Mol. Vision 6*, 125−131.
(40) Demchenko, A. P. (2001) Concepts and misconcepts in the analysis of simple kinetics of protein folding. *Curr. Protein Pept. Sci. 2*, 73−98.

(41) MacKenzie, K. R., Prestegard, J. H., and Engelman, D. M. (1997) A transmembrane helix dimer: Structure and implications. *Science 276*, 131−133.
(42) Buck, M. (1998) Trifluoroethanol and colleagues: Cosolvents come of age. Recent studies with peptides and proteins. *Q. Rev. Biophys. 31*, 297−355.
(43) Roccatano, D., Colombo, G., Fioroni, M., and Mark, A. E. (2002) Mechanism by which 2,2,2-trifluoroethanol/water mixtures stabilize secondary-structure formation in peptides: A molecular dynamics study. *Proc. Natl. Acad. Sci. U.S.A. 99*, 12179−12184.
(44) Tulumello, D. V., and Deber, C. M. (2009) SDS micelles as a membrane-mimetic environment for transmembrane segments. *Biochemistry 48*, 12096−12103.
(45) Singh, H., and Ashley, R. H. (2007) CLIC4 (p64H1) and its putative transmembrane domain form poorly selective, redox-regulated ion channels. *Mol. Membr. Biol. 24*, 41−52.
(46) Hierrezuelo, J. M., Aguiar, J., and Ruiz, C. C. (2004) Stability, interaction, size, and microenvironmental properties of mixed micelles of decanoyl-N-methylglucamide and sodium dodecyl sulfate. *Langmuir 20*, 10419−10426.
(47) Pace, C. N., and Scholtz, J. M. (1998) A helix propensity scale based on experimental studies of peptides and proteins. *Biophys. J. 75*, 422−427.
(48) Littler, D. R., Harrop, S. J., Brown, L. J., Pankhurst, G. J., Mynott, A. V., Luciani, P., Mandyam, R. A., Mazzanti, M., Tanda, S., Berryman, M. A., Breit, S. N., and Curmi, P. M. (2008) Comparison of vertebrate and invertebrate CLIC proteins: The crystal structures of *Caenorhabditis elegans* EXC-4 and *Drosophila melanogaster* DmCLIC. *Proteins 71*, 364−378.
(49) Cavatorta, P., Favilla, R., and Mazzini, A. (1979) Fluorescence quenching of tryptophan and related compounds by hydrogen peroxide. *Biochim. Biophys. Acta 578*, 541−546.
(50) Goodchild, S. C., Angstmann, C. N., Breit, S. N., Curmi, P. M., and Brown, L. J. (2011) Transmembrane extension and oligomerization of the CLIC1 chloride intracellular channel protein upon membrane interaction. *Biochemistry 50*, 10887−10897.
(51) Achilonu, I., Fanucchi, S., Cross, M., Fernandes, M., and Dirr, H. W. (2012) Role of individual histidines in the pH-dependent global stability of human chloride intracellular channel 1. *Biochemistry 51*, 995−1004.
(52) Legg-E'silva, D., Achilonu, I., Fanucchi, S., Stoychev, S., Fernandes, M., and Dirr, H. W. (2012) Role of Arginine 29 and Glutamic Acid 81 Interactions in the Conformational Stability of Human Chloride Intracellular Channel 1. *Biochemistry. 51*, 7854−7862.
(53) Bennett, M. J., Choe, S., and Eisenberg, D. (1994) Refined structure of dimeric diphtheria toxin at 2.0 Å resolution. *Protein Sci. 3*, 1444−1463.
(54) Garcia-Saez, A. J., Mingarro, I., Perez-Paya, E., and Salgado, J. (2004) Membrane-insertion fragments of Bcl-xL, Bax, and Bid. *Biochemistry 43*, 10930−10943.
(55) Singh, H. (2010) Two decades with dimorphic Chloride Intracellular Channels (CLICs). *FEBS Lett. 584*, 2112−2121.
(56) Jentsch, T. J. (2002) Chloride channels are different. *Nature 415*, 276−277.
(57) Ngubane, C. (2012) The Transmembrane Domain of CLIC1 is Helical in Membrane-Mimetic Environments. Unpublished M.Sc. Dissertation (http://hdl.handle.net/10539/11477).
(58) Walkenhorst, W. F., Merzlyakov, M., Hristova, K., and Wimley, W. C. (2009) Polar residues in transmembrane helices can decrease electrophoretic mobility in polyacrylamide gels without causing helix dimerization. *Biochim. Biophys. Acta 1788*, 1321−1331.
(59) Rath, A., Glibowicka, M., Nadeau, V. G., Chen, G., and Deber, C. M. (2009) Detergent binding explains anomalous SDS-PAGE migration of membrane proteins. *Proc. Natl. Acad. Sci. U.S.A. 106*, 1760−1765.

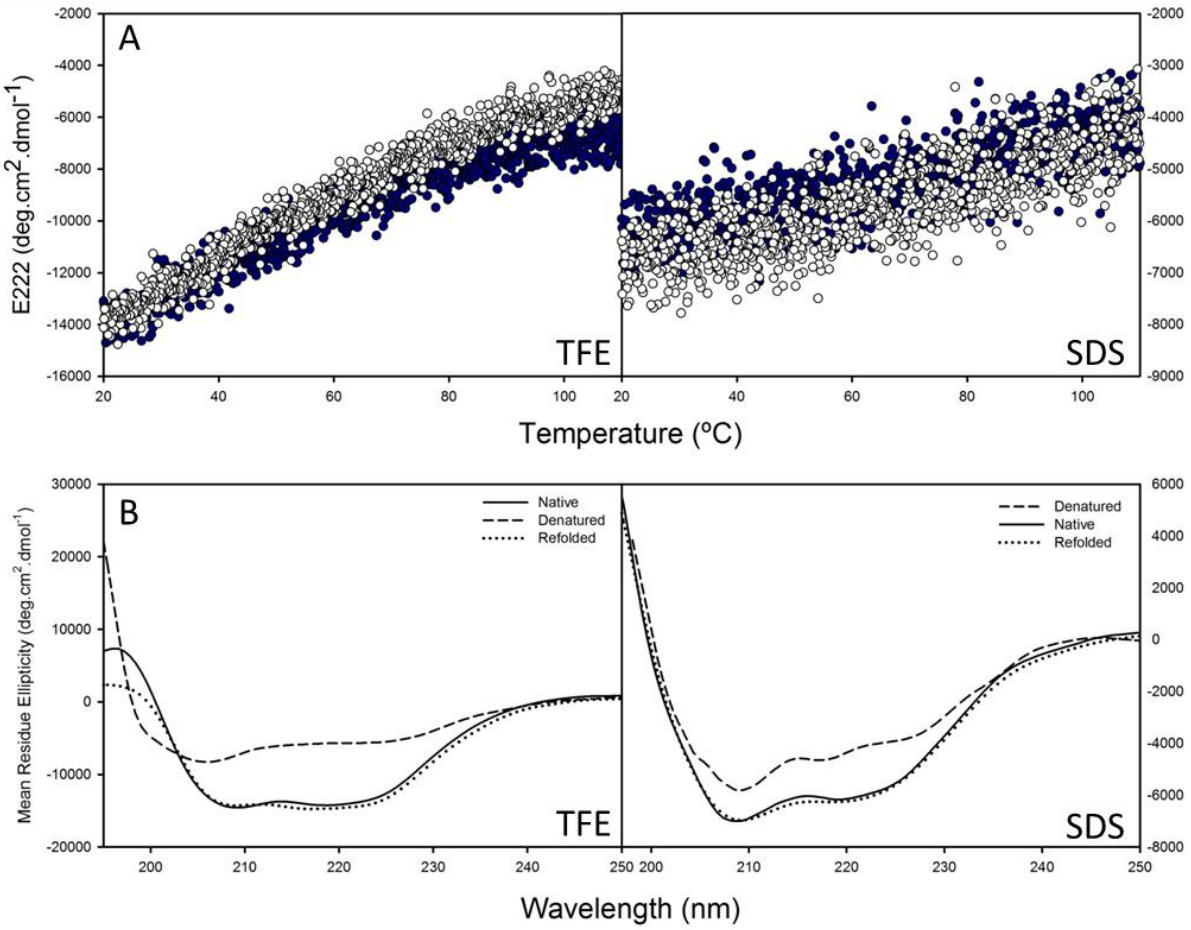

Figure S1 The CLIC1 TMD unfolds via a reversible and non-cooperative one-step pathway. (A) Thermal melts of 15 µM TMD peptide were monitored by ellipticity at 222 nm in 40 % (v/v) TFE and 15 mM SDS. The unfolding (closed circle) and refolding (open circle) pathways showed no hysteresis, suggesting that the process is reversible. The far-UV CD spectra (B) confirm this, with 100 % of the peptide assuming its native structure upon cooling. The approximately linear loss of structure suggests that the unfolding process is non-cooperative and follows a one-step pathway. Such a pathway comprises a transition from an initial folded state to a final unfolded state without the presence of stable intermediates. The absence of any native or denatured baselines precludes the determination of thermodynamic parameters. The buffer used was 20 mM Na_2PO_4, 1 mM DTT, 0.2 % (w/v) NaN_3, pH 5.5

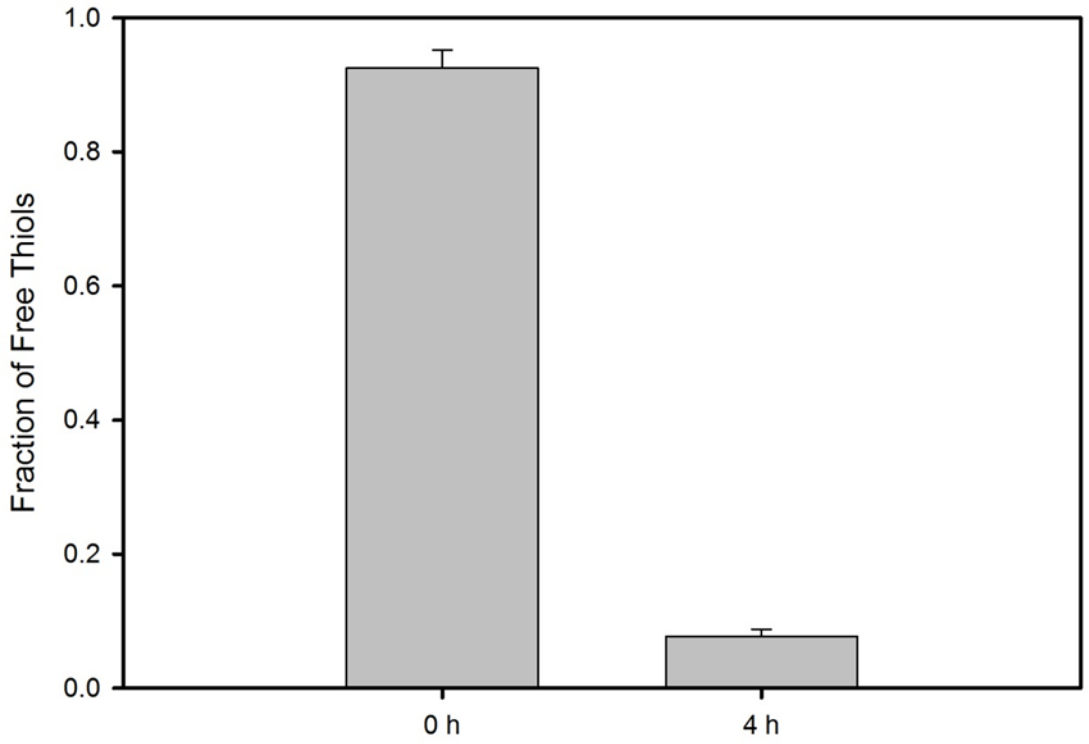

Figure S2 Oxidation of the CLIC1 TMD peptide results in disulfide formation. A DTNB assay was carried to confirm that the TMD peptide forms disulfide bonds under oxidising conditions. The fraction of free thiols of 15 µM TMD peptide was determined before and after the addition of 2 mM H_2O_2. Approximately 90 % of the peptide forms a disulfide with NTB, suggesting that most of the Cys24 residues in the oxidised SDS-PAGE control will form an intermolecular disulfide bond. The buffer used was 1 mM EDTA, 0.2 % (w/v) NaN_3, pH 7.0

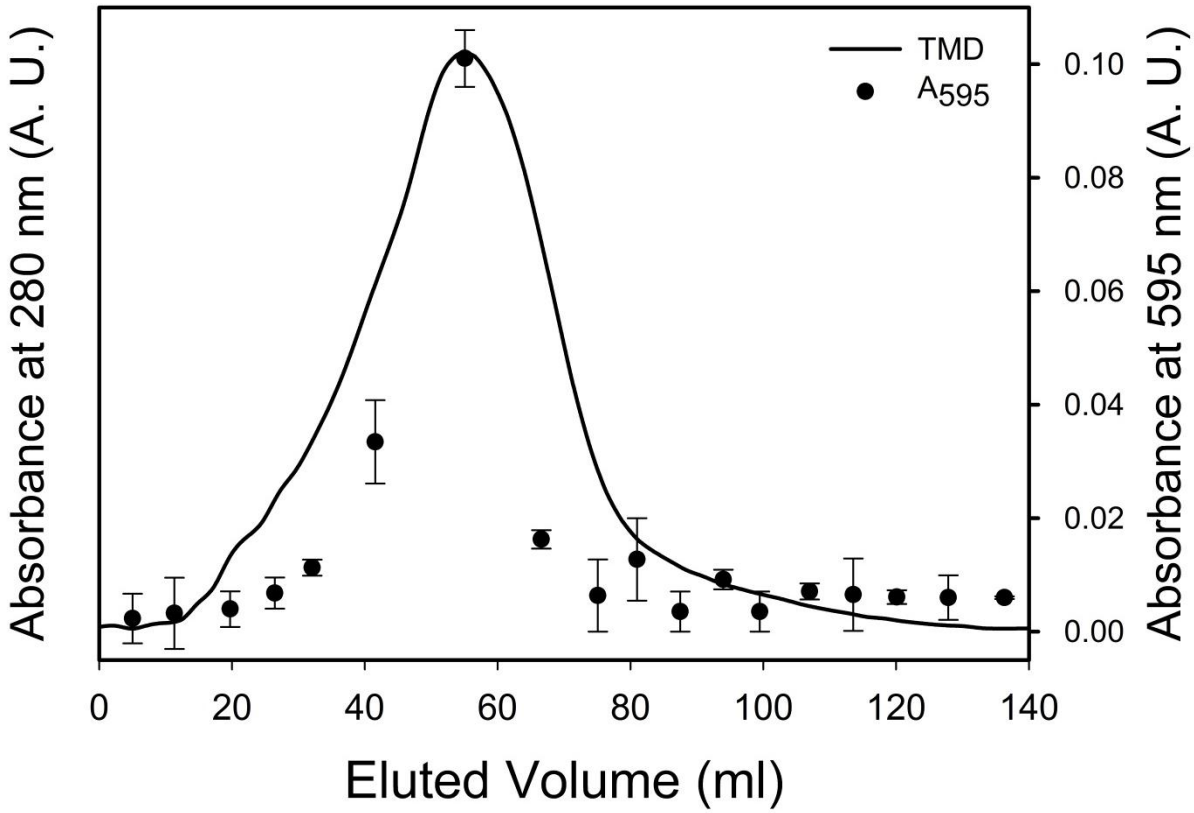

Figure S3 Detection of the CLIC1 TMD peptide using the Bradford assay. A Bradford assay was used to identify the CLIC1 TMD peptide in the absence of POPC liposomes following separation on a Sephadex G-25 size exclusion column. This peptide-only control shows that the assay is sufficiently sensitive to detect the small peptide, and that the amount of peptide detected in the absence and presence of POPC are comparable. The buffer used for equilibration of the size-exclusion column was 20 mM Na_2PO_4, 1 mM DTT, 0.2 % (w/v) NaN_3, pH 5.5

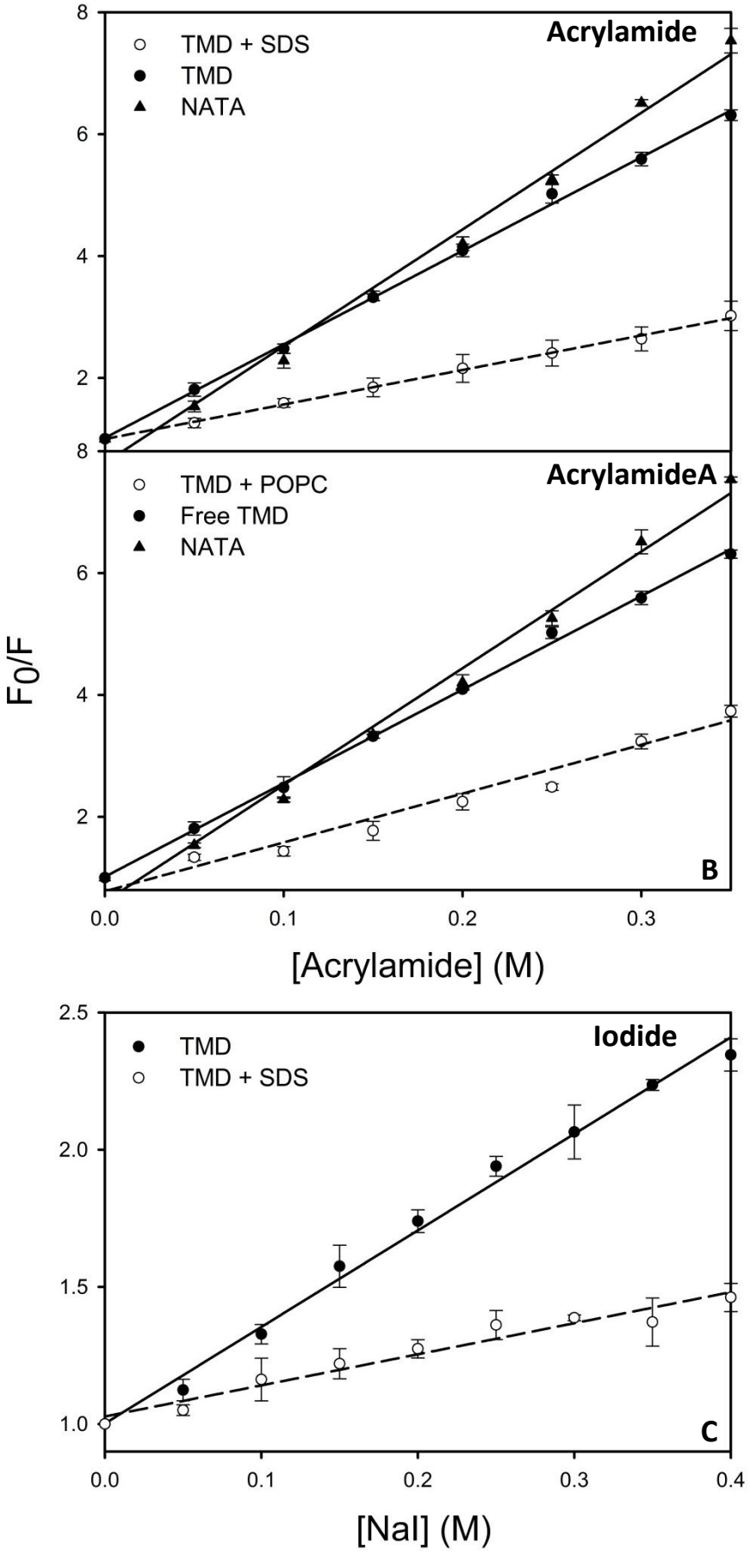
Acrylamide
TMD + SDS
TMD
NATA
AcrylamideA
TMD + POPC
Free TMD
NATA
B
F0/F
[Acrylamide] (M)
Iodide
TMD
TMD + SDS
C
[NaI] (M)

Figure S4 Stern-Volmer plots of the quenching of Trp35 fluorescence by acrylamide and iodide. Acrylamide **(A, B)** and iodide **(C)** quenching of 15 µM CLIC1 TMD peptide and 15 µM NATA was performed in buffer, 15 mM SDS **(A, C)** and 2.5 mM POPC **(B)**. The linear nature of these plots suggests that the quenching occurs via a dynamic process. Upon the addition of SDS and POPC, a significant reduction of the K_{SV} is observed, indicating decreased solvent exposure of Trp35. Iodide quenching was chosen as an additional probe in SDS owing to the ability of acrylamide to penetrate SDS micelles. Samples were analysed in 20 mM Na_2PO_4, 1 mM DTT, 0.2 % (w/v) NaN_3, pH 5.5.

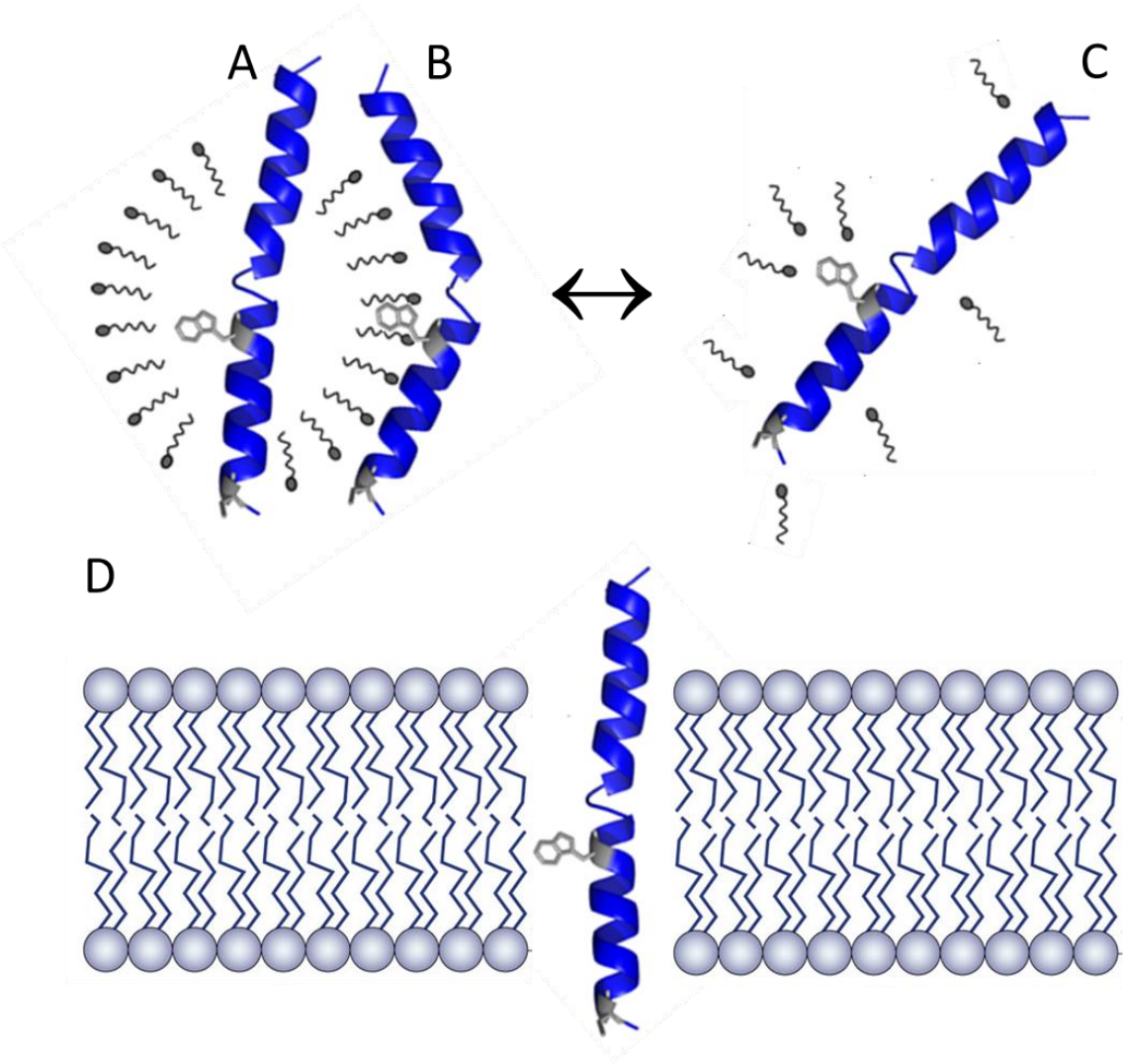

Figure S5 Proposed orientation of the CLIC1 TMD peptide in SDS micelles and POPC liposomes. Based on data obtained from quenching and DTNB studies, we propose that the core of the CLIC1 TMD either inserts into and is fully surrounded by SDS micelles **(A)** or is peripherally associated with the micelles in a manner which excludes Trp35 from the solvent **(B)**. Because detergent micelles exist in equilibrium with detergent monomers, the orientation shown in **(C)** is likely to co-exist with those interacting with micelles. Studies of thiol reactivity in POPC liposomes show that ~ 70 % of Cys24 residues are located at the *trans*-face of the liposomes (ie: the liposome interior) **(D)**. This is consistent with its predicted orientation at the membrane surface. It should be noted, however, that the entire peptide chain may not be helical as shown here.

Chapter 3

A Lys-Trp cation-π interaction mediates the dimerisation and function of the chloride intracellular channel protein 1 transmembrane domain

Peter, B., Polyansky, A. A., Fanucchi, S. and Dirr, H. W.
Biochemistry, **53(1):** 57-67

In this publication, electrostatic and hydrophobic interactions which stabilise the CLIC1 TMD dimer in the membrane were identified. In addition, a liposome flux assay was developed for functional characterisation of membrane-bound TMD.

Author contributions: Bradley Peter performed all experimental work except the modelling of the CLIC1 TMD dimer (Figure 2), analysed the data and wrote the manuscript. Anton A. Polyansky developed the PREDDIMER algorithm and performed the modelling of the CLIC1 TMD dimer. Sylvia Fanucchi and Heini W. Dirr supervised the project and assisted in data analysis and interpretation.

BIOCHEMISTRY
including biophysical chemistry & molecular biology

Article

pubs.acs.org/biochemistry

A Lys−Trp Cation−π Interaction Mediates the Dimerization and Function of the Chloride Intracellular Channel Protein 1 Transmembrane Domain

Bradley Peter,[†] Anton A. Polyansky,[‡,§] Sylvia Fanucchi,[†] and Heini W. Dirr*[,†]

[†]Protein Structure-Function Research Unit, School of Molecular and Cell Biology, University of the Witwatersrand, Johannesburg 2050, South Africa

[‡]Department of Structural and Computational Biology, Max F. Perutz Laboratories, University of Vienna, Campus Vienna Biocenter 5, Vienna AT-1030, Austria

[§]M. M. Shemyakin and Yu. A. Ovchinnikov Institute of Bioorganic Chemistry, Russian Academy of Sciences, Moscow 117997, Russia

Supporting Information

ABSTRACT: Chloride intracellular channel protein 1 (CLIC1) is a dual-state protein that can exist either as a soluble monomer or in an integral membrane form. The oligomerization of the transmembrane domain (TMD) remains speculative despite it being implicated in pore formation. The extent to which electrostatic and van der Waals interactions drive folding and association of the dimorphic TMD is unknown and is complicated by the requirement of interactions favorable in both aqueous and membrane environments. Here we report a putative Lys37−Trp35 cation−π interaction and show that it stabilizes the dimeric form of the CLIC1 TMD in membranes. A synthetic 30-mer peptide comprising a K37M TMD mutant was examined in 2,2,2-trifluoroethanol, sodium dodecyl sulfate micelles, and 1-palmitoyl-2-oleoyl-*sn*-glycero-3-phosphocholine liposomes using far-ultraviolet (UV) circular dichroism, fluorescence, and UV absorbance spectroscopy. Our data suggest that Lys37 is not implicated in the folding, stability, or membrane insertion of the TMD peptide. However, removal of this residue impairs the formation of dimers and higher-order oligomers. This is accompanied by a 30-fold loss of chloride influx activity, suggesting that dimerization modulates the rate of chloride conductance. We propose that, within membranes, individual TMD helices associate via a Lys37-mediated cation−π interaction to form active dimers. The latter findings are also supported by results of modeling a putative TMD dimer conformation in which Lys37 and Trp35 form cation−π pairs at the dimer interface. Dimeric helix bundles may then associate to form fully active ion channels. Thus, within a membrane-like environment, aromatic interactions involving a polar lysine side chain provide a thermodynamic driving force for helix−helix association.

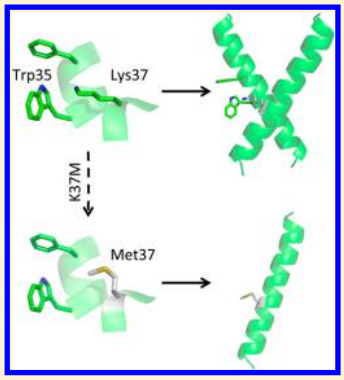

The two-step folding model proposed by Popot and Engelman[1,2] and the modified two-step model of White and Wimley[3] have been used to explain the mechanisms by which membrane proteins bind to, insert, and oligomerize in membranes. These models depict TMDs as independently stable and folded units capable of self-association. The self-association of transmembrane helices is a key step in membrane protein folding because it typically results in the protein adopting a functional form. Helix−helix association is thought to be mediated largely through noncovalent van der Waals and electrostatic forces.[4] The former utilizes small residue packing motifs to maximize helix contacts, such as GxxxG[5] and AxxxA,[6] whereas electrostatic interactions occur between polar side chains and side chain and backbone residues of interacting helices.[7−9] Although these two interactions predominate, other important subsets of noncovalent interactions involving aromatic residues exist. These may involve (i) two aromatic residues (π−π stacking) or (ii) a basic and an aromatic residue (cation−π). The latter is emerging as an important stabilizing force in membrane proteins,[10−12] being favorable in a hydrophobic medium[13−15] with an average strength of −6.5 kcal/mol.[16] The extent to which cation−π interactions direct membrane protein folding and transmembrane helix association is poorly understood, given that the energetics associated with the polar and aromatic groups differ substantially between membrane and water-soluble proteins.

Proteins capable of adopting multiple stable native states present an intriguing variation to these schemes. These proteins undergo large-scale structural rearrangements upon association with the lipid bilayer, resulting in the spontaneous conversion from a water-soluble to a membrane-bound form.[17] This requires interactions that are favorable in both aqueous and membrane environments, limiting the ensemble of potential helix−helix contacts. The eukaryotic chloride intracellular channel (CLIC) protein family is an example of a class of

Received: October 22, 2013
Revised: December 11, 2013
Published: December 11, 2013

amphitropic proteins that have evolved to overcome this limitation.

In their reduced monomeric state, the CLIC proteins adopt a topology similar to that of the GST superfamily, with a thioredoxin N-domain and an all-α-helical C-domain (Figure 1A).[18] CLICs are unique among all eukaryotic ion channels in

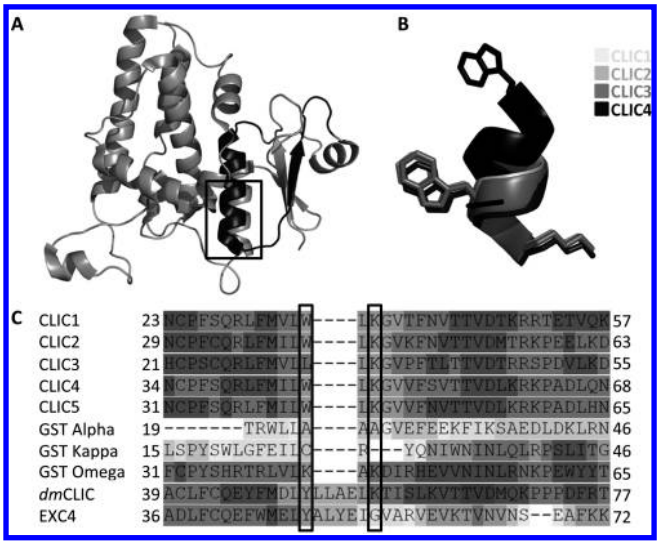

Figure 1. Structure and sequence conservation of the CLIC1 TMD. (A) The CLIC1 TMD comprises residues 24–46, which include most of helix α1 and sheet β2 (black) of the N-domain. This region shows strong sequence conservation across the vertebrate CLICs as well as the invertebrate homologues Exc4 (*Caenorhabditis elegans*) and dmCLIC (*Drosophila melanogaster*). The residues involved in a putative cation–π interaction are superimposed in panel B and boxed in panel C.

that they are dimorphic and can exist in either a soluble or membrane-bound form.[18] The best characterized member of this family is the p64 homolgue CLIC1. The soluble–membrane transition of CLIC1 likely involves the exposure of a single TMD. We have demonstrated that the isolated TMD undergoes structural modifications in a membrane environment, including the acquisition of helical secondary structure and dimerization.[19] Although the residues involved in dimerization are unknown, it is likely that they form noncovalent helix–helix interactions. The oligomerization process, which completes the two-step folding model, has been poorly characterized in CLIC1. To date, two models for the functional CLIC1 channel have been proposed.[20,21] However, neither of these models provides any indication about which interactions stabilize the TMD oligomers in the membrane. Modeling of the CLIC1 TMD dimer has identified a putative cation–π interaction at the dimer interface. This interaction, along with a network of hydrophobic contacts, may play an important role in stabilizing the dimer and higher-order oligomers in the membrane. This has both structural and functional implications, given that the single TMD of CLIC1 alone is insufficient to form an ion-conducting membrane channel.

To improve our understanding of the process of oligomerization in CLIC1, we probed the role of Lys37 as a key residue in maintaining the specificity and stability of dimerization in the TMD. In this study, we examined the secondary, tertiary, and quaternary structural changes of a K37M CLIC1 TMD mutant as it partitions between an aqueous and membrane-mimicking environment.

MATERIALS AND METHODS

Modeling of TMD Dimer Conformations. The CLIC1 TMD sequence (Figure 1) was built into uniform α-helices with ideal backbone torsion angles of −65° (φ) and −40° (ψ) using Chimera version 1.6.2. Side chain rotamers were chosen using the backbone-dependent rotamer library program SCWRL.[22] Subsequently, the dimeric structure of the CLIC1 TMD was reconstructed using the PREDDIMER algorithm (http://model.nmr.ru/preddimer/).[23] Packing efficiencies of the predicted conformations were estimated according to the PREDDIMER scoring function (F_{SCOR}).

Peptide Design and Synthesis. The 30-residue CLIC1 K37M TMD peptide (22-GNCPFSQRLFMVLWLMGVTFN-VTTVDTKRR-51) containing a carboxylated amino terminus and an amidated carboxyl terminus was synthesized using a solid phase continuous flow system by GL Biochem (Shanghai, China). Its purity was determined to be >95% using high-performance liquid chromatography.

Sample Preparation. Samples were solubilized in 100% (v/v) methanol to yield a 1 mM stock solution and prepared as previously described.[19] Incorporation of the peptide into SDS micelles and POPC liposomes was conducted according to an established protocol.[19] Lucigenin-encapsulated liposomes were prepared using a method identical to that described previously[19] with the inclusion of 10 mM Lucigenin (Sigma-Aldrich) and 15 mM potassium acetate in reconstitution buffer. Free Lucigenin was removed by size-exclusion chromatography on a Sephadex G-25 column equilibrated with reconstitution buffer.

CD and Fluorescence Spectroscopy. Far-UV CD and fluorescence spectra of the K37M peptide were recorded in TFE, SDS, and POPC as described previously.[19] Spectra were buffer-corrected and smoothed using the negative exponential method. CD spectra were normalized to mean residue ellipticity ($[\theta]$) using the equation

$$[\theta] = (100\theta)/(cnl)$$

where $[\theta]$ is the molar ellipticity (degrees square centimeter per decimole), θ is the ellipticity (millidegrees), c is the protein concentration (millimolar), n is the number of residues in the peptide, and l is the path length (centimeters). For all far-UV CD analyses, n = 30 and l = 0.1 cm. A quantitative estimation of the secondary structure content of the TMD peptide was made using the CDPro software package as described previously.[19,24] The standard error of the secondary structural elements was determined from four separate CDPro analyses.

To analyze the effect of oxidation, 10 μM peptide was incubated with 2 mM H_2O_2 for 0–24 h and analyzed as previously described.[19] Acrylamide and iodide quenching was also performed as described previously.[19] The fluorescence intensity at 345 nm was monitored and analyzed according to the Stern–Volmer relationship:

$$F_0/F = 1 + K_{SV}[Q]$$

where F_0 and F are the emission intensities in the absence and presence of the quencher, respectively, [Q] is the concentration of the quencher, and K_{SV} is the Stern–Volmer constant.

DTNB Assay. DTNB (5,5′-dithio-2-nitrobenzoic acid) is a water-soluble compound used to quantify free thiol (-SH) groups in solution based on their solvent accessibility. The

dx.doi.org/10.1021/bi401433f | *Biochemistry* 2014, 53, 57–67

CLIC1 K37M TMD contains a single cysteine residue at position 24. The DTNB assay was performed as described previously[19] in SDS and POPC. In the case of liposome samples, two versions of the DTNB assay were performed: (i) as described above with extrinsic DTNB added to samples and (ii) using DTNB encapsulated within the liposomes. The aim of these two methods was to probe whether Cys24 is located at the *cis* or *trans* face of the membrane mimetic. The concentration of 2-nitro-5-thiobenzoic acid (NTB) was determined spectrophotometrically at 412 nm using an extinction coefficient of 13600 M^{-1} cm^{-1}.[25] The proportion of free thiols was obtained from the ratio of NTB concentration to peptide concentration.

Tricine Sodium Dodecyl Sulfate–Polyacrylamide Gel Electrophoresis (SDS–PAGE). The oligomeric state of the K37M TMD peptide in SDS micelles was investigated by gel electrophoresis. A modified Tricine buffer system[26] with a 0.5% SDS gel was used. Samples were prepared and electrophoresed as described previously.[19] A dimer control was included by incubating samples with 2 mM H_2O_2 in the absence of β-mercaptoethanol, thereby inducing the formation of a Cys24–Cys24 disulfide bond between two peptides. Silver staining was performed using the SilverQuest kit (Life Technologies, Carlsbad, CA) according to the manufacturer's instructions. Band intensities were quantified using ImageJ (http://rsbweb.nih.gov/ij/).

UV Absorption. To probe whether a cation–π interaction occurs between Lys37 and Phe41/Trp35, UV absorption spectra of the wild-type and K37M peptides were recorded. This method of detecting cation–π interactions is based on the weakening of the B_b tryptophan absorbance (at ~220 nm) accompanied by a red shift to ~230 nm in the presence of these interactions.[27,28] The negative–positive peak pair at 220/230 nm is considered a marker of tryptophan residues involved in cation–π interactions. Samples of 10 μM wild-type or K37M peptides were analyzed in buffer [20 mM sodium phosphate and 1 mM DTT (pH 5.5)], 40% (v/v) TFE, or 15 mM SDS. Spectra were recorded between 200 and 300 nm in a 1 cm quartz cuvette using a Jasco V-630 spectrophotometer (Jasco, Tokyo, Japan) at 20 °C and are an average of three accumulations. Spectra were buffer-corrected and plotted as the difference between the SDS and TFE spectra (SDS − TFE). The TFE spectra serve as controls for no interaction as TFE inhibits quaternary contacts.[29]

Chloride Influx Assay. To determine whether (i) the TMD peptide has been functionally reconstituted into membranes and (ii) dimerization is required for function, a method for monitoring the movement of chloride ions across a phospholipid bilayer was developed. The assay is based on the quenching of an encapsulated chloride-sensitive fluorescent dye Lucigenin by extravesicular chloride ions.

Wild-type or K37M TMD peptides were mixed with Lucigenin-encapsulated liposomes (see Sample Preparation) and left to equilibrate covered for 2 h. The final lipid concentration was 2.5 mM, and final peptide concentrations were between 2 and 50 μM. Blank samples were supplemented with appropriate volumes of 100% (v/v) methanol. The CLIC1 activity has previously been shown to be pH-sensitive.[30] Therefore, samples were analyzed at either (i) pH 7.2, the pH of the cytosol, or (ii) pH 5.5, the pH at the membrane surface. Fluorescence emission spectra of the encapsulated dye were recorded between 400 and 600 nm in a 1 cm quartz cuvette using a Perkin-Elmer LS50B luminescence spectrometer (Perkin-Elmer, Waltham, MA) at 20 °C and are an average of five accumulations. An excitation wavelength of 368 nm, a scan speed of 250 nm/min, and 3.5 nm slit widths were used. Peptide samples were prepared and analyzed in 20 mM sodium phosphate, 15 mM potassium chloride, 1 mM DTT, and 0.02% sodium azide (pH 5.5 or 7.2). The percent quenching following the addition of 4 μM valinomycin was determined according to

$$(1 - F_{484P}/F_{484B}) \times 100\%$$

where F_{484P} and F_{484B} represent the emission intensity at 484 nm in the presence and absence of the TMD peptide, respectively. The kinetics of chloride influx was monitored at 484 nm as described, following the addition of 20 μM wild-type or K37M TMD peptide. Data were fit to either a single- or double-exponential decay model in SigmaPlot version 11.0 from which the observed rate constants (k_{obs}) were derived.

RESULTS

Predicted Structure of the CLIC1 TMD Dimers. We have previously demonstrated that the CLIC1 TMD forms stable dimers in membrane mimetics.[19] The putative conformation of the dimer was predicted by the PREDDIMER algorithm[23] (Figure 2). This model has the top-ranking score (F_{SCOR} = 3.1) among other possible variants and represents the

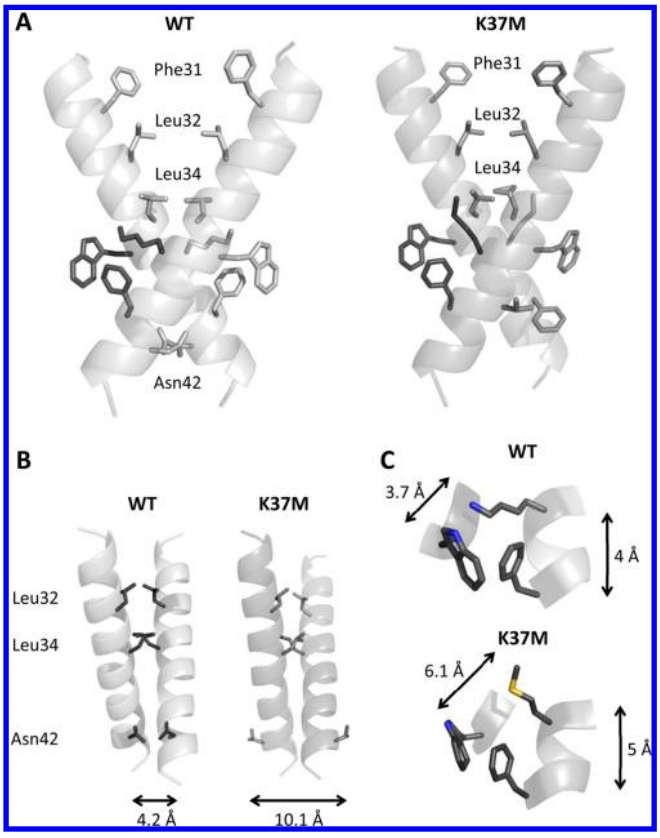

Figure 2. Modeled structure of the CLIC1 TMD dimers. (A) The dimeric wild-type and K37M CLIC1 TMD was modeled using the PREDDIMER algorithm.[23] The interacting helices cross at an angle of 60° to form a symmetric dimer ~32 Å in length. The dimer interface comprises a network of hydrophobic residues (B) as well as a cation–π interaction between Lys37 and Trp35/Phe41 (C). The C_α–C_α distances between Asn42 and Asn42, Trp35 and Lys37/Met37, and Phe41 and Lys37/Met37 are shown. All figures were rendered using PyMol version 1.3.

dx.doi.org/10.1021/bi401433f | *Biochemistry* 2014, 53, 57–67

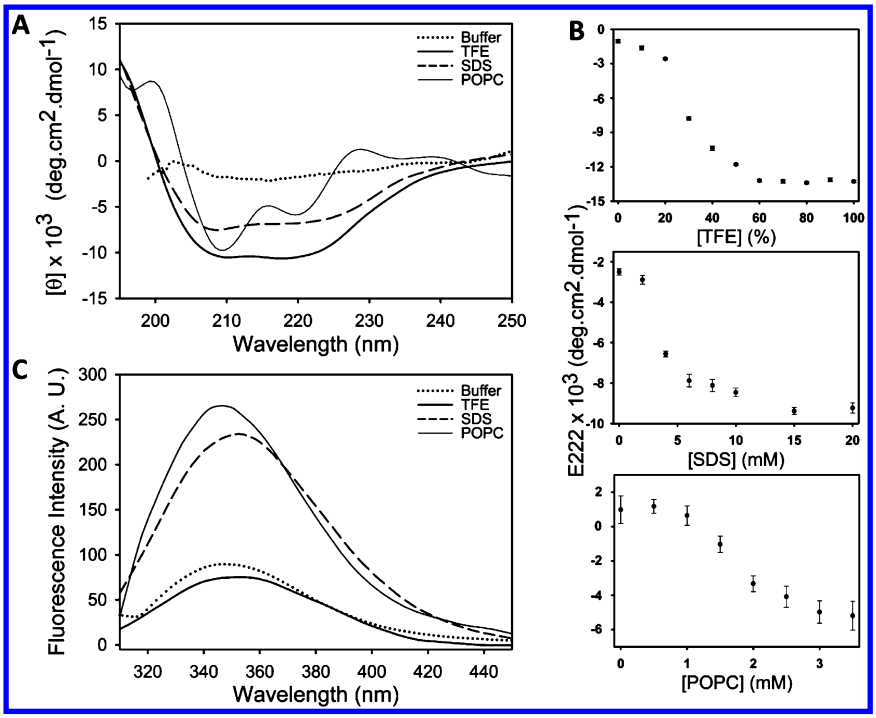

Figure 3. Secondary and tertiary structure of the CLIC1 K37M TMD peptide. Far-UV CD (A and B) and tryptophan fluorescence (C) spectra were recorded in buffer (dotted), in 40% (v/v) TFE (thick solid), in 15 mM SDS micelles (dashed), and in 2.5 mM POPC (thin solid). (A) In solution, the peptide is unstructured, whereas the addition of TFE, SDS, and POPC induces α-helical secondary structure. (B) The helical content of 15 μM peptide is maximal at 60% (v/v) TFE, 15 mM SDS, and 3 mM POPC, after which no further increase in helicity is observed. (C) In TFE, the peptide emits maximally at 353 nm, whereas SDS and POPC induce both a blue-shifted λ_{max} (346 and 339 nm) and a 2.5-fold increase in emission intensity. This indicates that Trp35 becomes located in a hydrophobic environment, presumably inserted into the SDS micelles or POPC liposomes. The buffer consisted of 20 mM sodium phosphate, 1 mM DTT, and 0.2% (w/v) sodium azide (pH 5.5). Error bars represent the standard deviation from four independent replicates.

dimer with the best packing efficiency. The model comprises TMD residues 22−46 with a total hydrophobic length of ∼32 Å. The helices form a symmetric right-handed dimer with a crossing angle of −60°. The dimer interface comprises a series of hydrophobic interactions that include Phe31, Leu32, Leu34, and Asn42. In addition, a cation−π interaction between Lys37 and Trp35 was identified. The residues involved in this interaction are conserved across the vertebrate CLICs as well as the *Drosophila melanogaster* CLIC homologue (Figure 1C). On the basis of this model, we created the K37M TMD mutant to probe whether the predicted cation−π interaction was involved in dimer formation and/or stabilization. The K37M TMD dimer has packing properties similar to those of the wild type (Figure 2A). However, the rotational angle of the helices is asymmetric compared to that of the wild type, which results in the loss of contact between Asn42 residues on opposite chains (Figure 2B). The proximity of Met37 to both Trp35 and Phe41 is also reduced (Figure 2C) compared to that of the wild type.

Secondary Structure Content. The far-UV CD spectra of the K37M TMD peptide in aqueous buffer, TFE, SDS micelles, and POPC liposomes are shown in Figure 3. In solution, the peptide is unstructured. Upon addition of TFE, SDS micelles, or POPC liposomes, the CD spectra exhibit two minima near 208 and 222 nm, which is characteristic of a predominantly α-helical conformation. Much like that of the wild-type peptide, the spectra in POPC displayed an additional maximum at ∼228 nm that can be attributed to aromatic side chains adopting an ordered conformation.[31] In addition, the molar ellipticity of the K37M TMD peptide in TFE was 25 ± 4% and 12 ± 2% higher than that in SDS micelles and POPC liposomes, respectively. This suggests that a greater proportion of peptide assumes an α-helical conformation under these conditions compared to a micellar/vesicle environment. Quantitative secondary structure analysis of the wild-type and K37M peptides is summarized in Table 1. Both peptides show a similar trend, with membrane mimetics inducing an increase in α-helical content and decreases in β-structure and unordered structure content (Table 1). The α-helical content of the K37M peptide increased sigmoidally with increasing TFE, SDS, and POPC concentrations, reaching a maximum at 60% (v/v) TFE, 15 mM SDS, or 3 mM POPC (Figure 3B). Compared to the wild-type peptide (see Table 1), the K37M mutant requires an additional 20% (v/v) TFE or 0.5 mM POPC to achieve maximal helicity. The thermal stability of the peptide was also analyzed by measuring the ellipticity at 222 nm in 40% TFE or 15 mM SDS at increasing temperatures (Figure S1 of the Supporting Information). Both the wild-type and K37M peptides unfolded via noncooperative and fully reversible pathways. The sequential, rather than simultaneous, disruption of amide hydrogen bonds resulting in this behavior is characteristic of transmembrane helices.[32]

Tertiary Structure. The K37M TMD peptide contains a lone tryptophan residue at position 35 that can be used as a reporter of local tertiary structural changes. In solution, the peptide exhibits a fluorescence emission spectrum with a low emission intensity and a maximal emission wavelength (λ_{max}) of 349 nm (Figure 3C). The introduction of a methionine at position 37 has caused a 6 nm blue shift of the λ_{max} compared to that of the wild-type peptide (see Table 1). In the presence of TFE, the emission intensity was reduced by ∼25% while

dx.doi.org/10.1021/bi401433f | *Biochemistry* 2014, 53, 57−67

Table 1. Structural Changes of the Wild-Type and K37M CLIC1 TMD Peptides in Response to Membrane Mimetics[a]

	buffer	TFE	SDS	POPC
α-helix (%)[b]	18 ± 5	64 ± 8	59 ± 10	56 ± 9
	17 ± 6	67 ± 9	60 ± 3	61 ± 5
β-sheet (%)[b]	23 ± 4	9 ± 2	7 ± 3	11 ± 6
	25 ± 6	8 ± 4	7 ± 4	8 ± 3
random coil (%)[b]	56 ± 9	22 ± 9	29 ± 7	31 ± 11
	54 ± 7	21 ± 5	31 ± 6	28 ± 9
NRMSD	0.23	0.095	0.11	0.17
	0.19	0.104	0.096	0.14
λ_{max} (nm)	355 ± 2	355 ± 1	343 ± 1	342 ± 3
	349 ± 3	353 ± 2	346 ± 3	339 ± 2
K_{SV} (M^{-1})[c]	15.35 ± 0.23, 3.52 ± 0.12	ND[e]	5.66 ± 0.1, 1.03 ± 0.09	7.01 ± 0.76
	8.6 ± 0.16, 2.53 ± 0.13	ND[e]	2.42 ± 0.08, 1.08 ± 0.13	2.79 ± 0.09
fraction of free thiols[d]	0.98 ± 0.01	ND[e]	0.64 ± 0.009	0.39 ± 0.01, 0.63 ± 0.03
	1 ± 0.02	ND[e]	0.67 ± 0.012	0.4 ± 0.011, 0.61 ± 0.014
thermal unfolding	ND[e]	linear	linear	ND[e]
	ND[e]	linear	linear	ND[e]

[a]Wild-type values are shown first. The results for the wild type have been published previously.[19] The standard deviation from four independent replicates is given. [b]CDPro reference set SP43. [c]Samples with two values represent the K_{SV} determined from acrylamide and iodide quenching, respectively. [d]In POPC, the first value represents external DTNB (*cis*) while the second value represents encapsulated DTNB (*trans*). [e]Not determined.

shifting the λ_{max} to 353 nm. Both SDS and POPC induced a blue-shifted λ_{max} (346 and 339 nm) and a 2.5-fold increase in emission intensity. This behavior is similar to that of the wild type and suggests that Trp35 of the TMD peptide is inserted into the SDS micelles or POPC liposomes. The local environment of Trp35 may also be influenced by quaternary interactions in addition to interactions with the mimetics, particularly if Trp35 is located at or near an oligomer interface.

We have previously demonstrated that, under oxidizing conditions, the emission spectra of Trp35 are quenched by H_2O_2 on the basis of solvent accessibility.[19] This is a result of the conversion of the indole ring to oxyindole over time. As with the wild-type peptide, the K37M peptide shows ~5% quenching in SDS and POPC, ~20% quenching in TFE, and ~30% quenching in solution over 24 h (Figure 4C). This reflects the nature of the mimetic, with the peptide being inserted into the POPC liposomes or SDS micelles and partially shielded by the TFE. The overall levels of quenching in the K37M peptide are, on average, 10−20% lower than in the wild type. This correlates well with the λ_{max} values that are blue-shifted relative to that of the wild-type peptide.

Solvent Accessibility of Trp35 and Cys24 in SDS Micelles or POPC Liposomes. The wild-type CLIC1 TMD peptide spontaneously associates with and inserts into SDS micelles or POPC liposomes.[19] To determine whether the K37M mutation interferes with this interaction, dynamic fluorescence quenching with acrylamide or iodide and a DTNB assay were conducted. Panels A and B of Figure 4, Figure S2 of the Supporting Information, and Table 1 show the Stern−Volmer constants (K_{SV}) obtained using acrylamide and iodide. This constant reflects residue accessibility, with low values indicating residues with a low level of exposure and vice versa. In the absence of membrane mimetics, both acrylamide

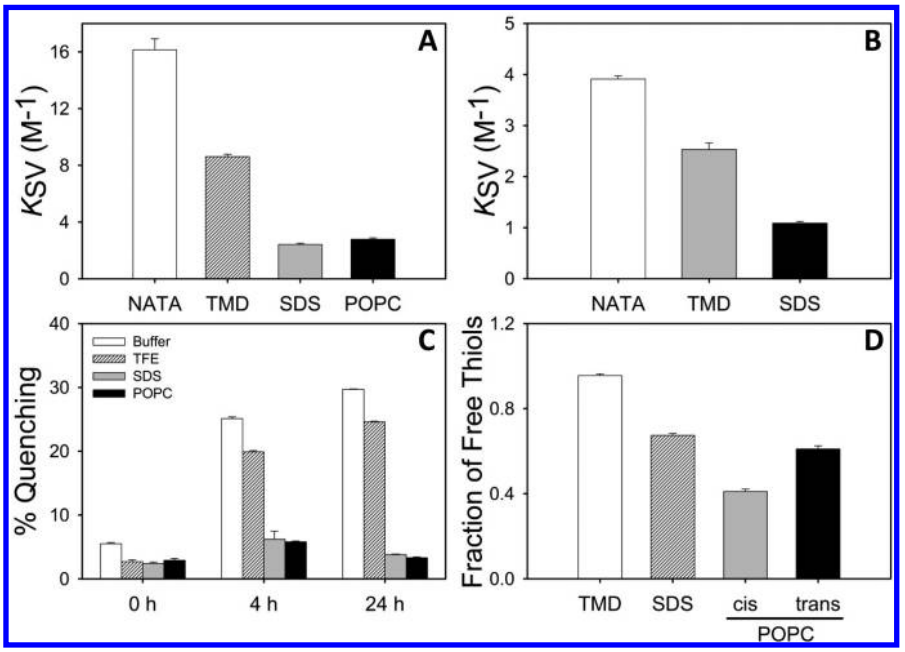

Figure 4. Solvent accessibility of the CLIC1 K37M TMD peptide in SDS micelles and POPC liposomes. Dynamic acrylamide (A), iodide (B), and H_2O_2 (C) quenching as well as a DTNB assay (D) were performed in the absence and presence of 40% (v/v) TFE (C only), 15 mM SDS, or 2.5 mM POPC. For panel C, samples were analyzed by fluorescence following the addition of 2 mM H_2O_2. In panel D, TMD refers to the free TMD peptide in solution, SDS refers to the TMD peptide inserted into SDS micelles, *cis* refers to external DTNB, and *trans* refers to encapsulated DTNB. The buffer consisted of 20 mM sodium phosphate, 1 mM DTT, and 0.2% (w/v) NaN_3 (pH 5.5) (quenching) or 20 mM Na_2PO_4, 1 mM EDTA, and 0.2% (w/v) sodium azide (pH 6.0) (DTNB assay). Error bars represent the standard deviation from four independent replicates.

dx.doi.org/10.1021/bi401433f | *Biochemistry* 2014, 53, 57−67

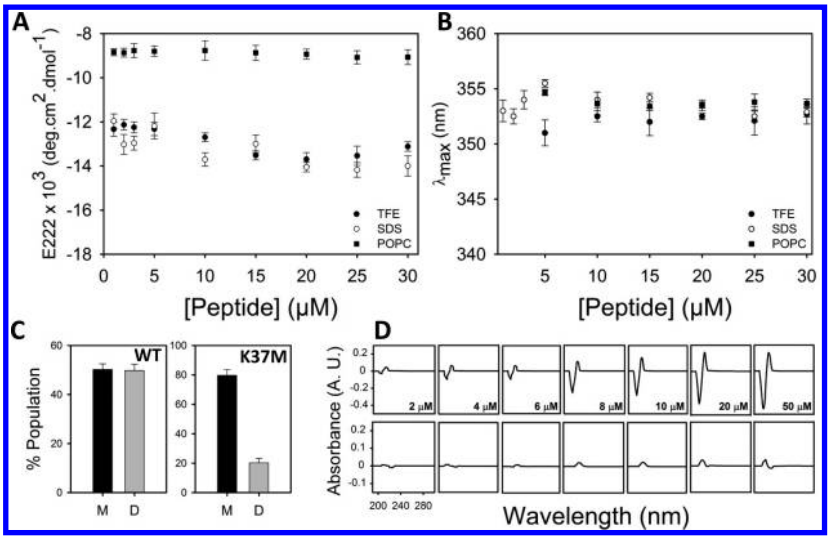

Figure 5. Lys37 mediates the noncovalent dimerization of the CLIC1 TMD peptide via a cation−π interaction. The E_{222} (A) and λ_{max} (B) values from K37M peptide samples incubated in SDS micelles or POPC liposomes show no change at increasing peptide concentrations and are identical to the values of samples incubated in TFE. (C) The monomeric and dimeric forms of 15 μM wild-type (left) and K37M (right) peptides were isolated using SDS−PAGE and band intensities quantified using ImageJ. Removal of Lys37 severely reduces the population of dimeric species compared to the population of the wild type. (D) UV absorption of the wild-type (top) and K37M (bottom) TMD peptides shows that Lys37 forms a cation−π interaction that presumably stabilizes the helical dimer. The negative−positive peak pair at 220/230 nm is considered a marker of tryptophan residues involved in cation−π interactions.[27,28] Error bars represent the standard deviation from four independent replicates.

(K_{SV} = 8.6 M^{-1}) and iodide (K_{SV} = 2.53 M^{-1}) quenching of the K37M peptide yield Stern−Volmer constants that are roughly 2-fold lower than that of either free NATA in solution (16.15 M^{-1} with acrylamide and 3.88 M^{-1} with iodide) or the wild-type peptide (15.35 M^{-1} with acrylamide and 3.52 M^{-1} with iodide). Upon addition of SDS micelles or POPC liposomes, a further 3-fold decrease in acrylamide accessibility occurs. This reduction is 2.5-fold greater for the K37M peptide than for the wild-type peptide (see Table 1). The iodide accessibility of the peptide in the presence of SDS, however, is similar to that of the wild type. This correlates well with data from H_2O_2-induced quenching and indicates that Trp35 (i) is protected from quenching by the micelles and liposomes and (ii) is less solvent accessible in the K37M mutant than in the wild type.[33]

Unlike that of Trp35, the solvent accessibility of Cys24 remains unchanged in the K37M peptide with an ∼35% reduction in the fraction of free thiols following the addition of SDS micelles (Figure 4D and Table 1). In POPC, a dual DTNB assay was employed whereby samples contained either extrinsic DTNB (*cis* face) or DTNB encapsulated within the liposomes (*trans* face). The data shown in Figure 4D suggest that the *trans* configuration is more prominent (∼60%) whereas only 30−35% of the residues react with extrinsic DTNB. This is identical to the case for the wild-type peptide (Table 1) and suggests that the orientation of Cys24 is not affected by the K37M mutation.

Role of Lys37 in Dimerization of the CLIC1 TMD. We have previously demonstrated, using concentration-dependent studies and SDS−PAGE, that the CLIC1 TMD forms stable dimers in membrane mimetics.[19] Panels A and B of Figure 5 show the results of concentration-dependent studies of K37M peptide samples incubated in TFE, SDS, and POPC. Both the E_{222} and λ_{max} values showed little to no change in either SDS or POPC and followed a trend similar to that of the samples incubated in TFE. Because TFE inhibits quaternary interactions,[29] the similar data from the three mimetics suggest that removal of Lys37 has severely impeded self-association of the peptide.

Tricine SDS−PAGE was subsequently used to assess the effect of the mutation on the formation of dimeric TMD (Figure S3 of the Supporting Information). The use of SDS−PAGE to monitor TMD association has been well-documented.[34−37] The K37M mutation has reduced the population of dimeric species by ∼30%, with the majority of the peptide remaining monomeric across all concentrations tested (Figure 5C and Figure S3 of the Supporting Information). The extent of smearing of the peptide band at high concentrations was also reduced relative to that of the wild type (Figure S3 of the Supporting Information). This suggests impaired formation of higher-order oligomers. Like that of the wild-type peptide, the migration patterns were independent of pH, denaturation, and reducing conditions. This agrees well with the reversible thermal denaturation (Figure S1 of the Supporting Information) and suggests that the helix−helix interactions between TMD peptides are noncovalent. The presence of a stabilizing noncovalent cation−π interaction is therefore probable.

To further investigate whether a cation−π interaction is involved in dimerization, the concentration dependence of UV absorption was examined in the wild-type and K37M TMD peptides. This method of detecting cation−π interactions is based on the weakening of B_b tryptophan absorbance (at ∼220 nm) accompanied by a red shift to ∼230 nm in the presence of these interactions.[27,28] The negative−positive peak pair at 220/230 nm is considered a marker of tryptophan residues involved in cation−π interactions.[27,28] Figure 5D compares the difference UV absorption spectra of the wild-type and K37M peptides. The wild-type peptide exhibits a positive peak at ∼230 nm and a weaker negative peak at ∼220 nm. This is consistent with previously described reports of tryptophan residues involved in cation−π interactions.[27,28] In the K37M peptide, the negative−positive peak pair at 220/230 nm is no longer observed. Instead, the spectra resemble those of the TFE control in which helix−helix interactions are absent. This

dx.doi.org/10.1021/bi401433f | *Biochemistry* 2014, 53, 57−67

observation suggests that Lys37 and Trp35 are involved in a cation−π interaction.

Chloride Influx Assay. Given that the single TMD of CLIC1 must oligomerize to form a functional channel, dimerization is likely to play a role in Cl^- conductance. The emission spectra of the liposome-encapsulated chloride-sensitive dye Lucigenin at pH 7.4 and 5.5 at various peptide concentrations are shown in Figure 6. The dye emits maximally

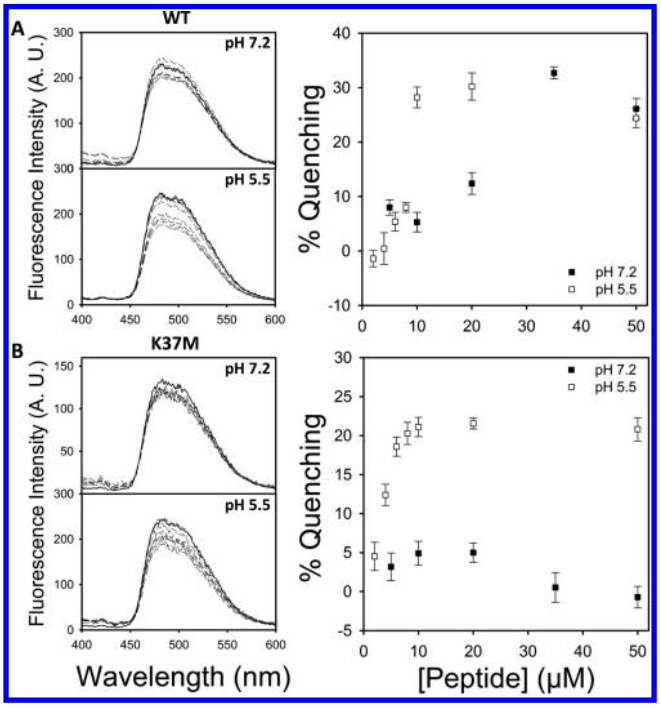

Figure 6. CLIC1 TMD alone is sufficient for chloride ion transport. A chloride influx assay was performed at increasing wild-type (A) and K37M (B) peptide concentrations, based on the quenching of the encapsulated dye Lucigenin. The solid line shows the sample in the absence of peptide, while the dashed lines are samples incubated with 2−50 μM peptide. Removal of Lys37 reduces the efficiency of transport at pH 5.5 and completely eliminates activity at pH 7.2. This is likely a result of (i) disrupted pore formation caused by impaired dimerization coupled with (ii) weakened membrane adsorption at neutral pH. The buffer consisted of 20 mM sodium phosphate, 15 mM potassium chloride, 1 mM DTT, and 0.02% sodium azide (pH 5.5 or 7.2). Error bars represent the standard deviation from four independent replicates.

at 484 nm at both pH values and at all peptide concentrations. Figure 6 shows the percentage quenching of the dye for the wild-type and K37M peptides. The wild-type peptide shows a concentration-dependent increase in the level of dye quenching at both pH values. Maximal quenching (~35%) is achieved between 10−20 μM (pH 5.5) and 30−40 μM (pH 7.2) peptide. The K37M mutation reduces the efficiency of chloride transport by 15% at pH 5.5. At pH 7.2, the K37M peptide shows neither concentration dependence nor significant chloride conductance. The contribution of the methanol solvent was shown to be negligible (Figure S4 of the Supporting Information).

In an attempt to improve our understanding of the mechanism of chloride influx and the role played by dimerization, we investigated the kinetics of chloride influx. Figure 7 shows averaged traces of peptide-mediated quenching of Lucigenin fluorescence. The observed rate constants for

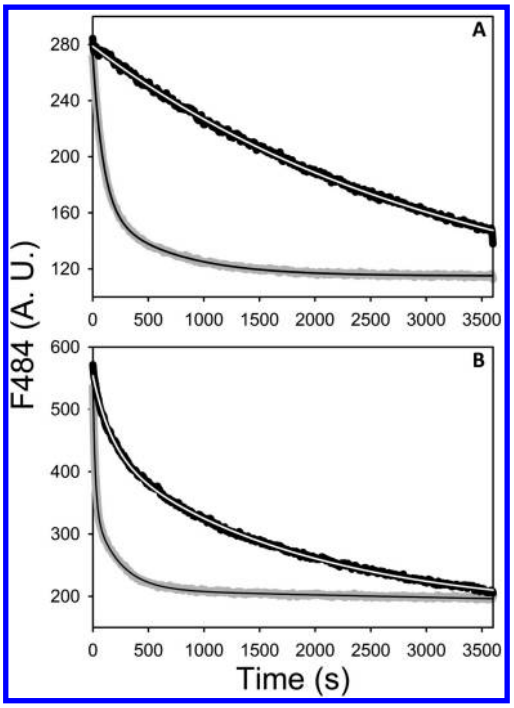

Figure 7. Dimerization modulates the kinetics of chloride influx. The kinetics of chloride influx in the wild-type (gray) and K37M (black) TMD peptides were measured at pH 7.2 (A) and pH 5.5 (B). The curves represent averages of four independent experiments. The data were fit to either a single- or double-exponential decay model using SigmaPlot version 11.0, and fits are shown as solid lines through the data. Removal of Lys37 severely impairs the rate of chloride influx, and the rate is 35-fold (pH 7.2) and 8-fold (pH 5.5) lower than that of the wild type. The buffer consisted of 20 mM sodium phosphate, 15 mM potassium chloride, 1 mM DTT, and 0.02% sodium azide (pH 5.5 or 7.2).

chloride influx (k_{obs}) are listed in Table 2. At pH 7.2, the wild-type peptide displays a two-state mechanism whereas the K37M peptide shows a single state. This is accompanied by an ~35-fold reduction in k_{obs} compared to that of the wild-type peptide. The additional state observed for the wild-type peptide may be attributable to the dimerization process. At pH 5.5, both the wild-type and K37M peptides display a two-state mechanism. The difference in k_{obs} between the wild-type and K37M peptides is reduced to 8- and 2-fold for the two states, respectively. This correlates well with the equilibrium quenching measurements that show that K37M-induced quenching reaches near wild-type levels at pH 5.5.

DISCUSSION

Membrane-bound CLIC1 plays key roles in cell signaling, homeostatic, and apoptotic processes.[38−40] To perform these functions, CLIC1 monomers must insert into membranes and oligomerize to form a chloride ion channel.[21] Despite its physiological relevance, the nature of CLIC1 oligomerization remains poorly understood. Here we report a cation−π interaction implicated in stabilizing the dimeric form of the CLIC1 TMD as it partitions between an aqueous and membrane-mimicking environment. The lysine side chain (Lys37) involved in the interaction was mutated to a methionine, and the resulting changes in the secondary, tertiary, and quaternary structure were observed.

dx.doi.org/10.1021/bi401433f | Biochemistry 2014, 53, 57−67

Table 2. Observed Rate Constants for Peptide-Mediated Chloride Influx[a]

	pH 7.2			pH 5.5		
	k_{obs1} (s^{-1})	k_{obs2} (s^{-1})	R^2	k_{obs1} (s^{-1})	k_{obs2} (s^{-1})	R^2
WT	0.0108 (2.2×10^{-5})	0.0016 (3.7×10^{-6})	0.9994	0.048 (2×10^{-4})	0.0044 (1.1×10^{-5})	0.9986
K37M	0.0003 (8.2×10^{-7})	not available	0.999	0.0058 (3.5×10^{-5})	0.0006 (2.1×10^{-6})	0.9991

[a]Data were fit to either a single- or double-exponential decay model[42] in SigmaPlot version 11.0, from which the observed rate constants (k_{obs}) were derived. The fit error from four independent replicates is given in parentheses.

Lys37 Does Not Direct Folding, Stability, or Membrane Insertion of the CLIC1 TMD. Removal of Lys37 has little impact on the secondary structure of the TMD peptide (Figure 3A,B). In the presence of membrane mimetics, the TMD still undergoes a dramatic structural rearrangement to form an α-helix. This is analogous to the case for the wild type and is consistent with the predicted membrane conformation of the TMD. This residue is therefore unlikely to be involved in the unfolding and/or refolding of the TMD, which is thought to occur at the membrane−cytosol interface.[19,41] The local tertiary structure of the peptide was, however, altered following the removal of Lys37 (Figure 3C). This is not surprising, given the proximity of Lys37 to the lone Trp35 probe. The observed effect can be explained by (i) the introduction of a hydrophobic pocket by methionine or (ii) the lowered local polarity resulting from the removal of Lys37. The latter is of particular interest as there have been several reports of lysine-induced quenching of tryptophan fluorescence when the two residues are involved in a cation−π interaction.[43,44] It is unlikely, however, that removal of Lys37 induces large-scale structural perturbations because the stability of the peptide in membrane mimetics is independent of this residue (Figure S1 of the Supporting Information). Surprisingly, Lys37 remains highly conserved throughout the CLIC family despite being implicated in neither folding nor stability (Figures 1 and 2 and Figure S1 of the Supporting Information). This is compounded by the fact that polar residues are often excluded from transmembrane segments on the basis of their unfavorable energetic contributions in a hydrophobic environment.[45] It is evident, then, that Lys37 must play a specialized role in insertion, oligomerization, and/or function. Fluorescence quenching studies indicate that Lys37 is not, in fact, required for the insertion of the peptide into SDS micelles or POPC liposomes (Figure 4A−C and Figure S7 of the Supporting Information), nor does it affect the orientation of the peptide in these mimetics (Figure 4D). The fact that the wild-type peptide does not show impaired membrane insertion (based on K_{SV} values) relative to those of other peptides lacking polar transmembrane residues[46,47] suggests an alternative role for Lys37.

Lys37 Provides a Driving Force for Helix−Helix Association. The insertion of Lys37 into the membrane requires the energetically unfavorable removal of polar groups from water. To compensate for this, a buried interaction involving Lys37 is likely required. An examination of the structures of several transmembrane domains[48] suggests that when lysine residues are present in transmembrane helices, they rarely occur in regions exposed to membrane lipids. Rather, the amide groups form intra- and interchain contacts with other regions of the peptide.[49] Thus, a buried interaction involving Lys37 may help to direct helix−helix contacts (i.e., oligomerization).

To confirm this theory, we modeled the putative CLIC1 TMD dimer to complement CD, UV, and SDS−PAGE analyses (Figures 2 and 5). The characteristic GxxxG motif[5] found in many transmembrane helical dimers is absent. A study by Doura and Fleming[51] showed that the GxxxG motif is, in fact, neither necessary nor sufficient for dimerization. Rather, the ability of helices to dimerize is governed by complex and detailed interactions at the helix−helix interface.[50] These small residue motifs are replaced by a network of hydrophobic interactions at the dimer interface that presumably contribute to stabilizing the dimeric conformation (Figure 2B). Perhaps most significant was the identification of a putative cation−π interaction between Lys37 and Phe41/Trp35. We validated this finding experimentally and showed that the removal of the lysine cation severely impairs the ability of the TMD to dimerize (Figure 5). The residual dimeric population is likely a result of the hydrophobic contacts (Figure 2B) that maintain weak helix−helix association. A stabilizing cation−π interaction involving Lys37 is therefore likely to play a key role in the dimerization of the CLIC1 TMD peptide. This is particularly relevant taking into account the estimated free energy gain associated with interacting Lys and Trp side chains in a hydrophobic medium (~6 kcal/mol).[16]

Dimerization Modulates the Rate of Cl^- Conductance. Given that CLIC1 contains a single TMD, subsequent oligomerization is required to form a functional pore. This process, which completes the two-step folding model, has been poorly characterized in CLIC1. It is clear that, in the absence of higher-order oligomers, CLIC1 is unlikely to function as a chloride channel. We investigated whether removal of Lys37 and the subsequent disruption of dimerization would impair CLIC1 TMD function. Our data suggest that the wild-type TMD alone is capable of conducting Cl^- ions (Figure 6). This highlights the fact that the CLIC1 TMD is a self-contained structural and functional unit when excised from the full-length protein. Removal of Lys37 does not prevent Cl^- transport but does significantly reduce the efficiency of the process. The retention of hydrophobic helix−helix contacts may explain the ability of the K37M peptide to weakly associate and transport Cl^- ions.

The most noticeable effect of removing Lys37 becomes apparent when analyzing the kinetics of chloride influx (Figure 7). Both the wild-type and K37M peptides showed enhanced activity at low pH. This is consistent with previous reports of the full-length protein[30] in which the pH at the membrane is ~2 units lower than in the cytosol. Lysine ($pK_a \sim 10.5$) is unlikely to undergo changes in its ionized state within the pH range tested. Therefore, the observed rate enhancement at low pH is likely a result of enhanced membrane adsorption resulting from changes in lipid charge. We assume that the rate-limiting step is the insertion and oligomerization of the peptide rather than Cl^- influx. This is the most conservative assumption given that diffusion of Cl^- ion to the pore as well as through the pore is rapid.[52] Hence, the apparent rate constant of Cl^- influx depends on the Gibbs free energies of membrane binding, insertion, and oligomerization. Because binding and insertion do not appear to be altered by the mutation (Figures 3 and 4

dx.doi.org/10.1021/bi401433f | Biochemistry 2014, 53, 57−67

and Figure S7 of the Supporting Information), the difference in the rate of Cl^- influx between the wild-type and K37M peptides is likely a result of oligomerization. Because there are few changes in the kinetics of membrane insertion (Figure S7 of the Supporting Information), we postulate that the decrease in rate is a result of an alteration in the equilibrium of pore formation. With only relatively weak hydrophobic interactions maintaining the dimer, dissociation of the dimer or oligomer would be frequent and the overall rate of chloride transport reduced. Studies by Warton et al.[30] suggest that a CLIC1 dimer may represent a weakly active protopore that subsequently oligomerizes to form the fully active channel. This could describe the observed two-step mechanism of Cl^- influx in the wild-type peptide and explain why the K37M peptide displays only a single step. Such behavior has been observed for other proteins that spontaneously insert into membranes, including diphtheria toxin,[53] Bax,[54] and Bcl-x_L.[55,56] It must be reiterated that the dimer itself is unlikely to represent the functional pore. Rather, it is likely an intermediate step for the formation of higher-order oligomers that then facilitate pore formation. The CLIC1 oligomerization scheme proposed by Singh[20] most closely matches the mechanism suggested by Warton et al.[30] as well as the data presented here. This scheme postulates a two-step process whereby (i) four TMD helices associate to form a protomer and (ii) four protomers interact to form the ion channel. The initial step may be mediated by the cation−π interaction described here, forming a stable and weakly active dimer or tetramer.

Because the cation−π interaction is not required for membrane partitioning or insertion (Figure S7 of the Supporting Information) but is required for Cl^- conductance, it is possible to propose a sequential mechanism for the membrane insertion of the CLIC1 TMD. (i) The unstructured peptide approaches the membrane interface where it refolds to form an α-helix. (ii) The helix partitions onto the membrane surface, followed by spontaneous insertion to form a membrane-spanning helix. (iii) Individual helices associate via a Lys37-mediated cation−π interaction to form dimers. (iv) Dimeric helix bundles associate to form ion channels. This is consistent with the two-step folding model proposed by Popot and Engelman.[2]

In conclusion, the results presented here represent the first study of the interactions that stabilize CLIC1 TMD oligomers in the membrane. We have identified a cation−π interaction involving Lys37 in addition to a network of hydrophobic contacts at the dimer interface. Although this residue is not required for folding, membrane binding, or insertion, it does facilitate CLIC1 TMD self-association. Mutation of Lys37 to Met37 essentially eliminates oligomerization of the membrane-bound peptide. Thus, within a membrane-like environment, interactions involving a polar lysine side chain provide a thermodynamic driving force for helix−helix association. Dimerization, in turn, is required for the effective transport of chloride ions. Further studies will be necessary to define the three-dimensional structure of the CLIC1 TMD, and future work will involve generating high-resolution structural data.

■ ASSOCIATED CONTENT

Supporting Information

Thermal unfolding of the CLIC1 TMD peptide in SDS and TFE (Figure S1), Stern−Volmer plots for acrylamide and iodide quenching (Figure S2), SDS−PAGE gels of the monomeric and dimeric TMD (Figure S3), the effect of methanol on Lucigenin fluorescence (Figure S4), residuals to the fits of the chloride influx kinetic data (Figure S5), contact maps derived from the PREDDIMER analysis of the wild-type and K37M TMD peptide (Figure S6), and membrane insertion kinetic data (Figure S7). This material is available free of charge via the Internet at http://pubs.acs.org.

■ AUTHOR INFORMATION

Corresponding Author

*E-mail: heinrich.dirr@wits.ac.za. Telephone: +27 11 7176352. Fax: +27 11 7176351.

Funding

This work was supported by the University of the Witwatersrand, South African National Research Foundation Grant 68898 to H.W.D., and the South African Research Chairs Initiative of the Department of Science and Technology and National Research Foundation (Grant 64788 to H.W.D.).

Notes

The authors declare no competing financial interest.

■ ABBREVIATIONS

CD, circular dichroism; CLIC1, chloride intracellular channel protein 1; DTNB, 5,5′-dithio-2-nitrobenzoic acid; DTT, dithiothreitol; λ_{max}, maximal emission wavelength; GST, glutathione transferase; HIV, human immunodeficiency virus; NATA, *N*-acetyl-tryptophanamide; POPC, 1-palmitoyl-2-oleoyl-*sn*-glycero-3-phosphocholine; SDS, sodium dodecyl sulfate; TFE, 2,2,2-trifluoroethanol; TMD, transmembrane domain of CLIC1 (residues 24−46).

■ REFERENCES

(1) Overington, J. P., Al-Lazikani, B., and Hopkins, A. L. (2006) How many drug targets are there? *Nat. Rev. Drug Discovery 5*, 993−996.

(2) Popot, J. L., and Engelman, D. M. (1990) Membrane protein folding and oligomerization: The two-stage model. *Biochemistry 29*, 4031−4037.

(3) White, S. H., and Wimley, W. C. (1999) Membrane protein folding and stability: Physical principles. *Annu. Rev. Biophys. Biomol. Struct. 28*, 319−365.

(4) Johnson, R. M., Hecht, K., and Deber, C. M. (2007) Aromatic and cation-π interactions enhance helix-helix association in a membrane environment. *Biochemistry 46*, 9208−9214.

(5) Russ, W. P., and Engelman, D. M. (2000) The GxxxG motif: A framework for transmembrane helix-helix association. *J. Mol. Biol. 296*, 911−919.

(6) MacKenzie, K. R., Prestegard, J. H., and Engelman, D. M. (1997) A transmembrane helix dimer: Structure and implications. *Science 276*, 131−133.

(7) Choma, C., Gratkowski, H., Lear, J. D., and DeGrado, W. F. (2000) Asparagine-mediated self-association of a model transmembrane helix. *Nat. Struct. Biol. 7*, 161−166.

(8) Gratkowski, H., Lear, J. D., and DeGrado, W. F. (2001) Polar side chains drive the association of model transmembrane peptides. *Proc. Natl. Acad. Sci. U.S.A. 98*, 880−885.

(9) Zhou, F. X., Merianos, H. J., Brunger, A. T., and Engelman, D. M. (2001) Polar residues drive association of polyleucine transmembrane helices. *Proc. Natl. Acad. Sci. U.S.A. 98*, 2250−2255.

(10) Ward, S. D., Curtis, C. A., and Hulme, E. C. (1999) Alanine-scanning mutagenesis of transmembrane domain 6 of the M(1) muscarinic acetylcholine receptor suggests that Tyr381 plays key roles in receptor function. *Mol. Pharmacol. 56*, 1031−1041.

(11) Aliste, M. P., MacCallum, J. L., and Tieleman, D. P. (2003) Molecular dynamics simulations of pentapeptides at interfaces: Salt bridge and cation-π interactions. *Biochemistry 42*, 8976−8987.

(12) Kamiyama, T., Miura, T., and Takeuchi, H. (2013) His-Trp cation-π interaction and its structural role in an α-helical dimer of HIV-1 Vpr protein. *Biophys. Chem. 173*−*174*, 8−14.
(13) Dougherty, D. A. (1996) Cation-π interactions in chemistry and biology: A new view of benzene, Phe, Tyr, and Trp. *Science 271*, 163−168.
(14) Waters, M. L. (2002) Aromatic interactions in model systems. *Curr. Opin. Chem. Biol. 6*, 736−741.
(15) Gromiha, M. M. (2003) Influence of cation-π interactions in different folding types of membrane proteins. *Biophys. Chem. 103*, 251−258.
(16) Polyansky, A. A., Volynsky, P. E., Arseniev, A. S., and Efremov, R. G. (2009) Adaptation of a membrane-active peptide to heterogeneous environment. I. Structural plasticity of the peptide. *J. Phys. Chem. B 113*, 1107−1119.
(17) Johnson, J. E., and Cornell, R. B. (1999) Amphitropic proteins: Regulation by reversible membrane interactions (review). *Mol. Membr. Biol. 16*, 217−235.
(18) Harrop, S. J., DeMaere, M. Z., Fairlie, W. D., Reztsova, T., Valenzuela, S. M., Mazzanti, M., Tonini, R., Qiu, M. R., Jankova, L., Warton, K., Bauskin, A. R., Wu, W. M., Pankhurst, S., Campbell, T. J., Breit, S. N., and Curmi, P. M. (2001) Crystal structure of a soluble form of the intracellular chloride ion channel CLIC1 (NCC27) at 1.4-Å resolution. *J. Biol. Chem. 276*, 44993−45000.
(19) Peter, B., Ngubane, N. C., Fanucchi, S., and Dirr, H. W. (2013) Membrane mimetics induce helix formation and oligomerization of the chloride intracellular channel protein 1 transmembrane domain. *Biochemistry 52*, 2739−2749.
(20) Singh, H. (2010) Two decades with dimorphic Chloride Intracellular Channels (CLICs). *FEBS Lett. 584*, 2112−2121.
(21) Goodchild, S. C., Angstmann, C. N., Breit, S. N., Curmi, P. M., and Brown, L. J. (2011) Transmembrane extension and oligomerization of the CLIC1 chloride intracellular channel protein upon membrane interaction. *Biochemistry 50*, 10887−10897.
(22) Canutescu, A. A., Shelenkov, A. A., and Dunbrack, R. L., Jr. (2003) A graph-theory algorithm for rapid protein side-chain prediction. *Protein Sci. 12*, 2001−2014.
(23) Polyansky, A. A., Volynsky, P. E., and Efremov, R. G. (2012) Multistate organization of transmembrane helical protein dimers governed by the host membrane. *J. Am. Chem. Soc. 134*, 14390−14400.
(24) Sreerama, N., and Woody, R. W. (2000) Estimation of protein secondary structure from circular dichroism spectra: Comparison of CONTIN, SELCON, and CDSSTR methods with an expanded reference set. *Anal. Biochem. 287*, 252−260.
(25) Habeeb, A. F. (1972) Reaction of protein sulfhydryl groups with Ellman's reagent. *Methods Enzymol. 25C*, 457−464.
(26) Schagger, H., and von Jagow, G. (1987) Tricine-sodium dodecyl sulfate-polyacrylamide gel electrophoresis for the separation of proteins in the range from 1 to 100 kDa. *Anal. Biochem. 166*, 368−379.
(27) Xue, Y., Davis, A. V., Balakrishnan, G., Stasser, J. P., Staehlin, B. M., Focia, P., Spiro, T. G., Penner-Hahn, J. E., and O'Halloran, T. V. (2008) Cu(I) recognition via cation-π and methionine interactions in CusF. *Nat. Chem. Biol. 4*, 107−109.
(28) Yorita, H., Otomo, K., Hiramatsu, H., Toyama, A., Miura, T., and Takeuchi, H. (2008) Evidence for the cation-π interaction between Cu^{2+} and tryptophan. *J. Am. Chem. Soc. 130*, 15266−15267.
(29) Roccatano, D., Colombo, G., Fioroni, M., and Mark, A. E. (2002) Mechanism by which 2,2,2-trifluoroethanol/water mixtures stabilize secondary-structure formation in peptides: A molecular dynamics study. *Proc. Natl. Acad. Sci. U.S.A. 99*, 12179−12184.
(30) Warton, K., Tonini, R., Fairlie, W. D., Matthews, J. M., Valenzuela, S. M., Qiu, M. R., Wu, W. M., Pankhurst, S., Bauskin, A. R., Harrop, S. J., Campbell, T. J., Curmi, P. M., Breit, S. N., and Mazzanti, M. (2002) Recombinant CLIC1 (NCC27) assembles in lipid bilayers via a pH-dependent two-state process to form chloride ion channels with identical characteristics to those observed in Chinese hamster ovary cells expressing CLIC1. *J. Biol. Chem. 277*, 26003−26011.
(31) Sreerama, N., Venyaminov, S. Y., and Woody, R. W. (2001) Analysis of protein circular dichroism spectra based on the tertiary structure classification. *Anal. Biochem. 299*, 271−274.
(32) Langosch, D., and Arkin, I. T. (2009) Interaction and conformational dynamics of membrane-spanning protein helices. *Protein Sci. 18*, 1343−1358.
(33) Eftink, M. R., and Ghiron, C. A. (1981) Fluorescence quenching studies with proteins. *Anal. Biochem. 114*, 199−227.
(34) Wigley, W. C., Vijayakumar, S., Jones, J. D., Slaughter, C., and Thomas, P. J. (1998) Transmembrane domain of cystic fibrosis transmembrane conductance regulator: Design, characterization, and secondary structure of synthetic peptides m1-m6. *Biochemistry 37*, 844−853.
(35) Melnyk, R. A., Partridge, A. W., and Deber, C. M. (2001) Retention of native-like oligomerization states in transmembrane segment peptides: Application to the *Escherichia coli* aspartate receptor. *Biochemistry 40*, 11106−11113.
(36) Rath, A., Glibowicka, M., Nadeau, V. G., Chen, G., and Deber, C. M. (2009) Detergent binding explains anomalous SDS-PAGE migration of membrane proteins. *Proc. Natl. Acad. Sci. U.S.A. 106*, 1760−1765.
(37) Walkenhorst, W. F., Merzlyakov, M., Hristova, K., and Wimley, W. C. (2009) Polar residues in transmembrane helices can decrease electrophoretic mobility in polyacrylamide gels without causing helix dimerization. *Biochim. Biophys. Acta 1788*, 1321−1331.
(38) Landry, D. W., Akabas, M. H., Redhead, C., Edelman, A., Cragoe, E. J., Jr., and Al-Awqati, Q. (1989) Purification and reconstitution of chloride channels from kidney and trachea. *Science 244*, 1469−1472.
(39) Fernandez-Salas, E., Sagar, M., Cheng, C., Yuspa, S. H., and Weinberg, W. C. (1999) p53 and tumor necrosis factor α regulate the expression of a mitochondrial chloride channel protein. *J. Biol. Chem. 274*, 36488−36497.
(40) Ronnov-Jessen, L., Villadsen, R., Edwards, J. C., and Petersen, O. W. (2002) Differential expression of a chloride intracellular channel gene, CLIC4, in transforming growth factor-β1-mediated conversion of fibroblasts to myofibroblasts. *Am. J. Pathol. 161*, 471−480.
(41) Fanucchi, S., Adamson, R. J., and Dirr, H. W. (2008) Formation of an unfolding intermediate state of soluble chloride intracellular channel protein CLIC1 at acidic pH. *Biochemistry 47*, 11674−11681.
(42) Demchenko, A. P. (2001) Concepts and misconcepts in the analysis of simple kinetics of protein folding. *Curr. Protein Pept. Sci. 2*, 73−98.
(43) Loewenthal, R., Sancho, J., and Fersht, A. R. (1991) Fluorescence spectrum of barnase: Contributions of three tryptophan residues and a histidine-related pH dependence. *Biochemistry 30*, 6775−6779.
(44) Vos, R., and Engelborghs, Y. (1994) A fluorescence study of tryptophan-histidine interactions in the peptide anantin and in solution. *Photochem. Photobiol. 60*, 24−32.
(45) Partridge, A. W., Melnyk, R. A., and Deber, C. M. (2002) Polar residues in membrane domains of proteins: Molecular basis for helix-helix association in a mutant CFTR transmembrane segment. *Biochemistry 41*, 3647−3653.
(46) Vincent, M., Gallay, J., Jamin, N., Garrigos, M., and de Foresta, B. (2007) The predicted transmembrane fragment 17 of the human multidrug resistance protein 1 (MRP1) behaves as an interfacial helix in membrane mimics. *Biochim. Biophys. Acta 1768*, 538−552.
(47) Freitas, M. S., Gaspar, L. P., Lorenzoni, M., Almeida, F. C., Tinoco, L. W., Almeida, M. S., Maia, L. F., Degreve, L., Valente, A. P., and Silva, J. L. (2007) Structure of the Ebola fusion peptide in a membrane-mimetic environment and the interaction with lipid rafts. *J. Biol. Chem. 282*, 27306−27314.
(48) Singh, H., and Ashley, R. H. (2007) CLIC4 (p64H1) and its putative transmembrane domain form poorly selective, redox-regulated ion channels. *Mol. Membr. Biol. 24*, 41−52.
(49) Groebke, K., Renold, P., Tsang, K. Y., Allen, T. J., McClure, K. F., and Kemp, D. S. (1996) Template-nucleated alanine-lysine helices are stabilized by position-dependent interactions between the lysine

side chain and the helix barrel. *Proc. Natl. Acad. Sci. U.S.A. 93*, 4025−4029.
(50) Burba, A. E., Lehnert, U., Yu, E. Z., and Gerstein, M. (2006) Helix Interaction Tool (HIT): A web-based tool for analysis of helix-helix interactions in proteins. *Bioinformatics 22*, 2735−2738.
(51) Doura, A. K., and Fleming, K. G. (2004) Complex interactions at the helix-helix interface stabilize the glycophorin A transmembrane dimer. *J. Mol. Biol. 343*, 1487−1497.
(52) Almeida, P. F., and Pokorny, A. (2009) Mechanisms of antimicrobial, cytolytic, and cell-penetrating peptides: From kinetics to thermodynamics. *Biochemistry 48*, 8083−8093.
(53) Bennett, M. J., Choe, S., and Eisenberg, D. (1994) Refined structure of dimeric diphtheria toxin at 2.0 Å resolution. *Protein Sci. 3*, 1444−1463.
(54) Garcia-Saez, A. J., Mingarro, I., Perez-Paya, E., and Salgado, J. (2004) Membrane-insertion fragments of Bcl-xL, Bax, and Bid. *Biochemistry 43*, 10930−10943.
(55) Thuduppathy, G. R., Craig, J. W., Kholodenko, V., Schon, A., and Hill, R. B. (2006) Evidence that membrane insertion of the cytosolic domain of Bcl-xL is governed by an electrostatic mechanism. *J. Mol. Biol. 359*, 1045−1058.
(56) Thuduppathy, G. R., and Hill, R. B. (2006) Acid destabilization of the solution conformation of Bcl-xL does not drive its pH-dependent insertion into membranes. *Protein Sci. 15*, 248−257.

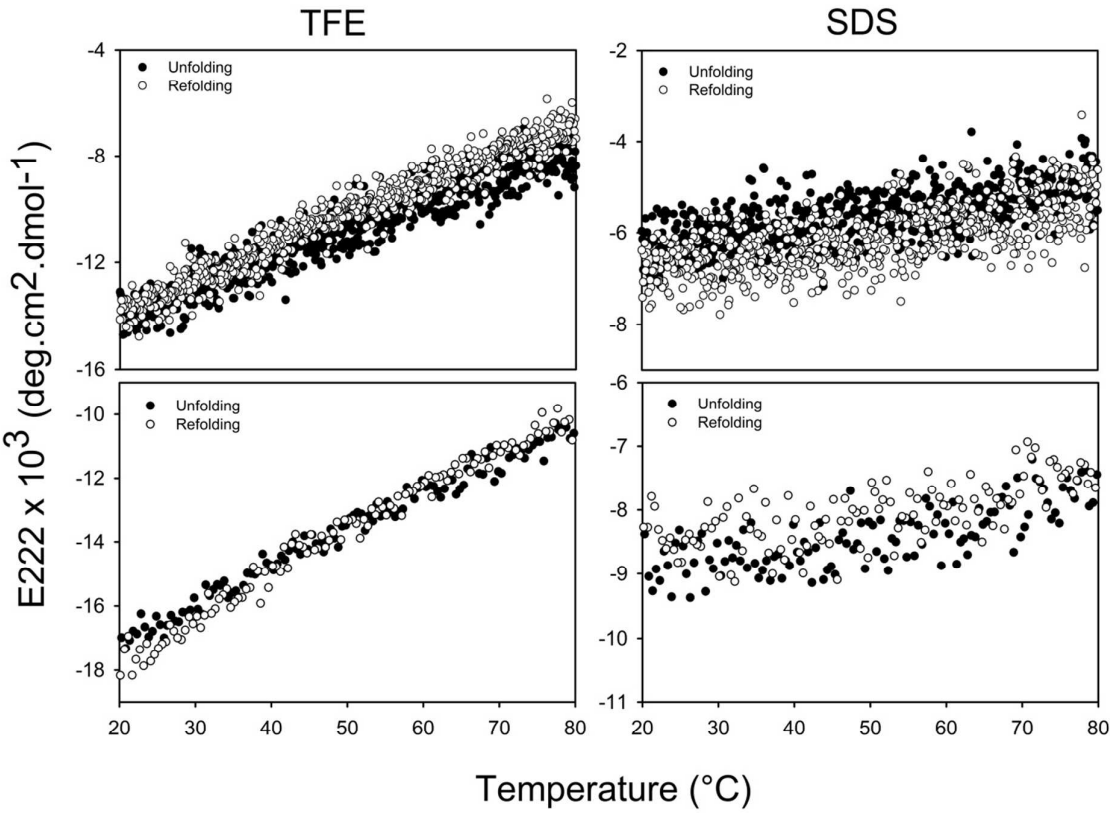

Figure S1 Lys37 is not implicated in maintaining the stability of the CLIC1 TMD. Thermal melts of 20 μM wild-type (top panel) or K37M (bottom panel) TMD peptide were monitored by ellipticity at 222 nm in 40 % (v/v) TFE and 15 mM SDS. The unfolding (closed circle) and refolding (open circle) pathways showed no hysteresis, suggesting that the process is reversible. The wild-type and K37M peptides appear to unfold via non-cooperative pathways, precluding Lys37 as a key residue in maintaining the stability of the folded structure. The approximately linear loss of structure suggests that the unfolding process is non-cooperative. The absence of any native or denatured baselines prevents the determination of thermodynamic parameters. The buffer used was 20 mM sodium phosphate, 1 mM DTT, 0.2 % (w/v) NaN_3, pH 5.5

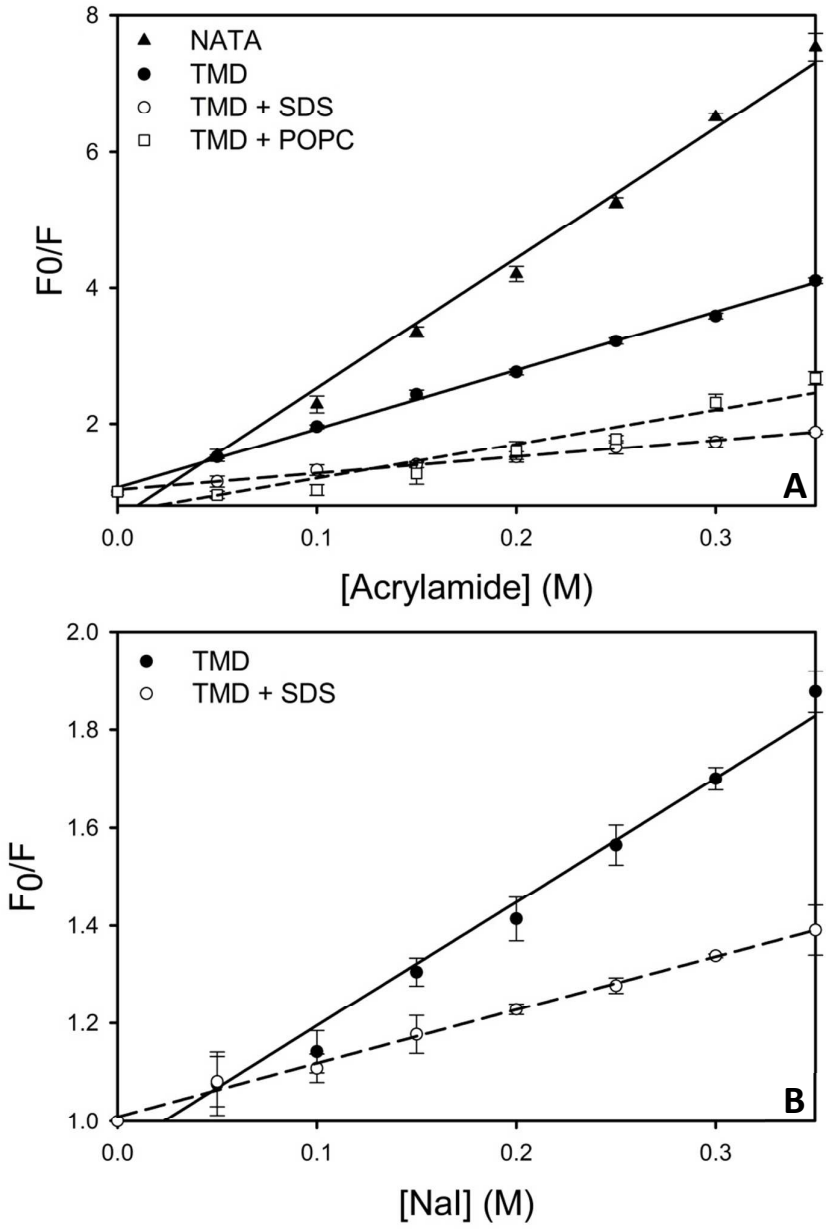

Figure S2 Stern-Volmer plots of the quenching of Trp35 fluorescence by acrylamide and iodide. Acrylamide (A) and iodide (B) quenching of 15 μM CLIC1 K37M TMD peptide and 15 μM NATA was performed in buffer, 15 mM SDS and 2.5 mM POPC. The linear nature of these plots suggests that the quenching occurs via a dynamic process. Upon the addition of SDS and POPC, a significant reduction of the K_{SV} is observed, indicating decreased solvent exposure of Trp35. Iodide quenching was chosen as an additional probe in SDS owing to the ability of acrylamide to penetrate SDS micelles. Samples were analysed in 20 mM sodium phosphate, 1 mM DTT, 0.2 % (w/v) NaN_3, pH 5.5. Error bars represent the standard deviation from four independent replicates

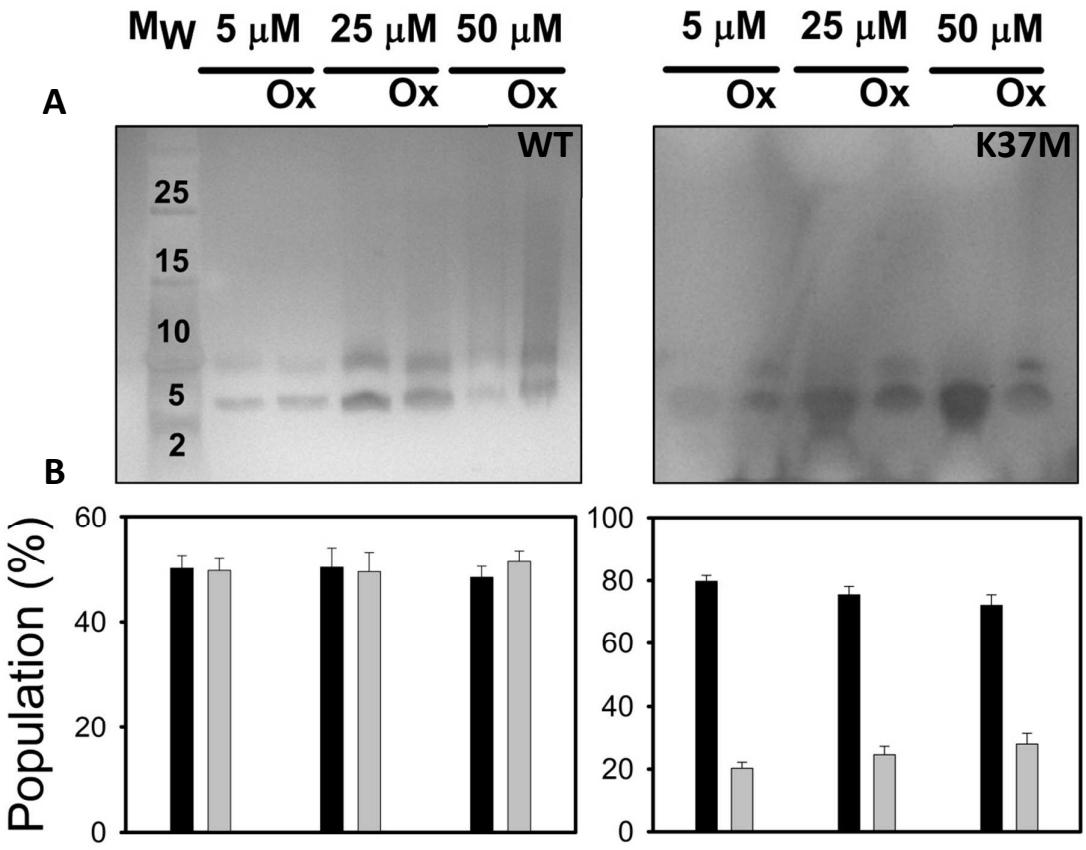

Figure S3 Dimerisation of the CLIC1 TMD peptide can be monitored using SDS-PAGE. (A) SDS-PAGE was used to investigate concentration-dependent oligomerisation of the TMD peptide in 15 mM SDS micelles. The lanes labelled 'Ox' refer to the oxidised dimer control at each peptide concentration. The wild-type peptide displays clear dimer formation at increasing peptide concentrations. The K37M mutant, however, shows little to no dimeric species. The ability of the oxidised control to form the dimer is also hampered, with the loss of the tetrameric species observed for the wild-type. (B) Band intensities confirm the ~ 30 % reduction of dimer (grey) in the K37M mutant relative to the wild-type. This suggests that the helix-helix interactions have been disrupted, pointing to the stabilising role of the Lys37-Trp35 cation-π interaction. Experimental details are given in the Materials and Methods. Error bars represent the standard deviation from four independent replicates

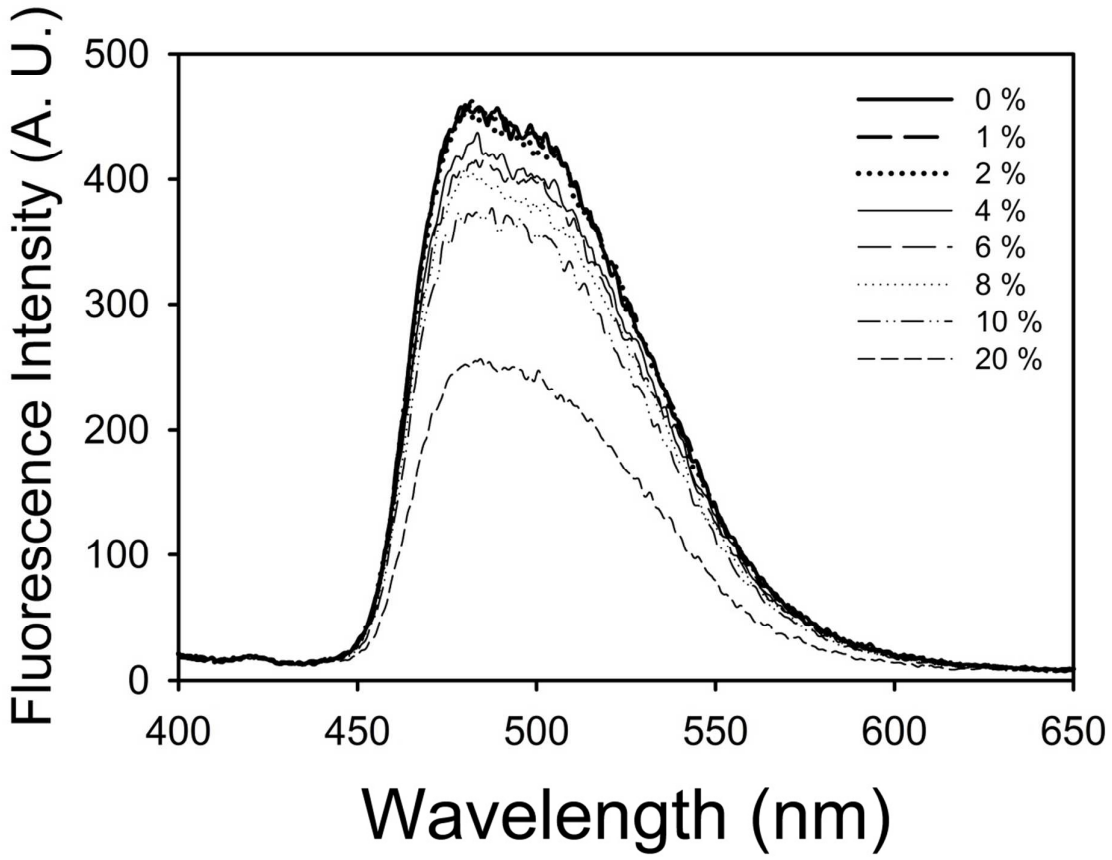

Figure S4 Lucigenin is quenched at high methanol concentrations. In order to determine whether the methanol solvent contributed to the observed reduction in Lucigenin fluorescence, dye-containing liposomes were titrated with increasing volumes of 100 % (v/v) methanol. Fluorescence quenching was observed at methanol concentrations above 4 % (v/v). The assay described in the text comprises no more than 2 % (v/v) methanol, ensuring that the contribution of the solvent to Lucigenin quenching is negligible. The buffer used was 20 mM sodium phosphate, 15 mM potassium chloride, 1 mM DTT, 0.02 % NaN_3, pH 5.5

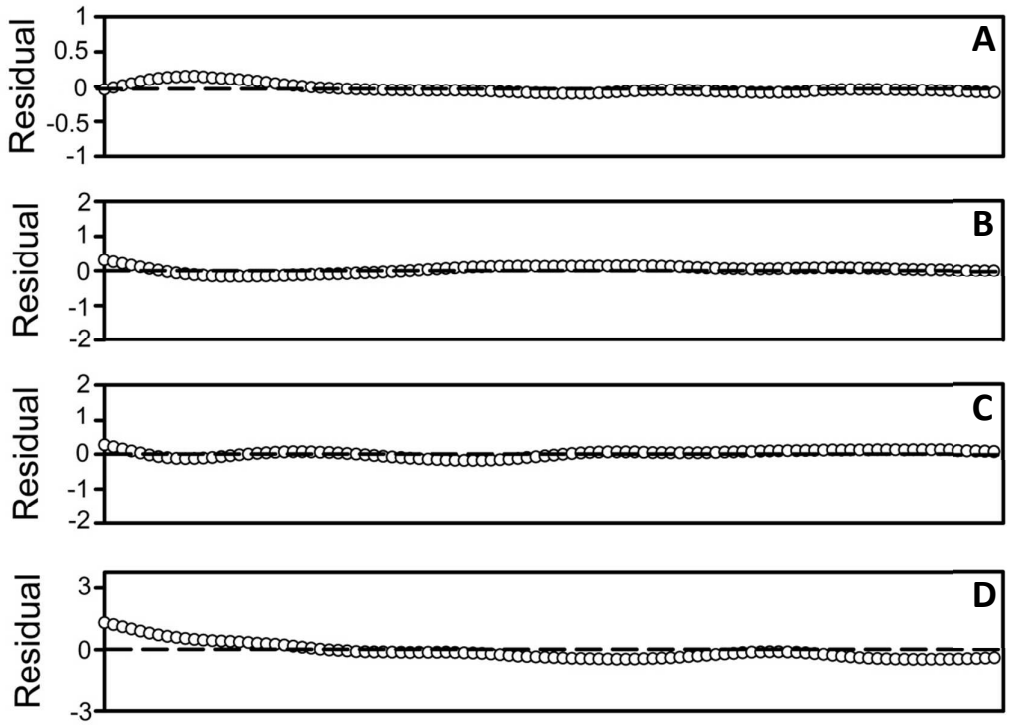

Figure S5 Residuals of the fits to the chloride influx data of the CLIC1 TMD peptide. The residuals from the single or double exponential decay fits are shown for (A) wild-type pH 7.2; (B) wild-type pH 5.5; (C) K37M pH 7.2 and; (D) K37M pH 5.5. The residuals suggest that the models used to fit to the data are accurate. The data were fit using SigmaPlot V 11.0

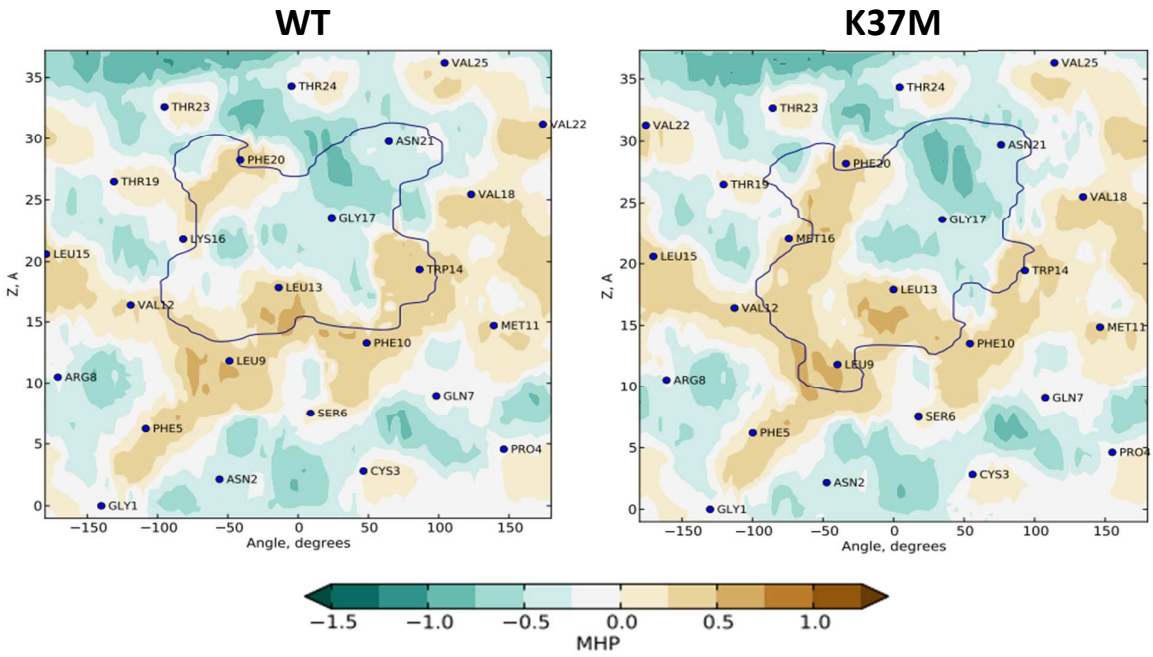

Figure S6 Contact maps derived from the PREDDIMER algorithm. The hydrophobic/ hydrophilic properties of the TMD peptide were mapped on a helical surface according to the molecular hydrophobicity potential (MHP) approach. Positive values of MHP correspond to hydrophobic regions whilst negative values correspond to hydrophilic regions. The residues comprising the dimer interface are indicated

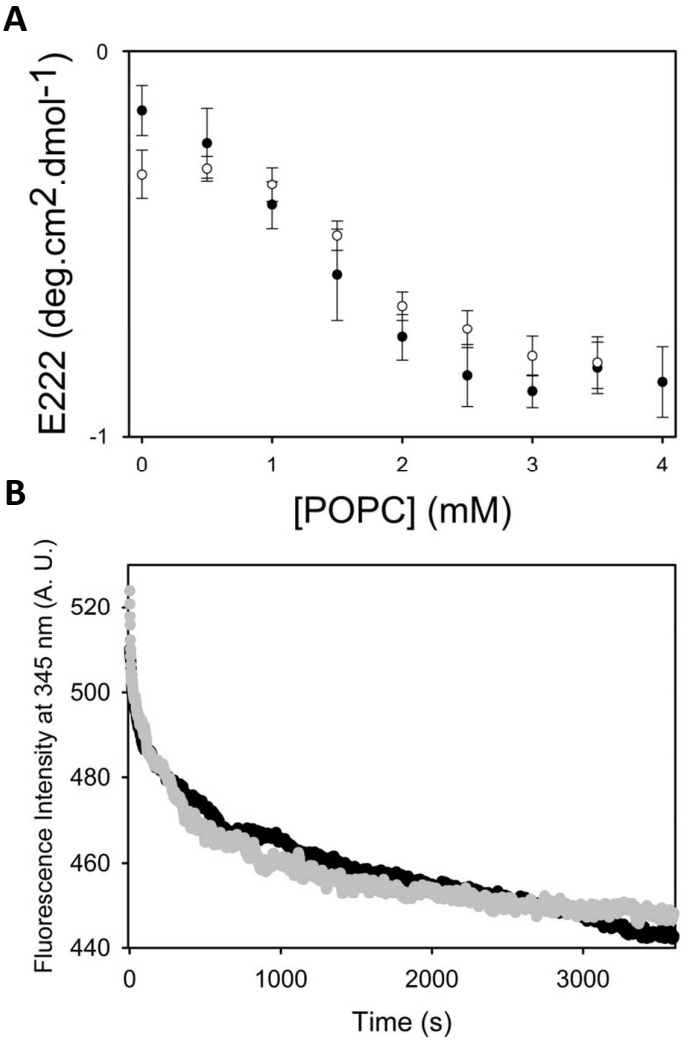

	k_{obs1} (s^{-1})	k_{obs2} (s^{-1})	R^2
WT	0.0055 (1.2 x10^{-4})	0.0008 (1.6 x10^{-5})	0.9927
K37M	0.0051 (6.3 x10^{-4})	0.0004 (2.7 x 10^{-5})	0.9888

Figure S7 Membrane binding and insertion is not affected by the K37M mutation. (A) Overlaid spectra of the wild-type (black) and K37M (white) helicity at increasing POPC concentrations suggest that there is no significant difference in membrane binding at equilibrium. (B) The binding kinetics of 20 μM wild-type (grey) or K37M (black) peptides to POPC membranes was monitored using Trp35 fluorescence following the addition of 3.5 mM POPC. The curves shown represent averages of four independent experiments and were fit to a double exponential model. The observed rate constants (k_{obs}) of both peptides are similar, suggesting that there are no significant differences in membrane binding or insertion.

Chapter 4

A conserved cationic motif enhances membrane binding and insertion of the chloride intracellular channel protein 1 transmembrane domain

Peter, B., Fanucchi, S. and Dirr, H. W.
Eur Biophys J, DOI: 10.1007/s00249-014-0972-y

In this publication, the contribution of electrostatic interactions to membrane binding, insertion and orientation of the CLIC1 TMD were identified.

Author contributions: Bradley Peter performed all experimental work, analysed the data and wrote the manuscript. Sylvia Fanucchi and Heini W. Dirr supervised the project and assisted in data analysis and interpretation.

Eur Biophys J
DOI 10.1007/s00249-014-0972-y

ORIGINAL PAPER

A conserved cationic motif enhances membrane binding and insertion of the chloride intracellular channel protein 1 transmembrane domain

Bradley Peter · Sylvia Fanucchi · Heini W. Dirr

Received: 7 March 2014 / Revised: 29 April 2014 / Accepted: 26 May 2014

Abstract The chloride intracellular channel protein 1 (CLIC1) is unique among eukaryotic ion channels in that it can exist as either a soluble monomer or an integral membrane channel. CLIC1 contains no known membrane-targeting signal sequences and the environmental factors which promote membrane binding of the transmembrane domain (TMD) are poorly understood. Here we report a positively charged motif at the C-terminus of the TMD and show that it enhances membrane partitioning and insertion. A 30-mer TMD peptide was synthesized in which the positively charged motif was replaced by three glutamate residues. The peptide was examined in 2,2,2-trifluoroethanol (TFE), sodium dodecyl sulfate micelles and 1-palmitoyl-2-oleoyl-*sn*-glycero-3-phosphocholine liposomes using size-exclusion chromatography, far-UV CD, and fluorescence spectroscopy. The motif appears to enhance membrane interaction via electrostatic contacts and functions as an electrostatic plug to anchor the TMD in membranes. In addition, the motif is also involved in orientating the TMD with respect to the *cis* and *trans* faces of the membrane. These findings shed light on the intrinsic and environmental factors that promote the spontaneous conversion of CLIC1 from a water-soluble to a membrane-bound protein.

Keywords CLIC · Spectroscopy · Transmembrane domain · Membrane binding · Membrane topology

Abbreviations

CD	Circular dichroism
CLIC1	Chloride intracellular channel protein 1
DTNB	5,5′-Dithio-2-nitrobenzoic acid
DTT	Dithiothreitol
EEE TMD	Transmembrane domain of CLIC1 containing Glu49-Glu50-Glu51
λ_{max}	Emission maximum wavelength
NATA	*N*-Acetyl-tryptophanamide
NLS	Nuclear localization sequence of CLIC4
NRMSD	Normalized root mean square deviation
POPC	1-Palmitoyl-2-oleoyl-*sn*-glycero-3-phosphocholine
SDS	Sodium dodecyl sulfate
TFE	2,2,2-Trifluoroethanol
TMD	Transmembrane domain of CLIC1 (residues 24–46)

Introduction

Over 50 % of all proteins interact with membranes at various levels. These proteins are responsible for a wide range of biochemical events occurring at the plasma membrane and within membrane-bound organelles. The two-step folding model used to explain how membrane proteins are targeted to, bind, and insert into membranes is simplified and does not take into account environmental factors that may influence these processes (Popot and Engelman 1990; White and Wimley 1999). The structure, folding, and insertion mechanisms of membrane proteins are, however, heavily influenced by the membrane environment (Olivella et al. 2002; Dewald et al. 2011; Barrera et al. 2012). As proteins approach the membrane interface, two competing short-range interactions come into effect: the unfavorable

Electronic supplementary material The online version of this article (doi:10.1007/s00249-014-0972-y) contains supplementary material, which is available to authorized users.

B. Peter · S. Fanucchi · H. W. Dirr (✉)
Protein Structure-Function Research Unit, School of Molecular and Cell Biology, University of the Witwatersrand, Johannesburg 2050, South Africa
e-mail: heinrich.dirr@wits.ac.za

Published online: 13 June 2014

desolvation of polar groups on the membrane/protein, and the favorable partitioning of non-polar groups into the membrane (Mulgrew-Nesbitt et al. 2006). The negative charge and low pH at the interface can alter a protein's electrostatic properties and induce considerable electrostatic attraction between the protein and membrane (Honig et al. 1986; McLaughlin et al. 2005). Electrostatic interactions may thus prime proteins for membrane targeting and insertion. These mechanisms are particularly important for proteins that adopt multiple stable native states. Such proteins spontaneously convert from a water-soluble to a membrane-bound form via large-scale structural rearrangements (Johnson and Cornell 1999). The eukaryotic chloride intracellular channel 1 (CLIC1) protein is an example of structural amphitropism, although its membrane insertion mechanism remains speculative.

In order for CLIC1 to form an ion-conducting channel, it must (1) translocate from the cytosol to the membrane interface and (2) bind to, insert, and remain inserted in the membrane. CLIC1 contains no known membrane-targeting signal sequences and the environmental factors that promote the transition from soluble to membrane-inserted are poorly understood. The oxidative state has been shown to play a role in CLIC1 ion-channel activity and membrane binding due to the presence of several redox-sensitive cysteine residues (Littler et al. 2004; Goodchild et al. 2009). However, not all CLICs and CLIC homologs have a redox-active cysteine at their active sites. CLIC1 also readily inserts into anionic lipid membranes where the pH at the membrane surface may be 1–2 pH units lower than that of the cytosol (Xia and Sui 2000; Singh and Ashley 2007). This hints at an electrostatic component in membrane binding/insertion. Interestingly, CLIC4 contains a lysine-rich nuclear localization sequence (NLS; residues 199–206) (Suh et al. 2004; Mynott et al. 2011). The NLS mediates nuclear translocation and membrane insertion by interacting with the nuclear import proteins importin-α and Ran (Malik et al. 2010). Although CLIC1 lacks a NLS, it does contain a lysine and arginine-rich motif at the C-terminus of the transmembrane domain (TMD) (Fig. 1). This motif is conserved across the vertebrate CLICs. Positively charged regions flanking the TMDs of membrane proteins are often considered topology determinants involved in the binding, insertion, and orientation of proteins in membranes (von Heijne 1984; Wallin and von Heijne 1995).

The TMD remains the focus of understanding the mechanism by which CLICs insert into the membrane. The sensitivity of the domain to pH as well as the presence of the conserved cationic motif suggests that the membrane binding and insertion mechanism of CLIC1 comprises an electrostatic component. In order to better understand the contribution of this motif to membrane binding and insertion of the CLIC1 TMD, we replaced Lys-Arg-Arg (KRR) with Glu-Glu-Glu (EEE). The resulting secondary, tertiary, and quaternary structural changes were examined within a membrane-mimicking environment.

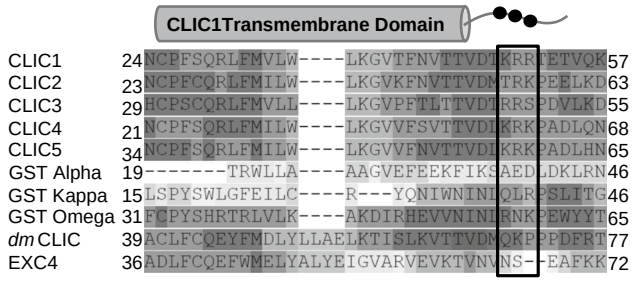

Fig. 1 Sequence conservation of a cationic motif in the CLIC1 TMD. The CLIC1 TMD comprises residues 24–46. This region shows strong sequence conservation across the vertebrate CLICs as well as the invertebrate homologs Exc4 (*Caenorhabditis elegans*) and dmCLIC (*Drosophila melanogaster*). The cationic motif (*boxed*) shows strong conservation across the vertebrate CLICs and membrane-bound omega GST, suggesting it plays a critical role in CLIC function/membrane binding

Materials and methods

Peptide design, synthesis, and sample preparation

The 30-residue CLIC1 EEE TMD peptide (22-GNCPFSQRLFMVLWLKGVTFNVTTVDT EEE-51) containing a carboxylated amino terminus and an amidated carboxyl terminus was synthesized using a solid-phase continuous flow system by GL Biochem (Shanghai, China). Its purity was determined as >95 % using HPLC.

The peptide was solubilized in 100 % (v/v) methanol to yield a 1-mM stock solution and prepared as previously described (Peter et al. 2013, 2014). Incorporation of the peptide into SDS micelles, POPC liposomes, and lucigenin-encapsulated liposomes was carried out according to an established protocol (Peter et al. 2014).

Spectroscopic analysis

Far-UV CD and fluorescence spectra of the peptide were recorded in TFE, SDS, and POPC as described (Peter et al. 2013). Spectra were buffer-corrected and smoothed using the negative exponential method. CD spectra were normalized to mean residue ellipticity ([θ]) using the equation:

$$[\theta] = (100.\theta)/\mathrm{cnl}$$

where [θ] is the molar ellipticity (deg cm^2 dmol^{-1}), θ is ellipticity (mdeg), c is the protein concentration (mM), n is the number of residues in the peptide, and l is the path length (cm). For all far-UV CD analyses: $n = 30$ and

l = 0.1 cm. The CDPro software package was used to estimate secondary-structural content (Sreerama and Woody 2000; Peter et al. 2013). The standard error of the secondary structural elements was determined from four separate CDPro analyses. Thermal melting studies were carried out between 10 and 100 °C.

Quenching studies of the Trp35 probe in the TMD peptide were performed using H_2O_2, acrylamide, and iodide as described (Peter et al. 2013, 2014). The fluorescence intensity at 345 nm was monitored and analyzed according to the Stern–Volmer relationship:

$$F_0/F = 1 + K_{SV}[Q]$$

where F_0 and F are the emission intensities in the absence and presence of quencher, respectively; [Q] is the concentration of quencher, and K_{SV} is the Stern–Volmer constant.

The solvent accessibility of the lone thiol of Cys24 in the TMD peptide was analyzed using DTNB (5,5′-dithio-2-nitrobenzoic acid) in SDS and POPC as described (Peter et al. 2013). The concentration of 2-nitro-5-thiobenzoic acid (NTB) was determined spectrophotometrically at 412 nm using an extinction coefficient of 13 600 M^{-1} cm^{-1} (Habeeb 1972). The proportion of free thiols was obtained from the ratio of NTB concentration to peptide concentration.

Size-exclusion chromatography

Size-exclusion chromatography was used to probe the electrostatic association of the peptide with POPC liposomes. Peptides bound to the membranes should elute in the void volume while unbound peptides are retarded. Wild-type or EEE CLIC1 TMD peptides (20 μM) were mixed with 2.5 mM POPC and 0–1 M NaCl and loaded onto a Sephadex G-25 column (Amersham Biosciences, Piscataway, NJ, USA) pre-equilibrated with buffer (20 mM sodium phosphate, 1 mM DTT, 0–1 M NaCl, pH 5.5). Elution profiles were corrected for scatter contribution by the liposomes using an identical sample in the absence of the TMD peptide.

Chloride influx assay

A chloride influx assay was used to monitor the effect of removing the cationic KRR motif on chloride transport. The assay is based on the quenching of an encapsulated chloride-sensitive fluorescent dye lucigenin by extravesicular chloride ions.

Samples were prepared and analyzed as described (Peter et al. 2014). Blank samples were supplemented with appropriate volumes of 100 % (v/v) methanol. An excitation wavelength of 368 nm, scan speed of 250 nm/min, and 3.5-nm slit widths were used. The % quenching following the addition of 4 μM valinomycin was determined according to:

$$[1 - (F484_P/F484_B)] \times 100\,\%$$

where $F484_P$ and $F484_B$ represent the emission intensity at 484 nm in the presence and absence of TMD peptide, respectively. The kinetics of chloride influx was monitored at 484 nm as described, following the addition of 20 μM EEE TMD peptide. Data were fit to a double exponential decay model in SigmaPlot V 11.0 from which the observed rate constants (k_{obs}) were derived.

Statistical analysis

All data were prepared for analysis with standard spreadsheet software (Microsoft Excel). Statistical analysis was done using Student's *t* test in Microsoft Excel.

Results

Secondary, tertiary, and quaternary structure

The far-UV CD spectra of the EEE TMD peptide in aqueous buffer, TFE, SDS micelles, and POPC liposomes are shown in Fig. 2a and b. Quantitative secondary structure analysis is summarized in Fig. 2b (EEE peptide) and Table S1 (wild-type peptide). The addition of membrane mimetics induces a two-state transition from unstructured to α-helical- characterized by two minima at 208 and 222 nm (Fig. 2a). The α-helical content of the peptide in TFE is ~10–15 % greater than in SDS or POPC. This suggests that a greater proportion of peptide assumes an α-helical conformation under these conditions compared to a micellar/vesicle environment. The gain in α-helical content is accompanied by decreases in β- and unordered structures (Fig. 2b). This pattern is identical to the wild-type peptide (Table S1; Peter et al. 2013). Compared to the wild type, however, the EEE peptide shows 8 % (SDS) and 7 % (POPC) less helicity overall, despite having an identical helical propensity (Pace and Scholtz 1998). The thermal stability of the peptide was also analyzed by measuring the ellipticity at 222 nm in 40 % TFE or 15 mM SDS at increasing temperature (Supplementary Fig. S1). Both the wild-type and EEE peptides unfold via non-cooperative and fully reversible pathways. This behavior is characteristic of transmembrane helices and results from the sequential, rather than simultaneous, disruption of amide hydrogen bonds (Langosch and Arkin 2009).

Tertiary structural changes induced by the membrane mimetics were monitored using the lone tryptophan residue at position 35. In solution, the peptide exhibits a fluorescence spectrum with a low emission intensity and an emission maximum wavelength (λ_{max}) of 352 nm (Fig. 2c). The

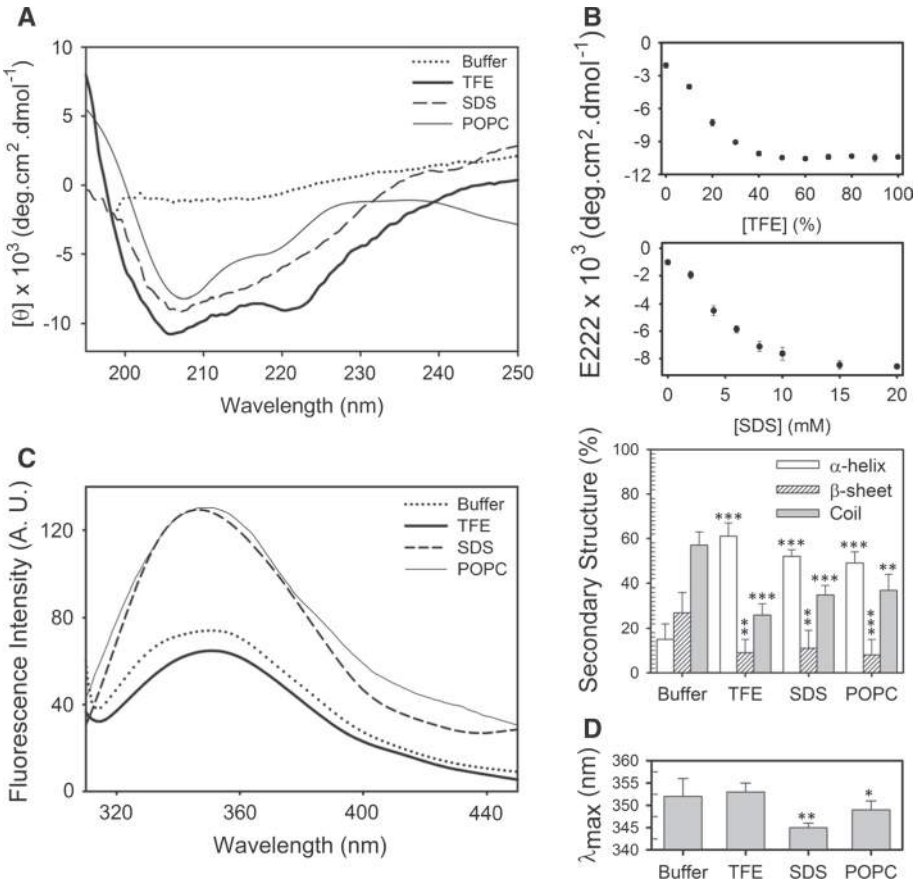

Fig. 2 Secondary and tertiary structure of the CLIC1 EEE TMD peptide. Far-UV CD and fluorescence spectra were recorded in buffer (*dotted line*), in 40 % (v/v) TFE (*thick solid line*), in 15 mM SDS micelles (*dashed line*) and in 2.5 mM POPC (*thin solid line*). **a** The peptide acquires α-helical secondary structure in the presence of TFE, SDS, and POPC. **b** The helical content of 15 μM peptide increases sigmoidally with increasing mimetic concentrations, reaching a maximum at 40 % (v/v) TFE and 15 mM SDS. The CDPro reference set SP43 was used to calculate secondary structural content. **c**, **d** In buffer, the peptide emits maximally at 352 nm. The addition of TFE reduces the emission intensity by 22 % but does not significantly alter the λ_{max}. The addition of SDS and POPC induce both a blue-shifted λ_{max} (345 and 349 nm, respectively) and a 200 % increase in emission intensity. This behavior is typical of a tryptophan that is buried in a hydrophobic interior, presumably inserted into the SDS micelles or POPC liposomes. The buffer used was 20 mM sodium phosphate, 1 mM DTT, 0.2 % (w/v) sodium azide, pH 5.5. *Error bars* represent the standard deviation from four independent replicates. *Asterisks* indicate ***$p < 0.001$, **$p < 0.01$, *$p < 0.05$, *t* test relative to buffer samples

addition of TFE reduces the emission intensity by 22 % but does not significantly alter the λ_{max} (Fig. 2d). The addition of SDS and POPC induce both a blue-shifted λ_{max} (345 and 349 nm) and a twofold increase in emission intensity. This behavior is typical of a tryptophan residue that is buried in a hydrophobic interior. Presumably, Trp35 becomes inserted into the SDS micelles or POPC liposomes. Although the data in SDS is consistent with the wild-type data, the λ_{max} in POPC for the EEE peptide is red-shifted 7 nm compared to that of the wild type (Table S1; Peter et al. 2013). This may be a result of altered interactions with the mimetics as well as altered quaternary interactions, particularly if Trp35 is located at or near an oligomer interface.

Self-association of the EEE peptide was probed using concentration-dependent studies (Fig. 3a and b) and SDS-PAGE (Supplementary Fig. S2). We have previously demonstrated that the wild-type CLIC1 TMD forms stable dimers in membrane mimetics (Peter et al. 2013). Both the E222 and λ_{max} values of the EEE peptide incubated in SDS show a concentration-dependent trend (Fig. 3a and b). The trend in E222 values deviates from that of the wild type (Fig. 3 inset), requiring threefold higher EEE peptide concentrations to achieve wild-type E222 levels. The λ_{max} values appear to follow a similar trend in the wild-type and EEE TMD peptides. Samples incubated in TFE show no concentration-dependence, as TFE inhibits quaternary interactions (Roccatano et al. 2002). Removal of the KRR motif thus appears to influence the secondary, tertiary, and quaternary structure of the CLIC1 TMD in membranes by reducing the overall helicity, increasing the local environmental polarity of Trp35 and shifting the equilibrium of oligomeric species.

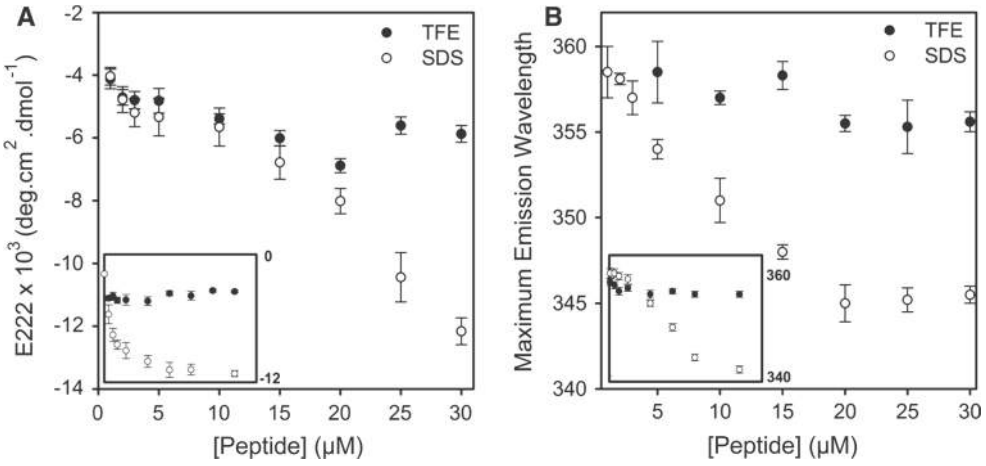

Fig. 3 Concentration-dependent secondary and tertiary structure of the CLIC1 EEE TMD peptide. The E222 (**a**) and λ_{max} (**b**) values from EEE peptide samples incubated in SDS micelles/POPC liposomes show a concentration-dependent trend. The trend in helical structure deviates from that of the wild type (*inset*) and requires threefold higher EEE peptide concentrations to achieve wild-type E222 levels. The λ_{max} values are similar for the wild-type and EEE peptides (**b**, *inset*). Samples incubated in TFE show no concentration-dependence. The *x*-axes of the insets are identical to those of the full-sized figures. *Error bars* represent the standard deviation from four independent replicates

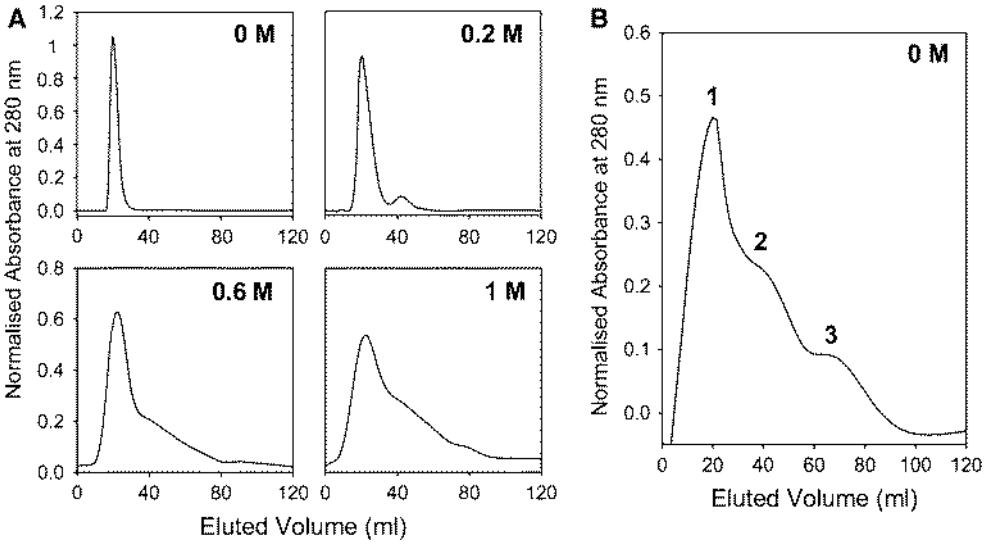

Fig. 4 The cationic motif influences membrane binding via an electrostatic mechanism. Size-exclusion chromatography was used to probe membrane adsorption on the basis that peptide adsorbed to the membrane will elute in the void volume while free peptide is retarded. **a** The wild-type TMD peptide in 2.5 mM POPC was analyzed on a Sephadex G-25 size-exclusion column equilibrated with 0–1 M NaCl. At increasing salt concentrations, there is a gradual reduction in the membrane-bound species and a corresponding rise in unbound peptide. **b** The elution profile of the EEE TMD peptide in 2.5 mM POPC and 0 M NaCl is heterogenous and comprises the membrane-bound peptide (*1*), free peptide dimer (*2*), and free peptide monomer (*3*). The profiles shown have been corrected for scatter contribution and normalized. The buffer used was 20 mM sodium phosphate, 0–1 M NaCl, 1 mM DTT, 0.2 % (w/v) sodium azide, pH 5.5

Membrane adsorption

In order to understand if/how the KRR motif facilitates membrane binding, size-exclusion chromatography was used (Fig. 4). Peptides adsorbed to the membrane will elute in the void volume while passage of free peptides will be retarded. If the interaction is largely electrostatic in nature, the inclusion of high salt concentrations should interfere with membrane binding and result in a larger population of free peptides. Figure 4a shows the elution profiles of the wild-type peptide at increasing salt concentrations. In the absence of salt, nearly all the peptide is bound to the

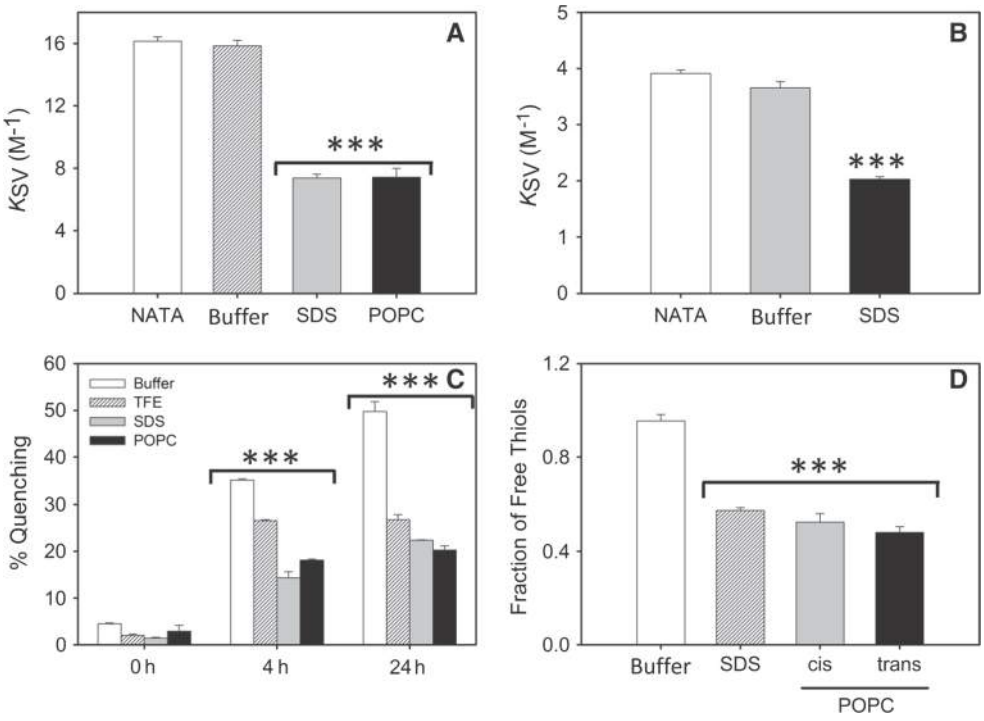

Fig. 5 The cationic motif acts as an electrostatic plug to anchor the CLIC1 TMD in membranes. Dynamic acrylamide (**a**), iodide (**b**), and H_2O_2 (**c**) quenching as well as a DTNB assay (**d**) were performed. "NATA" refers to *N*-acetyl tryptophanamide, "Buffer" refers to free TMD peptide in solution, "TFE" refers to TMD peptide in 40 % (v/v) TFE, "SDS" refers to TMD peptide in 15 mM SDS, and "POPC" refers to TMD peptide in 2.5 mM POPC. In **c**, samples were analyzed by fluorescence following the addition of 2 mM H_2O_2. In **d**, "*cis*" refers to external DTNB and "*trans*" refers to encapsulated DTNB. The buffer used was 20 mM sodium phosphate, 1 mM DTT, 0.2 % (w/v) sodium azide, pH 5.5 (Quenching) or 20 mM Na_2PO_4, 1 mM EDTA, 0.2 % (w/v) sodium azide, pH 6.0 (DTNB assay). *Error bars* represent the standard deviation from four independent replicates. *Asterisks* indicate ***$p < 0.001$, *t* test relative to buffer samples

membrane and elutes in the void volume. At increasing salt concentrations, there is a gradual reduction in the membrane-bound species and a corresponding rise in the free monomeric and dimeric species. Figure 4b shows the elution profile of the EEE peptide in the absence of salt. The elution profile is heterogenous and comprises three peaks. These peaks correspond to (1) the membrane-bound peptide, (2) free peptide dimer (~7.9 kDa), and (3) free peptide monomer (~3.7 kDa). Only approximately 50 % of the EEE peptide is bound to the membrane while the remainder is free in solution. At 1 M NaCl, the elution profile of the wild-type peptide resembles that of the EEE peptide in the absence of NaCl. Removal of the KRR motif thus appears to impede membrane association in a manner akin to salt-induced disruption of electrostatic interactions.

Solvent accessibility of Trp35 and Cys24

The role of the KRR motif in membrane insertion of the CLIC1 TMD was probed using H_2O_2, acrylamide, and iodide quenching in SDS micelles and POPC liposomes. In the presence of H_2O_2, the emission spectra of Trp35 are quenched on the basis of solvent accessibility due to the conversion of the indole ring to oxyindole over time. The EEE peptide shows 48 % (buffer), 28 % (TFE), 23 % (SDS), and 21 % (POPC) quenching over 24 h (Fig. 5c). Although there is a clear reduction in solvent accessibility following the addition of membrane mimetics, the overall levels of quenching in SDS and POPC are ~15–20 % greater than in the wild type (Peter et al. 2013).

A similar trend was observed using acrylamide and iodide as quenchers. Figure 5a and b as well as supplementary Fig. S3 and Table 1 show the Stern–Volmer constants (K_{SV}) obtained using acrylamide and iodide. This constant reflects residue accessibility, with low values, indicating residues of low exposure and vice versa. In the absence of membrane mimetics, both acrylamide ($K_{SV} = 15.85\ M^{-1}$) and iodide ($K_{SV} = 3.66\ M^{-1}$) quenching yield Stern–Volmer constants which are similar to both free *N*-acetyl tryptophanamide (NATA) in solution (16.15/3.88 M^{-1}) and the wild-type peptide (15.35/3.52 M^{-1}). The addition of SDS and POPC induce a twofold reduction in solvent accessibility. This reduction is between 1 (POPC) and 1.5-fold (SDS) less than the wild-type peptide (Table S1; Peter et al. 2013) and suggests that Trp35 of the EEE peptide is more solvent-exposed. This is consistent with the data obtained

Table 1 Solvent accessibility of the EEE CLIC1 TMD peptide in membrane mimetics

	Buffer	TFE	SDS	POPC
K_{SV} (M^{-1})[a]	15.85 (±0.36)/3.66 (±0.11)	ND	7.37 (±0.25)/2.03 (± 0.04)	7.41 (±0.57)
Fraction of free thiols[b]	0.96 (±0.03)	ND	0.57 (±0.02)	0.52 (±0.04)/0.47 (±0.02)

The results for the wild type have been published previously (Peter et al. 2013). *Values in brackets* represent the standard deviation from four independent replicates

[a] Samples with two values represent the K_{SV} determined from acrylamide and iodide quenching, respectively

[b] In POPC, the first value represents external DTNB (*cis*) while the second value represents encapsulated DTNB (*trans*)

using H_2O_2 (Fig. 5c) as well as the red-shifted λ_{max} in POPC (Fig. 2c and d).

The solvent accessibility of Cys24 in SDS and POPC was probed using a DTNB assay (Fig. 5d). The addition of SDS induces a ~40 % reduction in the fraction of free thiols, which is comparable to the wild-type (Fig. 5d and Table 1). In POPC, two versions of the DTNB assay were performed: (1) using extrinsic DTNB; and (2) using DTNB encapsulated within the liposomes. The aim of these two methods was to probe whether Cys24 is located at the *cis*- (1) or *trans*-face (2) of the membrane mimetic. The data shown in Fig. 5d suggest that the *cis* (~52 %) and *trans* (~47 %) orientations are equally favored. This differs from the wild-type peptide, which favors the *trans* orientation (63 %) over the *cis* orientation (39 %) (Table S1; Peter et al. 2013).

Chloride influx assay

The effect of removing the KRR motif in a functional context was probed using a dye-based chloride influx assay. The overall quenching of the dye at pH 5.5 and pH 7.2 is shown in Fig. 6a. A concentration-dependent increase in quenching is observed at both pH values, reaching a maximum of ~25 % at 20–30 µM (pH 5.5) and 50 µM (pH 7.2) peptide. This level of quenching is 5–10 % lower than the wild-type (Peter et al. 2014). In addition, the EEE peptide concentration at which maximal quenching occurs is shifted compared to the wild-type and requires a further 10 µM (pH 5.5) and 15 µM (pH 7.2) to achieve maximal quenching. The kinetics of chloride influx is shown in Fig. 6b. The observed rate constants for chloride influx (k_{obs}) are shown in Table 2. The peptide displays a two-phase mechanism at both pH values. Low pH enhances the rate of chloride influx sixfold (phase one) and threefold (phase two). Although this is similar to the wild-type peptide, the overall rate of chloride influx is ~twofold lower than for the wild type.

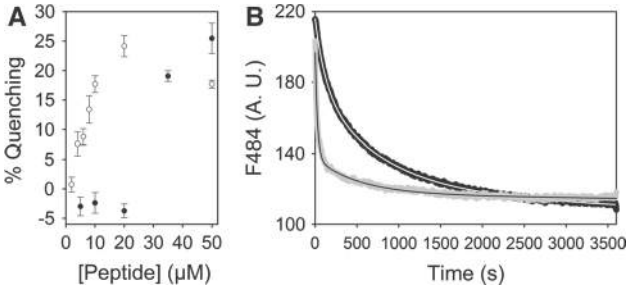

Fig. 6 The cationic motif enhances, but is not required for, chloride transport. Equilibrium (**a**) and kinetic (**b**) chloride influx assays were performed for the EEE TMD peptide. **a** Chloride influx is concentration-dependent at pH 5.5 (*open circle*) and pH 7.2 (*closed circle*). **b** The kinetic traces shown represent averages of four independent experiments at pH 5.5 (*grey*) and pH 7.2 (*black*). The data were fit to either a single or double exponential decay model using SigmaPlot V 11.0 and fits are shown as *solid lines* through the data. The buffer used was 20 mM sodium phosphate, 15 mM potassium chloride, 1 mM DTT, 0.02 % sodium azide, pH 5.5 or pH 7.2. *Error bars* represent the standard deviation from four independent replicates

Discussion

The factors that promote the cytosol-membrane transition of CLIC1 still remain uncertain, although pH and oxidative state are thought to be involved (Fanucchi et al. 2008; Goodchild et al. 2009). However, trends in membrane protein sequences suggest that intrinsic factors also play an important role in membrane binding and insertion (von Heijne and Gavel 1988; Gafvelin et al. 1997). In particular, regions flanking the transmembrane domain(s) of membrane proteins often direct membrane interactions and form a key component of the membrane insertion mechanism (von Heijne 1984; Wallin and von Heijne 1995). Here we report a cationic tripeptide motif located at the C-terminus of the CLIC1 TMD that is implicated in enhancing membrane binding and insertion. The polarity of the motif was reversed by mutating Lys-Arg-Arg (KRR) to Glu-Glu-Glu (EEE) and the resulting changes in structure, function, and membrane binding were observed.

The KRR motif facilitates membrane binding via an electrostatic interaction

Removal of the KRR motif severely disrupts the ability of the CLIC1 TMD to bind to membranes (Fig. 4b). The

Table 2 Observed rate constants for peptide-mediated chloride influx

	pH 7.2			pH 5.5		
	k_{obs1} (s^{-1})	k_{obs2} (s^{-1})	R^2	k_{obs1} (s^{-1})	k_{obs2} (s^{-1})	R^2
WT[a]	0.0108 (2.2×10^{-5})	0.0016 (3.7×10^{-6})	0.9994	0.048 (2×10^{-4})	0.0044 (1.1×10^{-5})	0.9986
EEE	0.0081 (5.3×10^{-5})	0.0013 (8.1×10^{-6})	0.9997	0.037 (3.1×10^{-4})	0.0019 (3.2×10^{-5})	0.9877

Data were fit to either a single or double exponential decay model in SigmaPlot V 11.0 from which the observed rate constants (k_{obs}) were derived. *Values in brackets* represent the standard deviation from four independent replicates

[a] Letter a refers to the reference from which the data was taken from (Peter et al. 2014)

severity of this disruption is similar to that caused to the wild type by high ionic strengths (Fig. 4a). Dissociation of the wild-type TMD from membranes at high ionic strength suggests that an electrostatic interaction is involved in membrane binding. This is common for many amphitropic and peripheral membrane proteins (Heimburg and Marsh 1995; Ben-Tal et al. 1997; McLaughlin and Murray 2005). Since the removal of the KRR motif shows a similar pattern at low ionic strength, it is likely that the KRR motif directs electrostatic adsorption to the membrane. The predominantly charged nature of the membrane interface is an ideal environment for ionic interactions. Salt bridges and hydrogen bonds between negatively charged phospholipid head groups and positively charged amino acid side chains may contribute between 3.5 and 10 kcal/mol to the binding energy (Hendsch and Tidor 1994; Xu et al. 1997). This may provide one source of energy, which is required for the energetically unfavorable translocation of polar residues across the membrane.

According to the two-step folding model of Popot and Engelman (1990), membrane partitioning/binding precedes the acquisition of secondary structure as well as membrane insertion and self-association. In order to move on to the next step, each preceding step must be satisfied. It is possible then that the reduction in α-helical secondary structure seen in the EEE peptide (Fig. 2b) is a result of impaired membrane adsorption caused by removal of the KRR motif. This theory is supported by similarities in helical content between EEE and wild-type peptides in TFE. As TFE is an isotropic solvent, no membrane binding is required and helix formation continues uninterrupted.

The KRR motif anchors and orientates the TMD in the membrane

Data obtained from fluorescence spectra (Fig. 2c and d) and quenching studies (Fig. 5a–c) suggest that removal of the KRR motif significantly increases the solvent accessibility of the peptide in the presence of membranes. This implies that either: (1) membrane insertion is impaired, (2) the peptide does not remain in the membrane following insertion, or (3) the peptide passes directly through the membrane. As described previously, the two-step folding model is a sequential rather than parallel mechanism. As such, the impaired membrane binding caused by removal of the KRR motif may in turn impair membrane insertion (point (1) above). However, the data likely reflect a mixture of free and inserted species (point (2) above) since a fair reduction in solvent accessibility is still observed following the addition of membranes (Fig. 5a–c). Rather than completely impairing membrane insertion, removal of the KRR motif may simply shift the equilibrium of the inserted species, causing a larger population to dissociate from the membrane following insertion. This is consistent with concentration-dependent secondary structural studies (Fig. 3a) and functional assays (Fig. 6a), which require a greater concentration of the EEE peptide to achieve wild-type levels of structure/function. Thus, increasing the concentration of soluble peptide shifts the equilibrium towards membrane insertion—allowing oligomerization and chloride transport to occur. The KRR motif may therefore act as an electrostatic plug that anchors the TMD in the membrane, preventing its dissociation and the resulting shift in equilibrium.

This role is similar to that of other positively charged residues that act as a topology determinant in many membrane proteins (von Heijne and Gavel 1988; Granseth et al. 2005). The so-called “positive-inside” rule refers to the uneven distribution of positively charged amino acids on the flanking regions of TMDs. These residues are thought to control which regions remain in the cytoplasm (high number of positive residues) and which regions translocate the lipid bilayer (low number of positive residues) (Granseth et al. 2005; Nilsson et al. 2005). Cytoplasmic retention of these positive residues occurs via electrostatic interactions with negatively charged phospholipid head groups (van Klompenburg et al. 1997). These interactions have also been observed in amphipathic helical peptides (Gallusser and Kuhn 1990; Mishra and Palgunachari 1996). The KRR motif is likely involved in a similar interaction.

In addition to anchoring the TMD in the membrane, the KRR motif may also be involved in orientating the peptide with respect to the *cis* and *trans* faces of the membrane. The wild-type peptide preferentially inserts

with Cys24 at the *trans* face of the membrane (Peter et al. 2013). Removal of the KRR motif removes this preference, with the *cis* and *trans* faces being equally favored (Fig. 5d and Table 1). In the cell, Cys24 would likely be at the *trans* face since the *cis* face requires the entire protein (including the charged KRR motif) to cross the membrane and then reinsert the N-terminal TMD from outside the cell. As CLIC1 is not known to be exocytosed, this orientation seems unlikely. However, the removal of the KRR motif greatly reduces the energy barrier of membrane translocation and thus allows for both *cis* and *trans* orientations.

The KRR motif and intracellular pH

The net negative charge at the membrane surface pools protons at the membrane-cytosol interface. As a result, the pH at the interface is typically 1–2 units lower than the cytosol (Xia and Sui 2000). It is this uneven distribution of pH, which is thought to act as a trigger for CLIC1 to insert into membranes and conduct chloride ions (Warton et al. 2002; Fanucchi et al. 2008). The low pH is thought to destabilize the soluble protein, lowering the activation energy barrier for its conversion and exposing key transmembrane hydrophobic residues (Manceva et al. 2004; Fanucchi et al. 2008; Stoychev et al. 2009; Legg E'Silva et al. 2013). At low pH, the KRR motif is likely to be fully protonated thereby maximizing electrostatic contacts with phospholipid head groups. Removal of the KRR motif does affect the pH sensitivity of the rate of chloride conductance 2.5-fold compared to the wild type (Fig. 6b). It can be argued that the introduction of three glutamate residues imparts a net-negative charge to the TMD, which may result in electrostatic repulsion from the membrane even at low pH. The pK_a of the free glutamate side chain is ~4.3 and ranges between 4.5 and 6.5 within a protein (Wallach and Zahler 1966; Smith et al. 1996). However, the greater proton concentration at the membrane interface should not favor ionization of glutamate side chains since the equilibrium is shifted towards the protonated (neutral) form. As a result, the pK_a is likely increased and the EEE motif would have a predominantly neutral charge.

In conclusion, the results presented here represent the first study of the specific interactions involved in the binding of the CLIC1 TMD to membranes. We have identified a cationic C-terminal motif, which is required for membrane partitioning and insertion. The motif appears to interact with membranes via electrostatic contacts and functions as an electrostatic plug to anchor the TMD in membranes. In addition, the motif is also involved in orientating the TMD with respect to the *cis* and *trans* faces of the membrane. This motif appears to function in a similar manner to many other membrane proteins and follows the so-called "positive-inside" rule. This sheds light on the factors that promote the spontaneous conversion of CLIC1 from a water-soluble to a membrane-bound protein.

Supporting information

Supporting information is available, and it includes four figures (Fig. S1 through Fig. S4) and one table (Table S1). The first figure describes the thermal unfolding of the CLIC1 TMD peptide in SDS and TFE, while the second figure shows the SDS-PAGE gels of the monomeric and dimeric TMD. The third figure shows the Stern–Volmer plots for acrylamide and iodide quenching and the fourth figure describes the residuals to the fits of the chloride influx kinetic data. Table S1 contains structural data for the wild-type CLIC1 TMD peptide.

Acknowledgments This work was supported by the University of the Witwatersrand, South African National Research Foundation Grant 68898 to H.W.D and South African Research Chairs Initiative of the Department of Science and Technology and National Research Foundation (Grant 64788 to H.W.D). Any opinion, findings, and conclusions or recommendations expressed in this material are those of the author(s) and therefore the National Research Foundation and the Department of Science and Technology do not accept any liability with regard thereto.

References

Barrera FN, Fendos J, Engelman DM (2012) Membrane physical properties influence transmembrane helix formation. Proc Natl Acad Sci USA 109:14422–14427

Ben-Tal N, Honig B, Miller C, McLaughlin S (1997) Electrostatic binding of proteins to membranes. Theoretical predictions and experimental results with charybdotoxin and phospholipid vesicles. Biophys J 73:1717–1727

Dewald AH, Hodges JC, Columbus L (2011) Physical determinants of beta-barrel membrane protein folding in lipid vesicles. Biophys J 100:2131–2140

Fanucchi S, Adamson RJ, Dirr HW (2008) Formation of an unfolding intermediate state of soluble chloride intracellular channel protein CLIC1 at acidic pH. Biochemistry 47:11674–11681

Gafvelin G, Sakaguchi M, Andersson H, von Heijne G (1997) Topological rules for membrane protein assembly in eukaryotic cells. J Biol Chem 272:6119–6127

Gallusser A, Kuhn A (1990) Initial steps in protein membrane insertion. Bacteriophage M13 procoat protein binds to the membrane surface by electrostatic interaction. EMBO J 9:2723–2729

Goodchild SC, Howell MW, Cordina NM, Littler DR, Breit SN, Curmi PM, Brown LJ (2009) Oxidation promotes insertion of the CLIC1 chloride intracellular channel into the membrane. Eur Biophys J 39:129–138

Granseth E, von Heijne G, Elofsson A (2005) A study of the membrane–water interface region of membrane proteins. J Mol Biol 346:377–385

Habeeb AF (1972) Reaction of protein sulfhydryl groups with Ellman's reagent. Methods Enzymol 25C:457–464

Heimburg T, Marsh D (1995) Protein surface-distribution and protein–protein interactions in the binding of peripheral proteins to charged lipid membranes. Biophys J 68:536–546

Hendsch ZS, Tidor B (1994) Do salt bridges stabilize proteins? A continuum electrostatic analysis. Protein Sci 3:211–226

Honig BH, Hubbell WL, Flewelling RF (1986) Electrostatic interactions in membranes and proteins. Annu Rev Biophys Biophys Chem 15:163–193

Johnson JE, Cornell RB (1999) Amphitropic proteins: regulation by reversible membrane interactions (review). Mol Membr Biol 16:217–235

Langosch D, Arkin IT (2009) Interaction and conformational dynamics of membrane-spanning protein helices. Protein Sci 18:1343–1358

Legg-E'silva D, Achilonu I, Fanucchi S, Stoychev S, Fernandes M, Dirr HW (2012) Role of Arginine 29 and Glutamic Acid 81 Interactions in the Conformational Stability of Human Chloride Intracellular Channel 1. Biochem 51(40):7854–7862

Littler DR, Harrop SJ, Fairlie WD, Brown LJ, Pankhurst GJ, Pankhurst S, DeMaere MZ, Campbell TJ, Bauskin AR, Tonini R et al (2004) The intracellular chloride ion channel protein CLIC1 undergoes a redox-controlled structural transition. J Biol Chem 279:9298–9305

Malik M, Shukla A, Amin P, Niedelman W, Lee J, Jividen K, Phang JM, Ding J, Suh KS, Curmi PM et al (2010) S-nitrosylation regulates nuclear translocation of chloride intracellular channel protein CLIC4. J Biol Chem 285:23818–23828

Manceva SD, Pusztai-Carey M, Butko P (2004) Effect of pH and ionic strength on the cytolytic toxin Cyt1A: a fluorescence spectroscopy study. Biochim Biophys Acta 1699:123–130

McLaughlin S, Murray D (2005) Plasma membrane phosphoinositide organization by protein electrostatics. Nature 438:605–611

McLaughlin S, Hangyas-Mihalyne G, Zaitseva I, Golebiewska U (2005) Reversible—through calmodulin: electrostatic interactions between basic residues on proteins and acidic lipids in the plasma membrane. Biochem Soc Symp 72:189–198

Mishra VK, Palgunachari MN (1996) Interaction of model class A1, class A2, and class Y amphipathic helical peptides with membranes. Biochemistry 35:11210–11220

Mulgrew-Nesbitt A, Diraviyam K, Wang J, Singh S, Murray P, Li Z, Rogers L, Mirkovic N, Murray D (2006) The role of electrostatics in protein-membrane interactions. Biochim Biophys Acta 1761:812–826

Mynott AV, Harrop SJ, Brown LJ, Breit SN, Kobe B, Curmi PM (2011) Crystal structure of importin-alpha bound to a peptide bearing the nuclear localisation signal from chloride intracellular channel protein 4. FEBS J 278:1662–1675

Nilsson J, Persson B, von Heijne G (2005) Comparative analysis of amino acid distributions in integral membrane proteins from 107 genomes. Proteins 60:606–616

Olivella M, Deupi X, Govaerts C, Pardo L (2002) Influence of the environment in the conformation of alpha-helices studied by protein database search and molecular dynamics simulations. Biophys J 82:3207–3213

Pace CN, Scholtz JM (1998) A helix propensity scale based on experimental studies of peptides and proteins. Biophys J 75:422–427

Peter B, Ngubane NC, Fanucchi S, Dirr HW (2013) Membrane mimetics induce helix formation and oligomerization of the chloride intracellular channel protein 1 transmembrane domain. Biochemistry 52:2739–2749

Peter B, Polyansky AA, Fanucchi S, Dirr HW (2014) A Lys-Trp cation-pi interaction mediates the dimerization and function of the chloride intracellular channel protein 1 transmembrane domain. Biochemistry 53:57–67

Popot JL, Engelman DM (1990) Membrane protein folding and oligomerization: the two-stage model. Biochemistry 29:4031–4037

Roccatano D, Colombo G, Fioroni M, Mark AE (2002) Mechanism by which 2,2,2-trifluoroethanol/water mixtures stabilize secondary-structure formation in peptides: a molecular dynamics study. Proc Natl Acad Sci U S A 99:12179–12184

Singh H, Ashley RH (2007) CLIC4 (p64H1) and its putative transmembrane domain form poorly selective, redox-regulated ion channels. Mol Membr Biol 24:41–52

Smith SO, Smith CS, Bormann BJ (1996) Strong hydrogen bonding interactions involving a buried glutamic acid in the transmembrane sequence of the neu/erbB-2 receptor. Nat Struct Biol 3:252–258

Sreerama N, Woody RW (2000) Estimation of protein secondary structure from circular dichroism spectra: comparison of CONTIN, SELCON, and CDSSTR methods with an expanded reference set. Anal Biochem 287:252–260

Stoychev SH, Nathaniel C, Fanucchi S, Brock M, Li S, Asmus K, Woods VL Jr, Dirr HW (2009) Structural dynamics of soluble chloride intracellular channel protein CLIC1 examined by amide hydrogen-deuterium exchange mass spectrometry. Biochemistry 48:8413–8421

Suh KS, Mutoh M, Nagashima K, Fernandez-Salas E, Edwards LE, Hayes DD, Crutchley JM, Marin KG, Dumont RA, Levy JM et al (2004) The organellular chloride channel protein CLIC4/mtCLIC translocates to the nucleus in response to cellular stress and accelerates apoptosis. J Biol Chem 279:4632–4641

van Klompenburg W, Nilsson I, von Heijne G, de Kruijff B (1997) Anionic phospholipids are determinants of membrane protein topology. EMBO J 16:4261–4266

von Heijne G (1984) Analysis of the distribution of charged residues in the N-terminal region of signal sequences: implications for protein export in prokaryotic and eukaryotic cells. EMBO J 3:2315–2318

von Heijne G, Gavel Y (1988) Topogenic signals in integral membrane proteins. Eur J Biochem 174:671–678

Wallach DF, Zahler PH (1966) Protein conformations in cellular membranes. Proc Natl Acad Sci U S A 56:1552–1559

Wallin E, von Heijne G (1995) Properties of N-terminal tails in G-protein coupled receptors: a statistical study. Protein Eng 8:693–698

Warton K, Tonini R, Fairlie WD, Matthews JM, Valenzuela SM, Qiu MR, Wu WM, Pankhurst S, Bauskin AR, Harrop SJ et al (2002) Recombinant CLIC1 (NCC27) assembles in lipid bilayers via a pH-dependent two-state process to form chloride ion channels with identical characteristics to those observed in Chinese hamster ovary cells expressing CLIC1. J Biol Chem 277:26003–26011

White SH, Wimley WC (1999) Membrane protein folding and stability: physical principles. Annu Rev Biophys Biomol Struct 28:319–365

Xia XF, Sui SF (2000) The membrane insertion of trichosanthin is membrane-surface-pH dependent. Biochem J 349(Pt 3):835–841

Xu D, Lin SL, Nussinov R (1997) Protein binding versus protein folding: the role of hydrophilic bridges in protein associations. J Mol Biol 265:68–84

European Biophysics Journal

A conserved cationic motif enhances membrane binding and insertion of the chloride intracellular channel protein 1 transmembrane domain

Bradley Peter[1], Sylvia Fanucchi[1] and Heini W. Dirr[1*]

[1]Protein Structure-Function Research Unit, School of Molecular and Cell Biology, University of the Witwatersrand, Johannesburg, 2050, South Africa

[*]Corresponding author; E-mail: heinrich.dirr@wits.ac.za; Tel: +27 11 7176352; Fax: +27 11 7176351

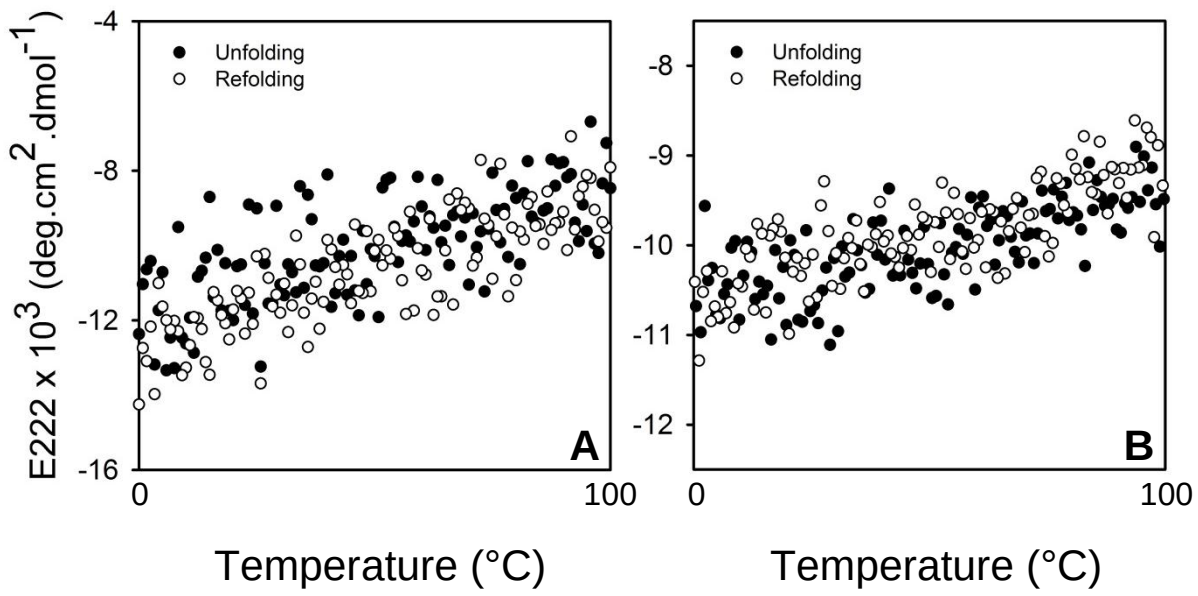

Figure S1 Thermal stability of the EEE CLIC1 TMD. Thermal melts of 20 µM EEE TMD peptide were monitored by ellipticity at 222 nm in 40 % (v/v) TFE (A) and 15 mM SDS (B). The unfolding (closed circle) and refolding (open circle) pathways showed no hysteresis, suggesting that the process is reversible. The peptide unfolds via a linear loss of structure, suggesting a non-cooperative pathway common for many transmembrane domains. The absence of any native or denatured baselines prevents the determination of thermodynamic parameters. The buffer used was 20 mM sodium phosphate, 1 mM DTT, 0.2 % (w/v) NaN_3, pH 5.5

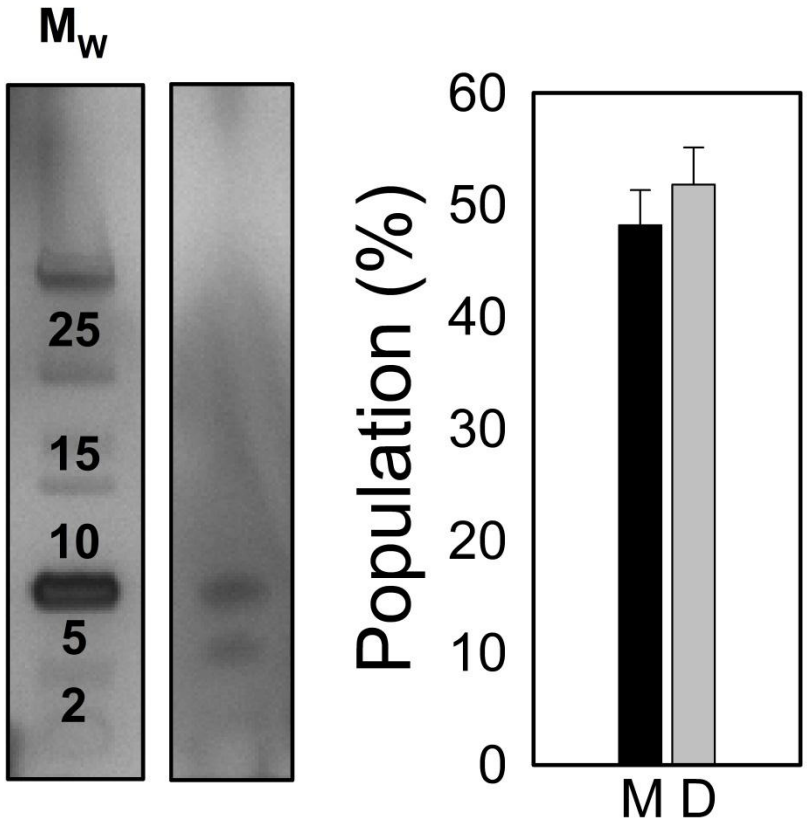

Figure S2 SDS-PAGE monitored dimerisation of the CLIC1 EEE TMD peptide. SDS-PAGE was used to investigate concentration-dependent oligomerisation of the TMD peptide in 15 mM SDS micelles. The peptide displays clear dimer formation at high concentrations, with band intensities confirming that ~ 53 % of the peptide exists as a dimer. This is comparable to the wild-type and suggests that the cationic motif is not involved in dimerisation. Experimental details are given below. Error bars represent the standard deviation from four independent replicates

Tricine SDS-PAGE

The oligomeric state of the EEE TMD peptide in SDS micelles was investigated by gel electrophoresis. A modified Tricine buffer system (Schägger and von Jagow, 1987) with a 0.5 % SDS gel was used. Samples were prepared and electrophoresed as described (Peter *et al.*, 2013). Silver staining was performed using the SilverQuest™ kit (Life Technologies, Carlsbad, California, USA) according to the manufacturer's instructions. Band intensities were quantified using the ImageJ program (http://rsbweb.nih.gov/ij/).

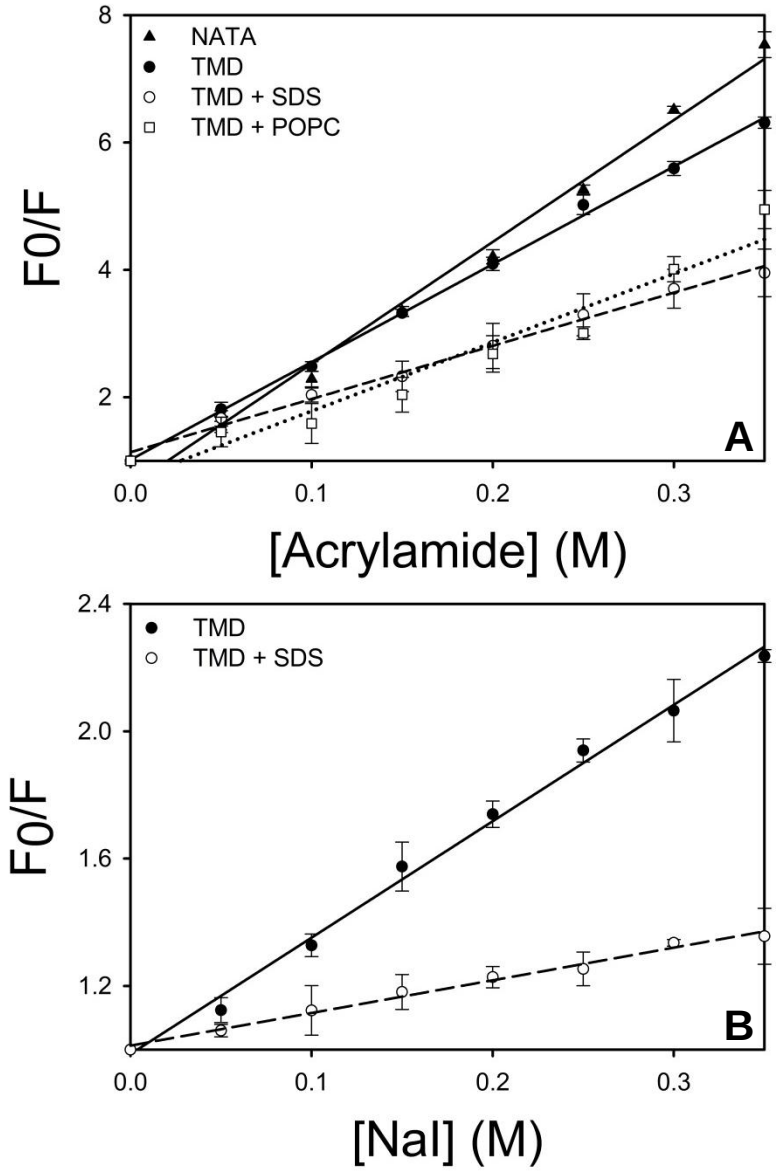

Figure S3 Stern-Volmer plots of the quenching of Trp35 fluorescence by acrylamide and iodide. Acrylamide (A) and iodide (B) quenching of 15 µM CLIC1 EEE TMD peptide and 15 µM NATA was performed in buffer, 15 mM SDS and 2.5 mM POPC. The linear nature of these plots suggests that the quenching occurs via a dynamic process. Iodide quenching was chosen as an additional probe in SDS owing to the ability of acrylamide to penetrate SDS micelles. Samples were analysed in 20 mM sodium phosphate, 1 mM DTT, 0.2 % (w/v) NaN_3, pH 5.5. Error bars represent the standard deviation from four independent replicates

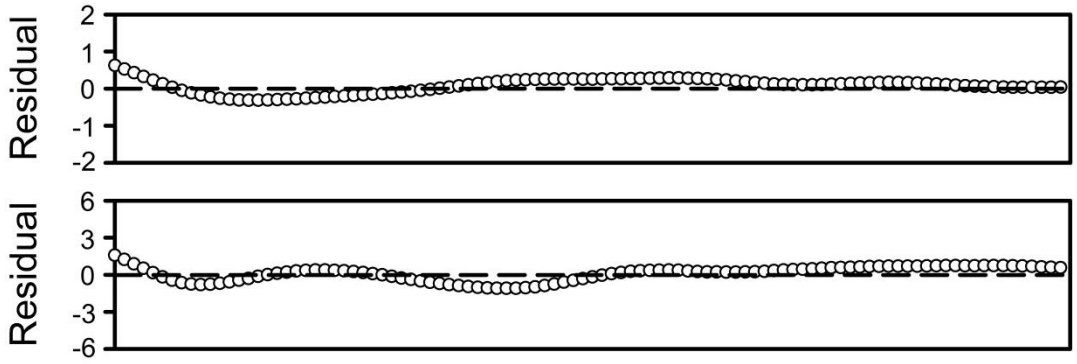

Figure S4 Residuals of the fits to the chloride influx data of the CLIC1 EEE TMD peptide. The residuals from the double exponential decay fits are shown for the EEE TMD peptide at pH 5.5 (top panel) and pH 7.2 (bottom panel). The residuals suggest that the models used to fit to the data are accurate. The data were fit using SigmaPlot V 11.0

Table S1 Structural changes of the wild-type CLIC1 TMD peptide in response to membrane mimetics. These results are taken from Peter *et al*., 2013

	Buffer	TFE	SDS	POPC
α-helix (%)[a]	18 (± 5)	64 (± 8)	59 (± 10)	56 (± 9)
β-sheet (%)[a]	23 (± 4)	9 (±2)	7 (± 3)	11 (± 6)
Random coil (%)[a]	56 (± 9)	22 (± 9)	29 (± 7)	31 (± 11)
NRMSD	0.23	0.095	0.11	0.17
λ_{max} (nm)	355 (± 2)	355 (± 1)	343 (± 1)	342 (± 3)
K_{SV} (M^{-1})[b]	15.35 (± 0.23)/3.52 (± 0.12)	ND	5.66 (± 0.1)/1.03 (± 0.09)	7.01 (± 0.76)
Fraction of free thiols[c]	0.98 (± 0.01)	ND	0.64 (± 0.009)	0.39 (± 0.01)/0.63 (± 0.03)

[a]CDPro reference set SP43

[b]Samples with two values represent the K_{SV} determined from acrylamide and iodide quenching, respectively

[c]In POPC, the first value represents external DTNB (*cis*) whilst the second value represents encapsulated DTNB (*trans*)

Chapter 5

General Discussion

5.1 Membrane-Induced Structural Transition of the CLIC1 Transmembrane Domain

This study has highlighted the structural plasticity of the CLIC1 TMD in response to a membrane environment. Upon interaction with membranes, the TMD undergoes a dramatic structural rearrangement to form a α-helix which is consistent with its predicted membrane conformation (Cromer *et al*., 2002; Fanucchi *et al*., 2008; Peter *et al*., 2013). The acquisition of helical secondary structure correlates with the insertion of the domain into lipid bilayers. This suggests that the membrane-catalysed refolding of the TMD is a prerequisite for insertion and subsequent chloride ion transport. The membrane environment also induces changes in the thermodynamic stability of the domain relative to that of the entire protein. When unfolded in aqueous solution, TMDs have a less compact structure with a high conformational entropy (Popot and Engelman, 2000). These unfolded conformations are stabilised by their relatively high hydration state in the absence of membranes (Jayasinghe *et al*., 2001; Finger *et al*., 2006). The addition of membranes/membrane-mimetics excludes water molecules from the domain and forces the TMD to adopt an entropically-lower helical/sheet conformation by inducing intrachain backbone interactions (Roccatano *et al*., 2002). The entropic loss resulting from folding is compensated for by strengthened backbone and hydrophobic interactions (Luo and Baldwin. 1998; Rohl *et al*., 1996; Wei *et al*., 2006). This leads to a folded domain which is resistant to unfolding. The thermal unfolding of the CLIC1 TMD is a prime example of membrane-enhanced stability, showing incomplete and non-cooperative unfolding in the presence of membrane mimetics (Peter *et al*., 2013; Peter *et al*., 2014).

A key regulator of both the structure and stability of full-length CLIC1 is pH. The lowered pH at the membrane interface (~ 4-5) relative to the cytosol (~ 7.4) is thought to act as the trigger for membrane insertion of CLIC1 in much the same way as bacterial PFTs (Fanucchi *et al*., 2008). The structure and stability of the CLIC1 TMD, however, is pH-insensitive (Ngubane, MSc Dissertation; URL: http://hdl.handle.net/10539/11477). CLIC1 contains a stabilising electrostatic network which is easily disrupted by changes in pH (Achilonu *et al*., 2012; Legg E'Silva *et al*., 2012). This network comprises residues which are not found within the TMD and thus do not influence the structure of the domain. Therefore, the initial refolding and insertion of the TMD is likely independent of pH and does not follow an identical mechanism to the bacterial PFTs. Changes in pH may, however, influence both exposure of the TMD in the full-length protein as well as ion-conducting activity (Warton *et al*., 2002; Fanucchi *et al*., 2008).

5.2 The Putative Pore Formed by the CLIC1 Transmembrane Domain

In order to form an ion-conducting pore, the single CLIC1 TMD must oligomerise. This study has identified a dimeric species of the TMD in membranes which is stabilised by a combination of hydrophobic and electrostatic (cation-π) interactions (Peter *et al*., 2013; Peter *et al*., 2014). Thus, within a membrane-like environment, buried electrostatic and hydrophobic interactions provide a thermodynamic driving force for the self-association of CLIC1 TMD helices. It must be reiterated that the dimer itself is unlikely to represent the functional pore of CLIC1. Rather, it is a weakly-active protopore intermediate during the formation of higher order oligomers which then facilitate pore formation. This is consistent with the two-step Cl^- influx observed for the TMD (Peter *et al*., 2014) and is similar to the association of bacterial PFTs (Bennett *et al*., 1994), Bax (Garcia-Saez *et al*., 2004) and Bcl-x_L (Thuduppathy and Hill, 2006).

Two models for the formation of the CLIC1 channel have been proposed, both comprising the TMD (Singh, 2010; Goodchild *et al*., 2011). The scheme presented by Singh (2010) closely matches ion-conductance data (Warton *et al*., 2002) as well as the data presented here. This model postulates that: (i) four TMD helices associate to form a pre-pore protomer and (ii) four protomers interact to form the functional channel. The interactions which stabilise these complexes are unknown, although the predominance of the dimeric form of the CLIC1 TMD suggests that it may play an important role in channel formation. A possible mechanism of channel formation involving the dimeric TMD is proposed in Figure 8. In this model, CLIC1 exists predominantly as a dimer in the membrane at low concentrations (Figure 8 A). The cation-π interaction between Trp35 and Lys37 plays a dual role of (i) stabilising the dimer and (ii) neutralising the positive charge on Lys37, thus allowing it to partition across the membrane with a minimal energetic cost. The charged Arg29 residues in the TMD dimer would be located near the lipid head groups and likely snorkel and interact with the negatively-charged phosphate moieties (Strandberg and Killian, 2003; Dorairaj and Allen, 2007). According to the Singh model, four TMD helices associate to form a symmetric pre-pore protomer (Figure 8 B). In order for the TMD dimer to assume this new conformation, the cation-π interaction must be broken. This would induce a conformational rearrangement thereby enabling Trp35 to interact with the lipid tails whilst allowing the positively-charged side chains of Arg29 and Lys37 to extend into the pore to form a series of charged rings at the top and centre of the pore. These charged rings would likely attract Cl^- to the pore as well as direct Cl^- transport through the pore. Four of these protopores would then associate to form the fully-functional channel complex.

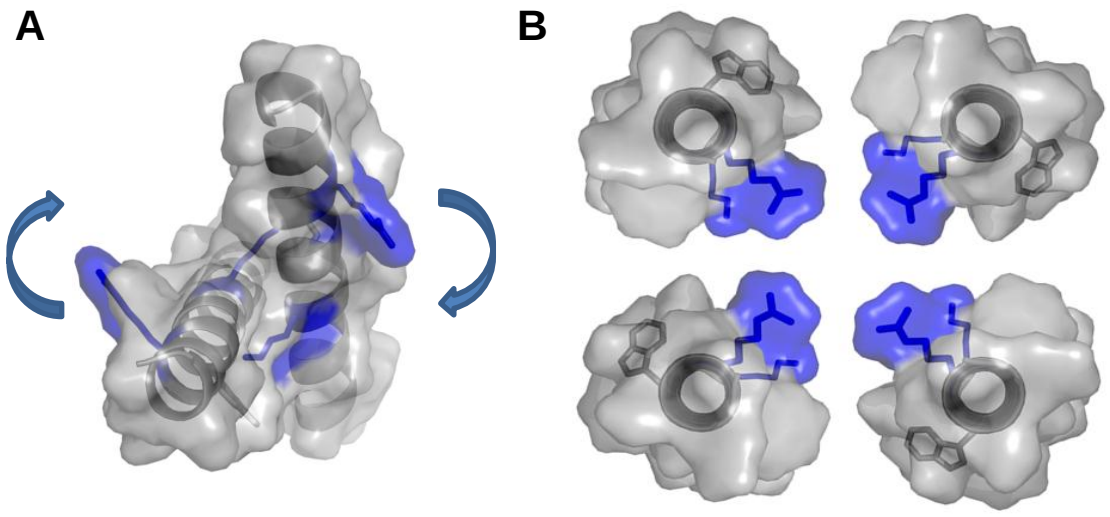

Figure 8 Role of the CLIC1 TMD in channel formation. (A) In the membrane, the CLIC1 TMD exists predominantly as a cation-π stabilised dimer. **(B)** In order to form a four helix protomer, the cation-π interaction is broken. This induces a conformational rearrangement which facilitates the association of two dimers. The new conformation forms a central pore lined by two charged rings comprising Arg29 and Lys37. These charged clusters may attract Cl^- to the pore as well as direct Cl^- transport through it. Four protomers subsequently associate to form the functional CLIC1 channel. The figure in **(A)** was modelled using the PREDDIMER algorithm whilst the figure in **(B)** was generated using PyMol V 1.3

5.3 Structural and Functional Regulation of the CLIC1 Transmembrane Domain

The CLIC1 TMD is a thermodynamically stable and independently folded unit capable of inserting into membranes in the absence of a signal peptide as well as conducting Cl^- across the membrane. The CLIC1 TMD is thus a self-contained structural and functional unit. This is consistent with the truncation studies carried out on CLIC4 by Singh and Ashley (2006). The domain may also be capable of independently regulating its folding/membrane insertion as well as Cl^- transport in the absence of the N- and C-domains.

The pH at the membrane interface has already been discussed as a contributing factor to the exposure of the TMD in full-length CLIC1. However, given the lack of ionisable residues within the TMD, pH is unlikely to promote local unfolding and refolding of the domain. The predominantly charged nature of the membrane interface is, however, ideal for ionic interactions (Honig, 1984; Hendsch and Tidor, 1994; Xu *et al.*, 1997). The cationic (KRR) motif identified in this study reversibly regulates membrane binding via electrostatic attraction with phosphate head groups. This interaction subsequently behaves as an electrostatic plug which anchors the TMD in the membrane (Peter *et al*., 2014). Electrostatic interactions at the membrane interface are, of course, heavily dependent on the lipid composition of the membrane itself (Träuble and Eibl, 1974). CLIC1 is primarily thought to localise to nuclear membranes (Valenzuela *et al*., 1997) which contain a greater proportion of the anionic lipid phosphatidylserine (PS) compared to the plasma membrane (Neitcheva and Peeva, 1995; Albi *et al*., 1997). The negative surface potential created by PS may serve two roles for insertion of the CLIC1 TMD: (i) it may raise the pK_a values of acidic residues to ensure that they are protonated (neutral) and able to cross the membrane and (ii) it may act as a means of attracting positively-charged residues to the membrane (as with the KRR motif). Should the lipid composition not be ideal, the domain will not bind to the membrane and no channel will be formed. The influence of membrane composition on protein binding and

insertion has been seen in both integral and amphipathic proteins (Kagan *et al*., 1981; Johnson *et al*., 2003).

The regulation of CLIC1 function has also been linked to pH and membrane composition, with Cl^- transport being maximal at low pH and in the presence of anionic lipids (Warton *et al*., 2002; Singh and Ashley, 2006). This is likely linked to variations in membrane binding of the TMD as described and, more specifically, the role played by the KRR motif. Channel activity is significantly reduced following the removal of this motif (Peter *et al*., 2014), lending support to this theory. Redox state is also thought to regulate the activity of the CLIC1 TMD (Littler *et al*., 2005). Although this was not tested in this study, Cys24 of the TMD is ideally situated to act as a redox-sensitive gating mechanism. In this study, dimerisation was also shown to influence Cl^- transport. The removal of dimer interactions resulted in a 30-40 % reduction in channel activity, suggesting that dimerisation modulates the rate of Cl^- conductance. Both chloride transport as well as helical structure were shown to be concentration-dependent (Peter *et al*., 2013; Peter *et al*., 2014). This suggests that, at low concentrations, the TMD may not assume a membrane-competent folded state. According to Figure 8, a reduction in membrane TMD dimer levels will likely result in fewer functional channels being formed. This is of particular interest to *in vivo* regulation of CLIC1 function since changes in the relative expression levels of the soluble protein will directly affect Cl^- transport. Overexpression of CLIC1 has been linked to colorectal cancer (Petrova *et al*., 2008) and Alzheimer's disease (Novarino *et al.*, 2004; Milton *et al.*, 2008) whereas lower expression levels of CLIC4 induce an antitumour response *in vitro* and reduced tumour growth *in vivo* (Suh *et al*., 2004). The expression, insertion and Cl^- transport of CLIC1 and its TMD must therefore be tightly regulated in order to maintain cellular homeostasis.

5.4 The Transmembrane Domain in the Context of Full-Length CLIC1

It can be argued that an understanding of how the TMD responds to a membrane environment does not necessarily indicate how the full-length protein binds to and inserts into membranes. The CLIC1 TMD itself occupies only a single αβ fold comprising < 15 % of the protein's amino acid content. Despite this, the TMD remains highly conserved across the CLICs and CLIC homologs compared to the N- and C-domains. In addition, truncation studies (Singh and Ashley, 2006) as well as the work presented here prove that the TMD alone can carry out the role of an amphitropic chloride channel as efficiently as the full-length protein. This is supported by the fact that (i) transmembrane domains are thermodynamically stable when excised from the parent protein (Popot and Engelman, 2000) and (ii) the TMD of CLIC1 likely forms the majority of membrane contacts. The CLIC1 TMD is thus an excellent candidate for studying membrane interactions of the full-length protein.

This naturally leads to the question as to why the N- and C-domains have not become redundant. Littler (2010) suggests that insertion and channel activity of the TMD are supported by the rest of the protein in several ways, including (i) membrane anchorage and (ii) funnelling of Cl^- to the pore. Other roles may include shielding the hydrophobic TMD from the cytosol (similar to the 'Umbrella' hypothesis of bacterial PFTs) (Cromer *et al*., 2002) or regulating the rate of Cl^- influx. Regardless, some form of supporting role in membrane binding/insertion and channel activity is likely since a functional role for the soluble protein has not yet been identified.

5.5 Membrane Insertion Mechanism of the CLIC1 Transmembrane Domain

The primary focus of this work was to understand how the CLIC1 TMD responded to a membrane environment in terms of its structure as well as its interaction with the membrane.

In doing so, aspects of the membrane insertion mechanism were elucidated. Based on this work, a possible mechanism for TMD insertion has been proposed (Figure 9). Under the influence of a signal, be it pH, oxidation state, cell cycle or apoptotic response, the unstructured TMD relocates to the membrane interface. Here, the net negative surface potential and lower dielectric constant cause the TMD to refold to form a α-helix. A combination of electrostatic attraction between the phosphate moieties and the KRR motif as well as hydrophobic interactions enable the TMD helix to partition onto the membrane surface. This is followed by the spontaneous insertion of the TMD to form a membrane-spanning helix. At this stage, the KRR motif likely acts as an electrostatic 'plug' to anchor the helices in the membrane. Individual helices then associate via hydrophobic interactions as well as a Lys37-mediated cation-π interaction to form stable dimers. These dimers subsequently oligomerise to form tetrameric helix bundles which further associate to form ion-channels. This mechanism, while only putative, is consistent with the folding models of α-helical membrane proteins proposed by Jacobs and White (1989), Popot and Engelman (1990) and White and Wimley (1999). It also shares similarities with other amphitropic proteins such as diphtheria toxin (Bennett *et al*., 1994; Vargas-Uribe *et al*., 2013), Bcl-x_L (Thuduppathy and Hill, 2006; Vargas-Uribe *et al*., 2013) and Bax (Garcia-Saez *et al*., 2004). Given the structure and sequence conservation between members of the CLIC family, it is possible that this mechanism is a shared feature of these amphitropic ion channels. An alternative mechanism of membrane insertion may exist, based on similarities to the bacterial PFTs, whereby the TMD tethers the inactive protein to the membrane surface. A subsequent stimulus (such as pH or lipid composition) would then trigger complete insertion of the TMD followed by channel formation.

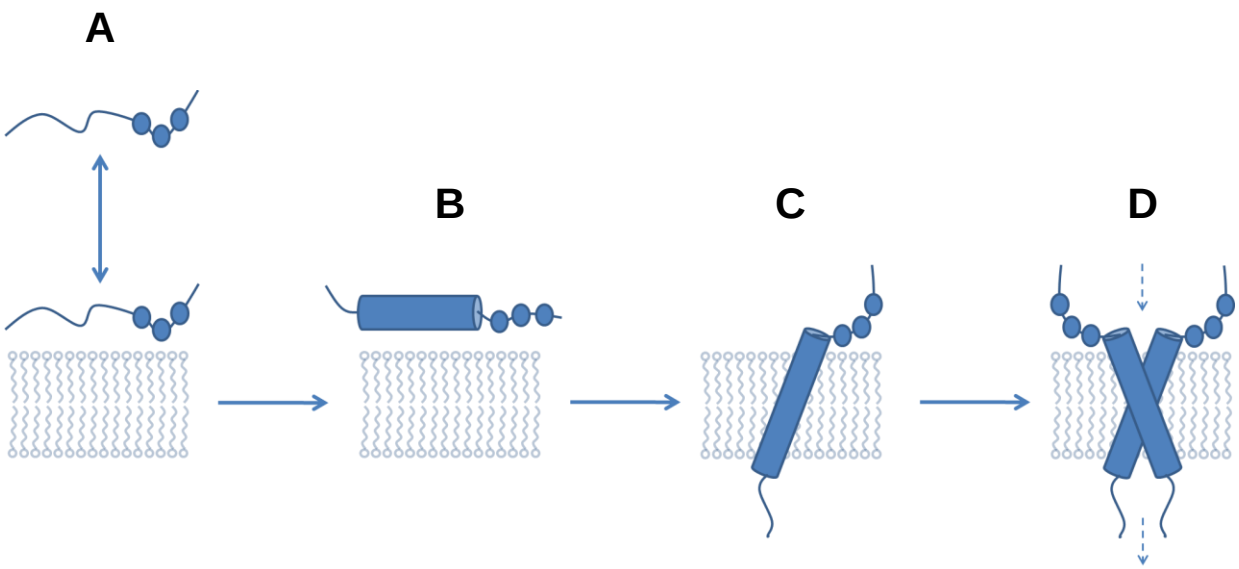

Figure 9 Membrane insertion mechanism of the CLIC1 TMD. (A) A cytoplasmic signal such as pH, oxidation state, cell cycle or apoptotic response triggers the TMD to translocate to the membrane. **(B)** As the unstructured domain approaches the membrane interface, it refolds to form a α-helix. **(C)** Electrostatic interactions between the anionic phosphate moieties and the cationic KRR motif (shown as three circles) allow the TMD to partition onto the membrane surface, followed by spontaneous insertion into the membrane. **(D)** Individual membrane-spanning helices then associate via a Lys37-mediated cation-π interaction to form dimers. These dimeric helix bundles subsequently associate to form the fully-functional ion channel.

5.6 Conclusions

The dimorphic nature of CLIC1 is unique among eukaryotic ion channels. Despite its biological significance, the mechanism by which CLIC1 spontaneously converts between a soluble and membrane-bound state is poorly understood. In addition, the transmembrane domain implicated in membrane insertion and channel activity has not been studied. In this research, the molecular basis of amphitropism in the CLIC1 transmembrane domain was determined. This comprised an analysis of both the membrane-induced structural plasticity of the domain as well as key domain-domain and domain-membrane interactions required for membrane binding and insertion. This is the first reported study directed at the CLIC1 transmembrane domain and represents an important step towards understanding how amphitropism occurs in CLIC1 as well as how the transmembrane domain regulates channel activity *in vivo*. This work thus offers a unique insight into how CLIC1 and other proteins defy the ‘one-sequence one-fold’ hypothesis.

Chapter 6

References

Achilonu, I., Fanucchi, S., Cross, M., Fernandes, M., and Dirr, H.W. (2012). Role of individual histidines in the pH-dependent global stability of human chloride intracellular channel 1. Biochemistry *51*, 995-1004.

Adams, J.M., and Cory, S. (1998). The Bcl-2 protein family: arbiters of cell survival. Science *281*, 1322-1326.

Albi, E., Tomassoni, M.L., and Viola-Magni, M. (1997). Effect of lipid composition on rat liver nuclear membrane fluidity. Cell Biochem Funct *15*, 181-190.

Alvaro, D., Cho, W.K., Mennone, A., and Boyer, J.L. (1993). Effect of secretion on intracellular pH regulation in isolated rat bile duct epithelial cells. J Clin Invest *92*, 1314-1325.

Andersen, O.S., and Koeppe, R.E., 2nd (2007). Bilayer thickness and membrane protein function: an energetic perspective. Annu Rev Biophys Biomol Struct *36*, 107-130.

Anderson, M.P., and Welsh, M.J. (1991). Calcium and cAMP activate different chloride channels in the apical membrane of normal and cystic fibrosis epithelia. Proc Natl Acad Sci U S A *88*, 6003-6007.

Arkin, I.T., and Brunger, A.T. (1998). Statistical analysis of predicted transmembrane alpha-helices. Biochim Biophys Acta *1429*, 113-128.

Armstrong, R.N. (1997). Structure, catalytic mechanism, and evolution of the glutathione transferases. Chem Res Toxicol *10*, 2-18.

Arreola, J., Melvin, J.E., and Begenisich, T. (1998). Differences in regulation of Ca(2+)-activated Cl- channels in colonic and parotid secretory cells. Am J Physiol *274*, C161-166.

Aurora, R., and Rose, G.D. (1998). Helix capping. Protein Sci *7*, 21-38.

Bateman, A. (1997). The structure of a domain common to archaebacteria and the homocystinuria disease protein. Trends Biochem Sci *22*, 12-13.

Bear, C.E., Li, C.H., Kartner, N., Bridges, R.J., Jensen, T.J., Ramjeesingh, M., and Riordan, J.R. (1992). Purification and functional reconstitution of the cystic fibrosis transmembrane conductance regulator (CFTR). Cell *68*, 809-818.

Belmonte, G., Pederzolli, C., Macek, P., and Menestrina, G. (1993). Pore formation by the sea anemone cytolysin equinatoxin II in red blood cells and model lipid membranes. J Membr Biol *131*, 11-22.

Ben-Ari, Y., Khazipov, R., Leinekugel, X., Caillard, O., and Gaiarsa, J.L. (1997). GABAA, NMDA and AMPA receptors: a developmentally regulated 'menage a trois'. Trends Neurosci *20*, 523-529.

Bennett, M.J., Choe, S., and Eisenberg, D. (1994). Refined structure of dimeric diphtheria toxin at 2.0 A resolution. Protein Sci *3*, 1444-1463.

Bergers, J.J., Vingerhoeds, M.H., van Bloois, L., Herron, J.N., Janssen, L.H., Fischer, M.J., and Crommelin, D.J. (1993). The role of protein charge in protein-lipid interactions. pH-dependent changes of the electrophoretic mobility of liposomes through adsorption of water-soluble, globular proteins. Biochemistry *32*, 4641-4649.

Berry, K.L., Bulow, H.E., Hall, D.H., and Hobert, O. (2003). A C. elegans CLIC-like protein required for intracellular tube formation and maintenance. Science *302*, 2134-2137.

Berry, K.L., and Hobert, O. (2006). Mapping functional domains of chloride intracellular channel (CLIC) proteins in vivo. J Mol Biol *359*, 1316-1333.

Berryman, M., and Bretscher, A. (2000). Identification of a novel member of the chloride intracellular channel gene family (CLIC5) that associates with the actin cytoskeleton of placental microvilli. Mol Biol Cell *11*, 1509-1521.

Berryman, M., Bruno, J., Price, J., and Edwards, J.C. (2004). CLIC-5A functions as a chloride channel in vitro and associates with the cortical actin cytoskeleton in vitro and in vivo. J Biol Chem *279*, 34794-34801.

Betz, H. (1990). Ligand-gated ion channels in the brain: the amino acid receptor superfamily. Neuron *5*, 383-392.

Board, P.G., Coggan, M., Chelvanayagam, G., Easteal, S., Jermiin, L.S., Schulte, G.K., Danley, D.E., Hoth, L.R., Griffor, M.C., Kamath, A.V., *et al.* (2000). Identification, characterization, and crystal structure of the Omega class glutathione transferases. J Biol Chem *275*, 24798-24806.

Bretscher, M.S. (1973). Membrane structure: some general principles. Science *181*, 622-629.

Brown, D.A., and London, E. (2000). Structure and function of sphingolipid- and cholesterol-rich membrane rafts. J Biol Chem *275*, 17221-17224.

Bryan, P.N., and Orban, J. (2010). Proteins that switch folds. Curr Opin Struct Biol *20*, 482-488.

Buckland, A.G., and Wilton, D.C. (2000). The antibacterial properties of secreted phospholipases A(2). Biochim Biophys Acta *1488*, 71-82.

Caffrey, M. (2003). Membrane protein crystallization. J Struct Biol *142*, 108-132.

Catterall, W.A. (1988). Molecular properties of voltage-sensitive sodium and calcium channels. Braz J Med Biol Res *21*, 1129-1144.

Chakrabarti, P., and Chakrabarti, S. (1998). C--H...O hydrogen bond involving proline residues in alpha-helices. J Mol Biol *284*, 867-873.

Chen, T.Y. (2005). Structure and function of clc channels. Annu Rev Physiol *67*, 809-839.

Chen, T.Y., and Miller, C. (1996). Nonequilibrium gating and voltage dependence of the ClC-0 Cl- channel. J Gen Physiol *108*, 237-250.

Choe, S., Bennett, M.J., Fujii, G., Curmi, P.M., Kantardjieff, K.A., Collier, R.J., and Eisenberg, D. (1992). The crystal structure of diphtheria toxin. Nature *357*, 216-222.

Cordes, F.S., Bright, J.N., and Sansom, M.S. (2002). Proline-induced distortions of transmembrane helices. J Mol Biol *323*, 951-960.

Cromer, B.A., Morton, C.J., Board, P.G., and Parker, M.W. (2002). From glutathione transferase to pore in a CLIC. Eur Biophys J *31*, 356-364.

Cunningham, S.A., Awayda, M.S., Bubien, J.K., Ismailov, II, Arrate, M.P., Berdiev, B.K., Benos, D.J., and Fuller, C.M. (1995). Cloning of an epithelial chloride channel from bovine trachea. J Biol Chem *270*, 31016-31026.

Deutsch, C. (2002). Potassium channel ontogeny. Annu Rev Physiol *64*, 19-46.

Diller, A., Loudet, C., Aussenac, F., Raffard, G., Fournier, S., Laguerre, M., Grelard, A., Opella, S.J., Marassi, F.M., and Dufourc, E.J. (2009). Bicelles: A natural 'molecular goniometer' for structural, dynamical and topological studies of molecules in membranes. Biochimie *91*, 744-751.

Dirr, H., Reinemer, P., and Huber, R. (1994a). Refined crystal structure of porcine class Pi glutathione S-transferase (pGST P1-1) at 2.1 A resolution. J Mol Biol *243*, 72-92.

Dirr, H., Reinemer, P., and Huber, R. (1994b). X-ray crystal structures of cytosolic glutathione S-transferases. Implications for protein architecture, substrate recognition and catalytic function. Eur J Biochem *220*, 645-661.

Dorairaj, S., and Allen, T.W. (2007). On the thermodynamic stability of a charged arginine side chain in a transmembrane helix. Proc Natl Acad Sci U S A *104*, 4943-4948.

Dulhunty, A.F., Pouliquin, P., Coggan, M., Gage, P.W., and Board, P.G. (2005). A recently identified member of the glutathione transferase structural family modifies cardiac RyR2 substate activity, coupled gating and activation by Ca2+ and ATP. Biochem J *390*, 333-343.

Duncan, R.R., Westwood, P.K., Boyd, A., and Ashley, R.H. (1997). Rat brain p64H1, expression of a new member of the p64 chloride channel protein family in endoplasmic reticulum. J Biol Chem *272*, 23880-23886.

Edwards, J.C. (1999). A novel p64-related Cl- channel: subcellular distribution and nephron segment-specific expression. Am J Physiol *276*, F398-408.

Fahlke, C., Yu, H.T., Beck, C.L., Rhodes, T.H., and George, A.L., Jr. (1997). Pore-forming segments in voltage-gated chloride channels. Nature *390*, 529-532.

Fanucchi, S., Adamson, R.J., and Dirr, H.W. (2008). Formation of an unfolding intermediate state of soluble chloride intracellular channel protein CLIC1 at acidic pH. Biochemistry *47*, 11674-11681.

Fernandez-Salas, E., Sagar, M., Cheng, C., Yuspa, S.H., and Weinberg, W.C. (1999). p53 and tumor necrosis factor alpha regulate the expression of a mitochondrial chloride channel protein. J Biol Chem *274*, 36488-36497.

Finger, C., Volkmer, T., Prodohl, A., Otzen, D.E., Engelman, D.M., and Schneider, D. (2006). The stability of transmembrane helix interactions measured in a biological membrane. J Mol Biol *358*, 1221-1228.

Friedli, M., Guipponi, M., Bertrand, S., Bertrand, D., Neerman-Arbez, M., Scott, H.S., Antonarakis, S.E., and Reymond, A. (2003). Identification of a novel member of the CLIC family, CLIC6, mapping to 21q22.12. Gene *320*, 31-40.

Garavito, R.M., and Ferguson-Miller, S. (2001). Detergents as tools in membrane biochemistry. J Biol Chem *276*, 32403-32406.

Garcia-Saez, A.J., Mingarro, I., Perez-Paya, E., and Salgado, J. (2004). Membrane-insertion fragments of Bcl-xL, Bax, and Bid. Biochemistry *43*, 10930-10943.

Goodchild, S.C., Angstmann, C.N., Breit, S.N., Curmi, P.M., and Brown, L.J. (2011). Transmembrane extension and oligomerization of the CLIC1 chloride intracellular channel protein upon membrane interaction. Biochemistry *50*, 10887-10897.

Goodchild, S.C., Howell, M.W., Cordina, N.M., Littler, D.R., Breit, S.N., Curmi, P.M., and Brown, L.J. (2009). Oxidation promotes insertion of the CLIC1 chloride intracellular channel into the membrane. Eur Biophys J *39*, 129-138.

Goodchild, S.C., Howell, M.W., Littler, D.R., Mandyam, R.A., Sale, K.L., Mazzanti, M., Breit, S.N., Curmi, P.M., and Brown, L.J. (2010). Metamorphic response of the CLIC1 chloride intracellular ion channel protein upon membrane interaction. Biochemistry *49*, 5278-5289.

Griffon, N., Jeanneteau, F., Prieur, F., Diaz, J., and Sokoloff, P. (2003). CLIC6, a member of the intracellular chloride channel family, interacts with dopamine D(2)-like receptors. Brain Res Mol Brain Res *117*, 47-57.

Grochulski, P., Masson, L., Borisova, S., Pusztai-Carey, M., Schwartz, J.L., Brousseau, R., and Cygler, M. (1995). Bacillus thuringiensis CryIA(a) insecticidal toxin: crystal structure and channel formation. J Mol Biol *254*, 447-464.

Gurezka, R., Laage, R., Brosig, B., and Langosch, D. (1999). A heptad motif of leucine residues found in membrane proteins can drive self-assembly of artificial transmembrane segments. J Biol Chem *274*, 9265-9270.

Gurtovenko, A.A., and Vattulainen, I. (2008). Membrane potential and electrostatics of phospholipid bilayers with asymmetric transmembrane distribution of anionic lipids. J Phys Chem B *112*, 4629-4634.

Harrop, S.J., DeMaere, M.Z., Fairlie, W.D., Reztsova, T., Valenzuela, S.M., Mazzanti, M., Tonini, R., Qiu, M.R., Jankova, L., Warton, K., *et al.* (2001). Crystal structure of a soluble

form of the intracellular chloride ion channel CLIC1 (NCC27) at 1.4-A resolution. J Biol Chem *276*, 44993-45000.

Heiss, N.S., and Poustka, A. (1997). Genomic structure of a novel chloride channel gene, CLIC2, in Xq28. Genomics *45*, 224-228.

Hendsch, Z.S., and Tidor, B. (1994). Do salt bridges stabilize proteins? A continuum electrostatic analysis. Protein Sci *3*, 211-226.

Hildebrand, P.W., Preissner, R., and Frommel, C. (2004). Structural features of transmembrane helices. FEBS Lett *559*, 145-151.

Honig, B. (1984). Electrostatic interactions in membrane proteins. Prog Clin Biol Res *164*, 149-152.

Honig, B.H., Hubbell, W.L., and Flewelling, R.F. (1986). Electrostatic interactions in membranes and proteins. Annu Rev Biophys Biophys Chem *15*, 163-193.

Howell, S., and Crine, P. (1996). Type VI membrane proteins? Trends Biochem Sci *21*, 171-172.

Hsu, Y.T., Wolter, K.G., and Youle, R.J. (1997). Cytosol-to-membrane redistribution of Bax and Bcl-X(L) during apoptosis. Proc Natl Acad Sci U S A *94*, 3668-3672.

Hunte, C., Screpanti, E., Venturi, M., Rimon, A., Padan, E., and Michel, H. (2005). Structure of a Na+/H+ antiporter and insights into mechanism of action and regulation by pH. Nature *435*, 1197-1202.

Jacobs, R.E., and White, S.H. (1989). The nature of the hydrophobic binding of small peptides at the bilayer interface: implications for the insertion of transbilayer helices. Biochemistry *28*, 3421-3437.

Jayasinghe, S., Hristova, K., and White, S.H. (2001). Energetics, stability, and prediction of transmembrane helices. J Mol Biol *312*, 927-934.

Jentsch, T.J., Stein, V., Weinreich, F., and Zdebik, A.A. (2002). Molecular structure and physiological function of chloride channels. Physiol Rev *82*, 503-568.

Jentsch, T.J., Steinmeyer, K., and Schwarz, G. (1990). Primary structure of Torpedo marmorata chloride channel isolated by expression cloning in Xenopus oocytes. Nature *348*, 510-514.

Johnson, J.E., and Cornell, R.B. (1999). Amphitropic proteins: regulation by reversible membrane interactions (review). Mol Membr Biol *16*, 217-235.

Johnson, J.E., Xie, M., Singh, L.M., Edge, R., and Cornell, R.B. (2003). Both acidic and basic amino acids in an amphitropic enzyme, CTP:phosphocholine cytidylyltransferase, dictate its selectivity for anionic membranes. J Biol Chem *278*, 514-522.

Kagan, B.L., Finkelstein, A., and Colombini, M. (1981). Diphtheria toxin fragment forms large pores in phospholipid bilayer membranes. Proc Natl Acad Sci U S A *78*, 4950-4954.

Kall, L., Krogh, A., and Sonnhammer, E.L. (2004). A combined transmembrane topology and signal peptide prediction method. J Mol Biol *338*, 1027-1036.

Kelly, R.B. (1985). Pathways of protein secretion in eukaryotes. Science *230*, 25-32.

Kidd, J.F., and Thorn, P. (2000). Intracellular Ca2+ and Cl- channel activation in secretory cells. Annu Rev Physiol *62*, 493-513.

Klein, P., Kanehisa, M., and DeLisi, C. (1985). The detection and classification of membrane-spanning proteins. Biochim Biophys Acta *815*, 468-476.

Koeppe, R.E., 2nd (2007). Concerning tryptophan and protein-bilayer interactions. J Gen Physiol *130*, 223-224.

Lacroix, E., Bruix, M., Lopez-Hernandez, E., Serrano, L., and Rico, M. (1997). Amide hydrogen exchange and internal dynamics in the chemotactic protein CheY from Escherichia coli. J Mol Biol *271*, 472-487.

Landolt-Marticorena, C., Williams, K.A., Deber, C.M., and Reithmeier, R.A. (1993). Non-random distribution of amino acids in the transmembrane segments of human type I single span membrane proteins. J Mol Biol *229*, 602-608.

Landry, D.W., Akabas, M.H., Redhead, C., Edelman, A., Cragoe, E.J., Jr., and Al-Awqati, Q. (1989). Purification and reconstitution of chloride channels from kidney and trachea. Science *244*, 1469-1472.

Langen, R., Isas, J.M., Hubbell, W.L., and Haigler, H.T. (1998). A transmembrane form of annexin XII detected by site-directed spin labeling. Proc Natl Acad Sci U S A *95*, 14060-14065.

Lawson, D., Raff, M.C., Gomperts, B., Fewtrell, C., and Gilula, N.B. (1977). Molecular events during membrane fusion. A study of exocytosis in rat peritoneal mast cells. J Cell Biol *72*, 242-259.

Lee, A.G. (2003). Lipid-protein interactions in biological membranes: a structural perspective. Biochim Biophys Acta *1612*, 1-40.

Lee, A.G. (2005). How lipids and proteins interact in a membrane: a molecular approach. Mol Biosyst *1*, 203-212.

Legg-E'silva, D., Achilonu, I., Fanucchi, S., Stoychev, S., Fernandes, M., and Dirr, H.W. (2012). Role of Arginine 29 and Glutamic Acid 81 Interactions in the Conformational Stability of Human Chloride Intracellular Channel 1. Biochemistry.

Li, J.D., Carroll, J., and Ellar, D.J. (1991). Crystal structure of insecticidal delta-endotoxin from Bacillus thuringiensis at 2.5 A resolution. Nature *353*, 815-821.

Lindstrom, J., Anand, R., Peng, X., Gerzanich, V., Wang, F., and Li, Y. (1995). Neuronal nicotinic receptor subtypes. Ann N Y Acad Sci *757*, 100-116.

Littler, D.R., Assaad, N.N., Harrop, S.J., Brown, L.J., Pankhurst, G.J., Luciani, P., Aguilar, M.I., Mazzanti, M., Berryman, M.A., Breit, S.N., *et al.* (2005). Crystal structure of the

soluble form of the redox-regulated chloride ion channel protein CLIC4. Febs J *272*, 4996-5007.

Littler, D.R., Harrop, S.J., Fairlie, W.D., Brown, L.J., Pankhurst, G.J., Pankhurst, S., DeMaere, M.Z., Campbell, T.J., Bauskin, A.R., Tonini, R., *et al.* (2004). The intracellular chloride ion channel protein CLIC1 undergoes a redox-controlled structural transition. J Biol Chem *279*, 9298-9305.

Littler, D.R., Harrop, S.J., Goodchild, S.C., Phang, J.M., Mynott, A.V., Jiang, L., Valenzuela, S.M., Mazzanti, M., Brown, L.J., Breit, S.N., *et al.* (2010). The enigma of the CLIC proteins: Ion channels, redox proteins, enzymes, scaffolding proteins? FEBS Lett *584*, 2093-2101.

Liu, Y., and Bolen, D.W. (1995). The peptide backbone plays a dominant role in protein stabilization by naturally occurring osmolytes. Biochemistry *34*, 12884-12891.

Locher, K.P., Bass, R.B., and Rees, D.C. (2003). Structural biology. Breaching the barrier. Science *301*, 603-604.

Lowe, G., and Gold, G.H. (1993). Nonlinear amplification by calcium-dependent chloride channels in olfactory receptor cells. Nature *366*, 283-286.

Luo, Y., and Baldwin, R.L. (1998). Trifluoroethanol stabilizes the pH 4 folding intermediate of sperm whale apomyoglobin. J Mol Biol *279*, 49-57.

Manceva, S.D., Pusztai-Carey, M., and Butko, P. (2004). Effect of pH and ionic strength on the cytolytic toxin Cyt1A: a fluorescence spectroscopy study. Biochim Biophys Acta *1699*, 123-130.

McLaughlin, S., Hangyas-Mihalyne, G., Zaitseva, I., and Golebiewska, U. (2005). Reversible - through calmodulin - electrostatic interactions between basic residues on proteins and acidic lipids in the plasma membrane. Biochem Soc Symp, 189-198.

Milton, R.H., Abeti, R., Averaimo, S., DeBiasi, S., Vitellaro, L., Jiang, L., Curmi, P.M., Breit, S.N., Duchen, M.R., and Mazzanti, M. (2008). CLIC1 function is required for beta-

amyloid-induced generation of reactive oxygen species by microglia. J Neurosci *28*, 11488-11499.

Mimms, L.T., Zampighi, G., Nozaki, Y., Tanford, C., and Reynolds, J.A. (1981). Phospholipid vesicle formation and transmembrane protein incorporation using octyl glucoside. Biochemistry *20*, 833-840.

Money, T.T., King, R.G., Wong, M.H., Stevenson, J.L., Kalionis, B., Erwich, J.J., Huisman, M.A., Timmer, A., Hiden, U., Desoye, G., *et al.* (2007). Expression and cellular localisation of chloride intracellular channel 3 in human placenta and fetal membranes. Placenta *28*, 429-436.

Morris, A.P., and Frizzell, R.A. (1993). Ca(2+)-dependent Cl- channels in undifferentiated human colonic cells (HT-29). I. Single-channel properties. Am J Physiol *264*, C968-976.

Mozafari, M.R. (2005). Liposomes: an overview of manufacturing techniques. Cell Mol Biol Lett *10*, 711-719.

Mulgrew-Nesbitt, A., Diraviyam, K., Wang, J., Singh, S., Murray, P., Li, Z., Rogers, L., Mirkovic, N., and Murray, D. (2006). The role of electrostatics in protein-membrane interactions. Biochim Biophys Acta *1761*, 812-826.

Munoz, V., and Serrano, L. (1997). Development of the multiple sequence approximation within the AGADIR model of alpha-helix formation: comparison with Zimm-Bragg and Lifson-Roig formalisms. Biopolymers *41*, 495-509.

Nagle, J.F., and Tristram-Nagle, S. (2000). Lipid bilayer structure. Curr Opin Struct Biol *10*, 474-480.

Neitcheva, T., and Peeva, D. (1995). Phospholipid composition, phospholipase A2 and sphingomyelinase activities in rat liver nuclear membrane and matrix. Int J Biochem Cell Biol *27*, 995-1001.

Nguyen, M., Millar, D.G., Yong, V.W., Korsmeyer, S.J., and Shore, G.C. (1993). Targeting of Bcl-2 to the mitochondrial outer membrane by a COOH-terminal signal anchor sequence. J Biol Chem *268*, 25265-25268.

Nilius, B., and Droogmans, G. (2001). Ion channels and their functional role in vascular endothelium. Physiol Rev *81*, 1415-1459.

Nishizawa, T., Nagao, T., Iwatsubo, T., Forte, J.G., and Urushidani, T. (2000). Molecular cloning and characterization of a novel chloride intracellular channel-related protein, parchorin, expressed in water-secreting cells. J Biol Chem *275*, 11164-11173.

Novarino, G., Fabrizi, C., Tonini, R., Denti, M.A., Malchiodi-Albedi, F., Lauro, G.M., Sacchetti, B., Paradisi, S., Ferroni, A., Curmi, P.M., *et al.* (2004). Involvement of the intracellular ion channel CLIC1 in microglia-mediated beta-amyloid-induced neurotoxicity. J Neurosci *24*, 5322-5330.

Nyholm, T.K., Ozdirekcan, S., and Killian, J.A. (2007). How protein transmembrane segments sense the lipid environment. Biochemistry *46*, 1457-1465.

Orzaez, M., Salgado, J., Gimenez-Giner, A., Perez-Paya, E., and Mingarro, I. (2004). Influence of proline residues in transmembrane helix packing. J Mol Biol *335*, 631-640.

Owens, D.F., Boyce, L.H., Davis, M.B., and Kriegstein, A.R. (1996). Excitatory GABA responses in embryonic and neonatal cortical slices demonstrated by gramicidin perforated-patch recordings and calcium imaging. J Neurosci *16*, 6414-6423.

Parbhoo, N., Stoychev, S.H., Fanucchi, S., Achilonu, I., Adamson, R.J., Fernandes, M., Gildenhuys, S., and Dirr, H.W. (2011). A conserved interdomain interaction is a determinant of folding cooperativity in the GST fold. Biochemistry *50*, 7067-7075.

Parker, M.W., and Feil, S.C. (2005). Pore-forming protein toxins: from structure to function. Prog Biophys Mol Biol *88*, 91-142.

Parker, M.W., and Pattus, F. (1993). Rendering a membrane protein soluble in water: a common packing motif in bacterial protein toxins. Trends Biochem Sci *18*, 391-395.

Parker, M.W., Postma, J.P., Pattus, F., Tucker, A.D., and Tsernoglou, D. (1992). Refined structure of the pore-forming domain of colicin A at 2.4 A resolution. J Mol Biol *224*, 639-657.

Parker, M.W., Tucker, A.D., Tsernoglou, D., and Pattus, F. (1990). Insights into membrane insertion based on studies of colicins. Trends Biochem Sci *15*, 126-129.

Paula, S., Volkov, A.G., and Deamer, D.W. (1998). Permeation of halide anions through phospholipid bilayers occurs by the solubility-diffusion mechanism. Biophys J *74*, 319-327.

Pelham, H.R., and Munro, S. (1993). Sorting of membrane proteins in the secretory pathway. Cell *75*, 603-605.

Peter, B., Ngubane, N.C., Fanucchi, S., and Dirr, H.W. (2013). Membrane mimetics induce helix formation and oligomerization of the chloride intracellular channel protein 1 transmembrane domain. Biochemistry *52*, 2739-2749.

Peter, B., Polyansky, A.A., Fanucchi, S., and Dirr, H.W. (2014). A Lys-Trp Cation-pi Interaction Mediates the Dimerization and Function of the Chloride Intracellular Channel Protein 1 Transmembrane Domain. Biochemistry *53*, 57-67.

Pethig, R., and Kell, D.B. (1987). The passive electrical properties of biological systems: their significance in physiology, biophysics and biotechnology. Phys Med Biol *32*, 933-970.

Petrova, D.T., Asif, A.R., Armstrong, V.W., Dimova, I., Toshev, S., Yaramov, N., Oellerich, M., and Toncheva, D. (2008). Expression of chloride intracellular channel protein 1 (CLIC1) and tumor protein D52 (TPD52) as potential biomarkers for colorectal cancer. Clin Biochem *41*, 1224-1236.

Ponce, A., Vega-Saenz de Miera, E., Kentros, C., Moreno, H., Thornhill, B., and Rudy, B. (1997). K+ channel subunit isoforms with divergent carboxy-terminal sequences carry distinct membrane targeting signals. J Membr Biol *159*, 149-159.

Ponting, C.P. (1997). CBS domains in CIC chloride channels implicated in myotonia and nephrolithiasis (kidney stones). J Mol Med (Berl) *75*, 160-163.

Popot, J.L., and Engelman, D.M. (1990). Membrane protein folding and oligomerization: the two-stage model. Biochemistry *29*, 4031-4037.

Popot, J.L., and Engelman, D.M. (2000). Helical membrane protein folding, stability, and evolution. Annu Rev Biochem *69*, 881-922.

Proutski, I., Karoulias, N., and Ashley, R.H. (2002). Overexpressed chloride intracellular channel protein CLIC4 (p64H1) is an essential component of novel plasma membrane anion channels. Biochem Biophys Res Commun *297*, 317-322.

Qian, Z., Okuhara, D., Abe, M.K., and Rosner, M.R. (1999). Molecular cloning and characterization of a mitogen-activated protein kinase-associated intracellular chloride channel. J Biol Chem *274*, 1621-1627.

Ramsay, G., Montgomery, D., Berger, D., and Freire, E. (1989). Energetics of diphtheria toxin membrane insertion and translocation: calorimetric characterization of the acid pH induced transition. Biochemistry *28*, 529-533.

Rawicz, W., Olbrich, K.C., McIntosh, T., Needham, D., and Evans, E. (2000). Effect of chain length and unsaturation on elasticity of lipid bilayers. Biophys J *79*, 328-339.

Redhead, C., Sullivan, S.K., Koseki, C., Fujiwara, K., and Edwards, J.C. (1997). Subcellular distribution and targeting of the intracellular chloride channel p64. Mol Biol Cell *8*, 691-704.

Reichling, D.B., Kyrozis, A., Wang, J., and MacDermott, A.B. (1994). Mechanisms of GABA and glycine depolarization-induced calcium transients in rat dorsal horn neurons. J Physiol *476*, 411-421.

Ren, J., Lew, S., Wang, Z., and London, E. (1997). Transmembrane orientation of hydrophobic alpha-helices is regulated both by the relationship of helix length to bilayer thickness and by the cholesterol concentration. Biochemistry *36*, 10213-10220.

Rigoutsos, I., Riek, P., Graham, R.M., and Novotny, J. (2003). Structural details (kinks and non-alpha conformations) in transmembrane helices are intrahelically determined and can be predicted by sequence pattern descriptors. Nucleic Acids Res *31*, 4625-4631.

Riordan, J.R., Rommens, J.M., Kerem, B., Alon, N., Rozmahel, R., Grzelczak, Z., Zielenski, J., Lok, S., Plavsic, N., Chou, J.L., *et al.* (1989). Identification of the cystic fibrosis gene: cloning and characterization of complementary DNA. Science *245*, 1066-1073.

Rivera, C., Voipio, J., Payne, J.A., Ruusuvuori, E., Lahtinen, H., Lamsa, K., Pirvola, U., Saarma, M., and Kaila, K. (1999). The K+/Cl- co-transporter KCC2 renders GABA hyperpolarizing during neuronal maturation. Nature *397*, 251-255.

Roccatano, D., Colombo, G., Fioroni, M., and Mark, A.E. (2002). Mechanism by which 2,2,2-trifluoroethanol/water mixtures stabilize secondary-structure formation in peptides: a molecular dynamics study. Proc Natl Acad Sci U S A *99*, 12179-12184.

Rohl, C.A., Chakrabartty, A., and Baldwin, R.L. (1996). Helix propagation and N-cap propensities of the amino acids measured in alanine-based peptides in 40 volume percent trifluoroethanol. Protein Sci *5*, 2623-2637.

Ronnov-Jessen, L., Villadsen, R., Edwards, J.C., and Petersen, O.W. (2002). Differential expression of a chloride intracellular channel gene, CLIC4, in transforming growth factor-beta1-mediated conversion of fibroblasts to myofibroblasts. Am J Pathol *161*, 471-480.

Rosen, C.G., and Weber, G. (1969). Dimer formation from 1-amino-8-naphthalenesulfonate catalyzed by bovine serum albumin. A new fluorescent molecule with exceptional binding properties. Biochemistry *8*, 3915-3920.

Sakai, H., and Tsukihara, T. (1998). Structures of membrane proteins determined at atomic resolution. J Biochem *124*, 1051-1059.

Sanchez, S.A., Tricerri, M.A., Ossato, G., and Gratton, E. (2010). Lipid packing determines protein-membrane interactions: challenges for apolipoprotein A-I and high density lipoproteins. Biochim Biophys Acta *1798*, 1399-1408.

Sanders, C.R., 2nd, and Landis, G.C. (1995). Reconstitution of membrane proteins into lipid-rich bilayered mixed micelles for NMR studies. Biochemistry *34*, 4030-4040.

Sathish, H.A., Cusan, M., Aisenbrey, C., and Bechinger, B. (2002). Guanidine hydrochloride induced equilibrium unfolding studies of colicin B and its channel-forming fragment. Biochemistry *41*, 5340-5347.

Schendel, S.L., and Cramer, W.A. (1994). On the nature of the unfolded intermediate in the in vitro transition of the colicin E1 channel domain from the aqueous to the membrane phase. Protein Sci *3*, 2272-2279.

Schlesinger, P.H., Blair, H.C., Teitelbaum, S.L., and Edwards, J.C. (1997). Characterization of the osteoclast ruffled border chloride channel and its role in bone resorption. J Biol Chem *272*, 18636-18643.

Schriever, A.M., Friedrich, T., Pusch, M., and Jentsch, T.J. (1999). CLC chloride channels in Caenorhabditis elegans. J Biol Chem *274*, 34238-34244.

Sheehan, D., Meade, G., Foley, V.M., and Dowd, C.A. (2001). Structure, function and evolution of glutathione transferases: implications for classification of non-mammalian members of an ancient enzyme superfamily. Biochem J *360*, 1-16.

Sheppard, D.N., and Welsh, M.J. (1993). Inhibition of the cystic fibrosis transmembrane conductance regulator by ATP-sensitive K+ channel regulators. Ann N Y Acad Sci *707*, 275-284.

Singh, H. (2010). Two decades with dimorphic Chloride Intracellular Channels (CLICs). FEBS Lett *584*, 2112-2121.

Singh, H., and Ashley, R.H. (2006). Redox regulation of CLIC1 by cysteine residues associated with the putative channel pore. Biophys J *90*, 1628-1638.

Singh, H., and Ashley, R.H. (2007). CLIC4 (p64H1) and its putative transmembrane domain form poorly selective, redox-regulated ion channels. Mol Membr Biol *24*, 41-52.

Skou, J.C. (1957). The influence of some cations on an adenosine triphosphatase from peripheral nerves. Biochim Biophys Acta *23*, 394-401.

Smith, S.S., Liu, X., Zhang, Z.R., Sun, F., Kriewall, T.E., McCarty, N.A., and Dawson, D.C. (2001). CFTR: covalent and noncovalent modification suggests a role for fixed charges in anion conduction. J Gen Physiol *118*, 407-431.

Spector, A.A., and Yorek, M.A. (1985). Membrane lipid composition and cellular function. J Lipid Res *26*, 1015-1035.

Stoychev, S.H., Nathaniel, C., Fanucchi, S., Brock, M., Li, S., Asmus, K., Woods, V.L., Jr., and Dirr, H.W. (2009). Structural dynamics of soluble chloride intracellular channel protein CLIC1 examined by amide hydrogen-deuterium exchange mass spectrometry. Biochemistry *48*, 8413-8421.

Strandberg, E., and Killian, J.A. (2003). Snorkeling of lysine side chains in transmembrane helices: how easy can it get? FEBS Lett *544*, 69-73.

Stuhmer, W., Ruppersberg, J.P., Schroter, K.H., Sakmann, B., Stocker, M., Giese, K.P., Perschke, A., Baumann, A., and Pongs, O. (1989). Molecular basis of functional diversity of voltage-gated potassium channels in mammalian brain. EMBO J *8*, 3235-3244.

Suginta, W., Karoulias, N., Aitken, A., and Ashley, R.H. (2001). Chloride intracellular channel protein CLIC4 (p64H1) binds directly to brain dynamin I in a complex containing actin, tubulin and 14-3-3 isoforms. Biochem J *359*, 55-64.

Suh, K.S., Mutoh, M., Nagashima, K., Fernandez-Salas, E., Edwards, L.E., Hayes, D.D., Crutchley, J.M., Marin, K.G., Dumont, R.A., Levy, J.M., *et al.* (2004). The organellular chloride channel protein CLIC4/mtCLIC translocates to the nucleus in response to cellular stress and accelerates apoptosis. J Biol Chem *279*, 4632-4641.

Tejuca, M., Serra, M.D., Ferreras, M., Lanio, M.E., and Menestrina, G. (1996). Mechanism of membrane permeabilization by sticholysin I, a cytolysin isolated from the venom of the sea anemone Stichodactyla helianthus. Biochemistry *35*, 14947-14957.

Thomas, M.J., Pang, K., Chen, Q., Lyles, D., Hantgan, R., and Waite, M. (1999). Lipid exchange between mixed micelles of phospholipid and triton X-100. Biochim Biophys Acta *1417*, 144-156.

Thuduppathy, G.R., Craig, J.W., Kholodenko, V., Schon, A., and Hill, R.B. (2006). Evidence that membrane insertion of the cytosolic domain of Bcl-xL is governed by an electrostatic mechanism. J Mol Biol *359*, 1045-1058.

Thuduppathy, G.R., and Hill, R.B. (2006). Acid destabilization of the solution conformation of Bcl-xL does not drive its pH-dependent insertion into membranes. Protein Sci *15*, 248-257.

Tonini, R., Ferroni, A., Valenzuela, S.M., Warton, K., Campbell, T.J., Breit, S.N., and Mazzanti, M. (2000). Functional characterization of the NCC27 nuclear protein in stable transfected CHO-K1 cells. Faseb J *14*, 1171-1178.

Trauble, H., and Eibl, H. (1974). Electrostatic effects on lipid phase transitions: membrane structure and ionic environment. Proc Natl Acad Sci U S A *71*, 214-219.

Tulk, B.M., Kapadia, S., and Edwards, J.C. (2002). CLIC1 inserts from the aqueous phase into phospholipid membranes, where it functions as an anion channel. Am J Physiol Cell Physiol *282*, C1103-1112.

Tusnady, G.E., and Simon, I. (1998). Principles governing amino acid composition of integral membrane proteins: application to topology prediction. J Mol Biol *283*, 489-506.

Ulmasov, B., Bruno, J., Woost, P.G., and Edwards, J.C. (2007). Tissue and subcellular distribution of CLIC1. BMC Cell Biol *8*, 8.

Valenzuela, S.M., Martin, D.K., Por, S.B., Robbins, J.M., Warton, K., Bootcov, M.R., Schofield, P.R., Campbell, T.J., and Breit, S.N. (1997). Molecular cloning and expression of a chloride ion channel of cell nuclei. J Biol Chem *272*, 12575-12582.

Valenzuela, S.M., Mazzanti, M., Tonini, R., Qiu, M.R., Warton, K., Musgrove, E.A., Campbell, T.J., and Breit, S.N. (2000). The nuclear chloride ion channel NCC27 is involved in regulation of the cell cycle. J Physiol *529 Pt 3*, 541-552.

van der Goot, F.G., Gonzalez-Manas, J.M., Lakey, J.H., and Pattus, F. (1991). A 'molten-globule' membrane-insertion intermediate of the pore-forming domain of colicin A. Nature *354*, 408-410.

Vannier, C., and Triller, A. (1997). Biology of the postsynaptic glycine receptor. Int Rev Cytol *176*, 201-244.

Vargas-Uribe, M., Rodnin, M.V., and Ladokhin, A.S. (2013). Comparison of membrane insertion pathways of the apoptotic regulator Bcl-xL and the diphtheria toxin translocation domain. Biochemistry *52*, 7901-7909.

von Heijne, G. (1984). Analysis of the distribution of charged residues in the N-terminal region of signal sequences: implications for protein export in prokaryotic and eukaryotic cells. EMBO J *3*, 2315-2318.

von Heijne, G., and Gavel, Y. (1988). Topogenic signals in integral membrane proteins. Eur J Biochem *174*, 671-678.

Wallin, E., and von Heijne, G. (1995). Properties of N-terminal tails in G-protein coupled receptors: a statistical study. Protein Eng *8*, 693-698.

Warton, K., Tonini, R., Fairlie, W.D., Matthews, J.M., Valenzuela, S.M., Qiu, M.R., Wu, W.M., Pankhurst, S., Bauskin, A.R., Harrop, S.J., *et al.* (2002). Recombinant CLIC1

(NCC27) assembles in lipid bilayers via a pH-dependent two-state process to form chloride ion channels with identical characteristics to those observed in Chinese hamster ovary cells expressing CLIC1. J Biol Chem *277*, 26003-26011.

Wei, X., Ding, S., Jiang, Y., Zeng, X.G., and Zhou, H.M. (2006). Conformational changes and inactivation of bovine carbonic anhydrase II in 2,2,2-trifluoroethanol solutions. Biochemistry (Mosc) *71 Suppl 1*, S77-82.

White, S.H., and Wimley, W.C. (1998). Hydrophobic interactions of peptides with membrane interfaces. Biochim Biophys Acta *1376*, 339-352.

White, S.H., and Wimley, W.C. (1999). Membrane protein folding and stability: physical principles. Annu Rev Biophys Biomol Struct *28*, 319-365.

Whittam, R., and Chipperfield, A.R. (1975). The reaction mechanism of the sodium pump. Biochim Biophys Acta *415*, 149-171.

Wilce, M.C., and Parker, M.W. (1994). Structure and function of glutathione S-transferases. Biochim Biophys Acta *1205*, 1-18.

Wimley, W.C., and White, S.H. (1996). Experimentally determined hydrophobicity scale for proteins at membrane interfaces. Nat Struct Biol *3*, 842-848.

Winterhalter, M., and Lasic, D.D. (1993). Liposome stability and formation: experimental parameters and theories on the size distribution. Chem Phys Lipids *64*, 35-43.

Xu, D., Lin, S.L., and Nussinov, R. (1997). Protein binding versus protein folding: the role of hydrophilic bridges in protein associations. J Mol Biol *265*, 68-84.

Yeagle, P.L. (1989). Regulation of membrane function through composition, structure, and dynamics. Ann N Y Acad Sci *568*, 29-34.

Zakerhamidi, M.S., Ahmadi-Kandjani, S., Moghadam, M., Ortyl, E., and Kucharski, S. (2012). Solvatochromism effects on the dipole moments and photo-physical behavior of some azo sulfonamide dyes. Spectrochim Acta A Mol Biomol Spectrosc *85*, 105-110.